UNIVERSITY OF CALIFORNIA, SAN DIEGO

The Role of the Innate Immune System in Cancer Immunoediting and Rejection

A dissertation submitted in partial satisfaction of the

requirements for the degree Doctor of Philiosophy

in

Biomedical Sciences

by

Timothy Edward O'Sullivan

Committee in charge:

Professor Jack Bui, Chair
Professor John Chang
Professor Shane Crotty
Professor Richard Klemke
Professor Cornelius Murre
Professor Elina Zuniga

2012

The Dissertation of Timothy Edward O'Sullivan is approved, and is acceptable

In quality and form for publication on microfilm and electronically:

_____

_____

_____

_____

_____

_____

Chair

University of California, San Diego

2012

DEDICATION

In recognition of her selflessness and understanding, this dissertation is dedicated to my mother Catherine Jane O'Sullivan.

EPIGRAPH

I wanted to change the world. But I have found that the only thing one can be sure of changing is oneself

Aldous Huxley

TABLE OF CONTENTS

LIST OF FIGURES

LIST OF TABLES

ACKNOWLEDGEMENTS

I would like to acknowledge Professor Jack Bui for his support as the chair of my committee. His patience and zen-like guidance have helped me overcome many obstacles, both personally and scientifically. His ideas and scientific work form the foundation for all the results in this dissertation.

I would also like to acknowledge Robert Saddawi-Konefka for his valuable support with experiments and unyielding optimism, and Miller Tran for producing reagents that were critical for the completion of this dissertation.

Chapter 1, in full, is an adapted version that has been submitted for publication of the material as it may appear in The Journal of Experimental Medicine, 2012, Saddawi-Konefka, Robert; Smyth Mark J.; Schreiber, Robert D.; Bui, Jack D.; The Rockefeller University Press. The disseration author was the primary co-author of this paper.

Chapter 2, in full, is an adapted version of the material as it appears in The Journal of Immunology, 2011, Schreiber, Robert D.; Bui, Jack D.; The American Association of Immunologists, Inc. The dissertation author was the primary author of this paper.

Chapter 3, in part, is an adapted version of material that is currently being prepared for submission for publication. Saddawi-Konefka, Robert; Bui, Jack D.; Mayfield, Stephen P.; Tran, Miller. The dissertation author was the primary author of this material.

VITA

2008 Bachelor of Science, Cornell University

2012 Doctor of Philosophy, University of California, San Diego

PUBLICATIONS

O'Sullivan, T., R.D. Schreiber, and J.D. Bui. Cancer Immunoediting of the NK Group 2D Ligand H60a. *J. Immunol*. 187:3538–3545 (2011).

FIELDS OF STUDY

Major Field: Biomedical Sciences

Studies in Cancer Immunology
Professor Jack Bui

ABSTRACT OF THE DISSERTATION

The Role of the Innate Immune System in Cancer Immunoediting and Rejection

by

Timothy Edward O'Sullivan

Doctor of Philosophy in Biomedical Sciences

University of California, San Diego, 2012

Professor Jack Bui, Chair

Cancer immunoediting is the process whereby immune cells protect against cancer formation and sculpt the immunogenicity of developing tumors. In its most complex form, this process involves the initial elimination of highly immunogenic tumor cells from an "unedited" heterogeneous cell repertoire, followed by the eventual escape

of non-immunogenic, "edited" cells. Edited cell lines, which are derived from tumors that develop in wild-type (WT) mice, are termed "progressors" because they are poorly immunogenic and grow progressively when transplanted into syngeneic naïve WT mice. Unedited cell lines, which are derived from immune deficient mice, are often highly immunogenic and are termed "regressors" because they are rejected when transplanted into syngeneic naïve WT mice. Although the full process depends on innate and adaptive immunity, it remains unclear whether innate immunity alone is capable of immunoediting, and the molecular differences between regressor and progressor tumors remain largely undefined. To determine whether the innate immune system can edit tumor cells in the absence of adaptive immunity, we compared the incidence and immunogenicity of 3'methylcholanthrene-induced sarcomas in syngeneic wild-type, $RAG2^{-/-}$, and $RAG2^{-/-}$x $\gamma c^{-/-}$ mice. We found that innate immune cells could indeed manifest cancer immunoediting activity in the absence of adaptive immunity. While natural killer (NK) cells can directly edit the natural killer group 2D (NKG2D) ligand H60a when expression levels are heterogenous within a tumor, these cells also indirectly edit through the production of IFNγ by polarizing M1 macrophages, which act as important effectors during cancer immunoediting. Using a non-biased microarray approach, we found that interleukin 17D (IL-17D) expression in tumors leads to the recruitment of NK cells through indirect production of MCP-1, which mediates the rejection of progressor tumors and leads to priming of the adaptive immune system and subsequent immunological memory of the host. All together these studies showcase the central role of NK cells in both cancer immunoediting and elimination, and implicate a novel tumor secreted factor IL-17D for use in tumor immunotherapy.

INTRODUCTION

The process of cancer immunoediting generates a repertoire of cancer cells that can persist in immune competent hosts (1-5). In its most complex form, this process involves the initial elimination of highly immunogenic tumor cells from an "unedited" heterogeneous cell repertoire, followed by the eventual escape of non-immunogenic, "edited" cells. Edited cell lines, which are derived from tumors that develop in wild-type (WT) mice, are termed "progressors" because they are poorly immunogenic and grow progressively when transplanted into syngeneic naïve WT mice. Unedited cell lines, which are derived from immune deficient mice, are often highly immunogenic and are termed "regressors" because they are rejected when transplanted into syngeneic naïve WT mice. Immune cells can infiltrate, recognize, become activated, and eliminate regressor but not progressor tumor cells (3-6). Edited tumors possess antigens (7,8), but the adaptive immune response to edited tumors ultimately fails, leading to cancer progression and death (5).

Several studies have revealed the contribution of adaptive and innate immunity in cancer immunoediting (1,9-16), but it is not clear whether the un-manipulated innate immune system can suppress tumor formation without adaptive immunity. We therefore examined the ability of the innate immune system to control tumor formation in the absence of adaptive immunity. It has been shown that natural killer (NK) cells (17, 18) and classically activated M1 macrophages (19,20) support a Th1 response that can ultimately lead to tumor rejection in the presence of adaptive immunity, but it is not clear

whether these cells interact in the absence of adaptive immunity to suppress tumor formation in primary tumor models. In contrast, other studies have found that the innate immune system can promote tumor formation via alternatively activated M2 macrophages (21) that augment angiogenesis and promote tissue invasion. M2 macrophages also inhibit the formation of anti-tumor adaptive immunity, and therefore, it is possible that innate immunity would promote tumor formation in the absence of adaptive immunity.

Using the 3'methylcholanthrene (MCA) model of sarcomagenesis, we previously found that the immune system in wild-type (WT) mice could edit tumors more effectively than the immune system in $RAG2^{-/-}$ mice (which lack adaptive immunity) (1), but we did not assess whether tumors from $RAG2^{-/-}$ mice were edited by the innate immune system. Since $RAG2^{-/-}$ mice and other immunodeficient mice such as nude and SCID mice are routinely used as "immunodeficient" models for xenotransplantation and pre-clinical studies, it is critical to assess whether the innate immune system in these mice could impact, positively or negatively, on tumor growth.

Towards this end, we set out to quantitate tumor editing in WT versus $RAG2^{-/-}$ versus $RAG2^{-/-}$ x $\gamma c^{-/-}$ mice. $RAG2^{-/-}$x $\gamma c^{-/-}$ mice lack all lymphocytes including NK, NK-T, γδ-T, classical $CD4^+$ and $CD8^+$ αβ-T cells and B cells and thus show deficits in both innate and adaptive immunity. If cells of the innate immune system could hinder tumor growth, then we would expect $RAG2^{-/-}$ x $\gamma c^{-/-}$ mice to demonstrate increased tumor incidence and decreased tumor editing compared to $RAG2^{-/-}$ mice. Indeed, when we compared MCA-induced sarcoma incidence and tumor cell immunogenicity between the groups of mice, we found both increased incidence and immunogenicity of MCA-induced

sarcomes in RAG2$^{-/-}$x γc$^{-/-}$ mice compared to RAG2$^{-/-}$ mice, which, consistent with previous results (1), had increased incidence and immunogenicity of tumors compared to WT mice.

To understand the basis of cellular recognition during immunediting, we then compared the edited and unedited tumor cell repertoire by examining MCA sarcoma cell lines generated in carcinogen-treated syngeneic WT and immunodeficient mice (1, 9). We focused on evaluating the expression of ligands for the activating receptor Natural Killer Group 2D (NKG2D) (22) within the unedited tumor repertoire. NKG2D is a receptor expressed on NK cells, CD8$^+$ T cells, gd-T cells, and NK-T cells that mediates the detection of stressed cells that are infected by viruses or undergoing transformation (23-27). It binds a ligand family that is generally not expressed at functional levels in normal tissues, but can be up-regulated by certain stimuli, including DNA damage and virus infection (28, 29).

Others have shown that the NKG2D ligand H60a (30-33), but not other NKG2D ligands, is down-regulated by IFNγ in MCA sarcomas (33). Considering the important role of IFNγ and NKG2D in preventing tumor formation (9,18), we wished to determine whether the IFNγ-regulated NKG2D ligand H60a could participate in the surveillance of developing tumors. Whereas H60a can mediate tumor rejection when expressed at very high levels (34), its endogenous role in tumor immunosurveillance is not known. Furthermore, previous studies with NKG2D-deficient mice (25, 26) were done on the C57BL/6 background, which does not express H60a, and therefore does not address the role of H60a in tumor editing. Interestingly, H60a can be induced within days of

carcinogen exposure in mouse skin (35), but its expression in the unedited tumor cell repertoire has not been studied.

We examined the expression of NKG2D ligands in MCA sarcoma cell lines derived from mice with varying levels of immune activity. We show that the heterogeneity of NKG2D ligand levels is inversely correlated with the degree of cancer immunoediting. This heterogeneity can be detected by the level of H60a expression in groups of tumor cell lines or can manifest in a single tumor cell line via bimodal distribution of H60a expression. When a cell line expressing bimodal levels of H60a was passaged through a $RAG2^{-/-}$ mouse and subjected to innate immune pressure, the H60a expression was reduced, indicating that H60a had been edited.

However, when transplanted into $RAG2^{-/-}$ recipients, $RAG2^{-/-}$x $\gamma c^{-/-}$ regressor sarcoma cell lines formed tumors that became heavily infiltrated with M1 macrophages. The infiltration of M1 macrophages was associated with tumor editing and required host NK cells and IFNγ activity. In contrast, in the absence of NK cells and IFNγ function, $RAG2^{-/-}$x $\gamma c^{-/-}$ regressors were infiltrated with more M2 macrophages, which can promote tumor formation (19). We also found that M1 macrophages can be elicited by CD40 agonistic antibodies to restore the editing capacity of $RAG2^{-/-}$x $\gamma c^{-/-}$ mice. These studies document that components of the innate immune system present in $RAG2^{-/-}$ mice can manifest certain types of cancer immunoediting capacity in the absence of adaptive immunity and point, specifically, to M1 macrophages as important effectors in this process. We propose that cancer immunoediting acts in part by limiting the heterogeneity of a diverse primary repertoire of tumor cells. H60a may be a suitable substrate or a surrogate marker for the editing process, while NK cells can act as direct or indirect

editors during immunoediting depending on tumor NKG2D ligand expression levels and hetergeneity.

Because the overall levels of NKG2D ligand expression was not found to be different between edited and unedited tumors, and the molecular differences between these tumors are poorly defined, we postulated that regressor tumors contained more antigens than progressor tumors. In order to test this, we mixed regressor tumor cell lines with progressor tumor cell lines and found that these tumor mixtures rejected in immunocompetent mice. However, this process was not dependent on common antigen expression, as mice pre-immunized wth regressor tumors could not reject transplanted progressor tumors. Whereas progressor-derived factors such as TGF-b (36) and B7-H1 (37) have been shown to actively suppress immune responses, thereby providing a potentially "dominant" mechanism for tumor escape, our results suggest an alternate mechanism of regressor secreted molecules that lead to tumor rejection. Using an unbiased global expression analysis approach, we identified a single gene, IL-17D, as sufficient and necessary for the rejection of edited MCA sarcoma cell lines. Interestingly, IL-17D mRNA expression can be found in skeletal muscle and can stimulate human umbilical vein endothelial cells to produce IL-6, IL-8, and GM-CSF (38). However, there have been no studies addressing the expression or function of IL-17D in cancer or any other disease system. We document that IL-17D can recruit NK cells via the induction of MCP-1, leading to the accumulation of M1 macrophages and priming of adaptive immune responses.

RESULTS

CHAPTER 1: CANCER IMMUNOEDITING BY THE INNATE IMMUNE SYSTEM

MCA-induced sarcoma incidence is increased in RAG2$^{-/-}$x γc$^{-/-}$ mice compared to syngeneic RAG2$^{-/-}$ and WT mice.

To determine whether the innate immune system of RAG2$^{-/-}$ mice was capable of tumor immunosurveillance, we compared the incidence of MCA-induced sarcomas in immunologically intact WT C57BL/6 mice to that of C57BL/6 mice with defects in either adaptive immunity only (RAG2$^{-/-}$ mice) or in both adaptive and innate immunity (RAG2$^{-/-}$x γc$^{-/-}$ mice). Figure 1.1 shows that the incidence of sarcomas was higher in RAG2$^{-/-}$x γc$^{-/-}$ mice compared to RAG2$^{-/-}$ mice at all doses tested. In addition, at MCA doses of 25 μg or 100 μg, RAG2$^{-/-}$x γc$^{-/-}$ mice developed sarcomas slightly faster than RAG2$^{-/-}$ mice, indicating that the innate immune system in RAG2$^{-/-}$ mice controlled MCA-induced tumor outgrowth to some extent.

Growth of MCA-induced sarcoma cell lines derived from RAG2$^{-/-}$ x γc$^{-/-}$ mice is inhibited when transplanted into syngeneic WT mice.

To study tumor editing, low passage cell lines were derived from primary MCA tumor masses generated in C57BL/6 WT, RAG2$^{-/-}$, and RAG2$^{-/-}$x γc$^{-/-}$ mice, and the

immunogenicity of each cell line was assessed by transplanting them into naïve WT syngeneic mice and monitoring their growth (reviewed in 5). As described previously (1) , we observed two divergent growth phenotypes among the transplanted sarcomas: a regressor phenotype, defined by a failure to form a mass of >9 mm in diameter in more than 50% of transplantations into syngeneic WT mice, and a progressor phenotype, defined by the formation of masses >9 mm in more than 50% of transplantations into WT mice. When we examined groups of MCA-induced sarcoma cell lines generated from WT, $RAG2^{-/-}$, and $RAG2^{-/-}$x $\gamma c^{-/-}$ mice, we found that the proportion of regressor MCA-induced sarcoma cell lines was 0/9 WT, 3/10 $RAG2^{-/-}$, and 6/10 $RAG2^{-/-}$x $gc^{-/-}$ (Fig. 1.2 A, right panels). All cell lines grew when transplanted into $RAG2^{-/-}$ mice (Fig. 1.2 A, left panels), indicating that their rejection was due to the adaptive immune system and was not simply a failure to grow in vivo.

To determine the overall immunogenicity of each group of tumors, we examined the tumor-free survival of large cohorts of WT and $RAG2^{-/-}$ mice challenged with panels of tumor cell lines derived from WT, $RAG^{-/-}$, or $RAG2^{-/-}$x $\gamma c^{-/-}$ mice (Fig. 1.2 B). All MCA-induced sarcoma cell lines formed tumors in $RAG2^{-/-}$ mice by 36 days post-tumor cell transplant (data not shown). In contrast, the kinetics and frequency of tumor formation in WT recipients was dependent upon the level of immune function of the original source from which the tumor cells were derived. Specifically, when 17 tumor cell lines derived from $RAG2^{-/-}$x $\gamma c^{-/-}$ mice were transplanted into a total of 132 naïve, syngeneic WT mice, only 46% of the mice formed tumors by 70 days post-transplant (Fig. 1.2 B, $p < 0.001$ for all comparisons). Over a similar time course, MCA-induced sarcoma cell lines from 15 $RAG2^{-/-}$ and 9 WT mice formed tumors in 64% and 97% of

WT recipients, respectively. These results were reproduced in an independent MCA induction experiment, and the combined results of these two experiments, encompassing 71 total MCA-induced sarcoma cell lines transplanted into 474 WT mice, 94 $RAG2^{-/-}$ mice, or 51 $RAG2^{-/-}$x $\gamma c^{-/-}$ mice, are shown in Table 1. Altogether, these results support the hypothesis that tumors from mice with greater immunodeficiency undergo decreased levels of immunoediting.

Tumor cell lines generated in $RAG2^{-/-}$x $\gamma c^{-/-}$ mice show an increased regressor frequency compared to cell lines from WT and $RAG2^{-/-}$ mice.

Previous work has shown that the percentage of regressors within a group of MCA-induced sarcoma cell lines, the "regressor frequency" was 40% when the MCA-induced sarcoma cell lines were generated in $RAG2^{-/-}$ mice and 0% when the cell lines were generated in WT mice (1). These percentages are remarkably reproducible and have remained so even when experiments have been conducted in our three independent laboratories in La Jolla, St. Louis, and Melbourne (Fig. 1.3). Specifically, we found a consistent regressor frequency of 0% when MCA-induced sarcoma cell lines are generated in WT mice (50 cell lines from two strains and four independent experiments). Notably, MCA-induced sarcoma cell lines derived from $RAG2^{-/-}$ mice displayed a 30-44% regressor frequency (82 cell lines from three strains and four independent experiments). MCA-induced sarcoma cell lines derived from $RAG2^{-/-}$ x $\gamma c^{-/-}$ mice had the highest regressor frequency (60-70%), indicating that as a group, these cell lines were the most immunogenic and least edited.

RAG2$^{-/-}$x γc$^{-/-}$ regressors undergo editing when transplanted into RAG2$^{-/-}$ mice.

Since regressor cell lines generated from RAG2$^{-/-}$x γc$^{-/-}$ mice displayed the highest levels of immunogenicity and, subsequently, the lowest levels of immunoediting compared to RAG2$^{-/-}$ and WT mice, we hypothesized that the innate immune system of RAG2$^{-/-}$ mice could edit these tumor cell lines in vivo. We tested this by transplanting two independent sarcoma cell lines generated from RAG2$^{-/-}$x γc$^{-/-}$ mice into either RAG2$^{-/-}$ or RAG2$^{-/-}$x γc$^{-/-}$ mice. To determine if in vivo passaging altered the immunogenicity of these cell lines, tumor masses were harvested at day 25 and converted into cell lines. When these cell lines were transplanted into WT mice, 88% of RAG2$^{-/-}$-passaged tumor cell lines formed progressively growing tumor masses by day 40 compared to 46% of RAG2$^{-/-}$x γc$^{-/-}$-passaged and 10% of unpassaged cell lines (Fig. 1.4 A, $p = 0.025$). These results suggest a higher level of editing by the innate immune system in RAG2$^{-/-}$ versus RAG2$^{-/-}$x γc$^{-/-}$ mice but also indicate that there is some level of measurable tumor sculpting in RAG2$^{-/-}$x γc$^{-/-}$ mice, which could be due to residual immune function or a non-immunologic editing process.

NK cells do not preferentially kill regressor versus progressor tumor cells.

Having shown that γc is important for the ability of innate immunity to control and edit MCA-induced sarcomas, we predicted that NK cells, dependent upon γc for development (39), would participate in this editing process in vivo. To explore whether NK cells preferentially recognize regressors over progressors, we performed standard

chromium release cytotoxicity assays (40) and also examined the NK cell content in regressor versus progressor tumors. We found that the overall susceptibility to NK cell killing of 10 MCA-induced sarcoma cell lines from RAG2$^{-/-}$x γc$^{-/-}$ mice did not differ from that of 10 MCA-induced sarcoma cell lines from RAG2$^{-/-}$, or 9 MCA-induced sarcomas from WT mice (Fig. 1.4 B). Even when all tumors were grouped based on phenotypic growth in WT mice – grouped into progressors or regressors – we observed no difference in NK cell-specific lysis (Fig. 1.4 B). Additionally, we did not detect a difference in NK1.1^{+} cell infiltration (approximately 5%) into any of the MCA-induced sarcomas after they were transplanted into RAG2$^{-/-}$ mice (Fig. 1.4 C).

MHC class II positive macrophages are selectively present in regressor tumors during immunoediting.

We therefore re-directed our focus on myeloid cells as they represent the major hematopoietic lineage cell type that infiltrates either rejecting or progressively growing tumors (19). To examine this issue, two RAG2$^{-/-}$x γc$^{-/-}$ regressor cell lines were transplanted into either RAG2$^{-/-}$ or RAG2$^{-/-}$x γc$^{-/-}$ hosts, and tumors were harvested at day 15 and analyzed by immunohistochemistry to assess the number and phenotypes of infiltrating myeloid cells. No differences were detected in the total number of CD68^{+} macrophages infiltrating tumors growing in either RAG2$^{-/-}$ or RAG2$^{-/-}$x γc$^{-/-}$ hosts (Fig. 1.5 B, right panels). In contrast, we observed significantly higher numbers of MHC class II positive cells in tumors growing in RAG2$^{-/-}$ versus RAG2$^{-/-}$ x γc$^{-/-}$ hosts (Fig. 1.5 A, B, $p = 0.00156, 0.0071$). A similar preferential accumulation of MHC class II positive cells

was also observed in unedited versus edited tumors growing in RAG2$^{-/-}$ mice (Fig. 1.5 C,D,E).

Editing of regressor tumor cells from RAG2$^{-/-}$x yc$^{-/-}$ mice and induction of MHC class II on tumor infiltrating cells requires NK cells and IFNγ production in vivo.

Since γc was important for editing, but NK cell-dependent tumor cell killing was not, we hypothesized that NK cell-derived IFNγ was critical for the editing process we observed in RAG2$^{-/-}$ mice. We therefore transplanted a regressor cell line derived from a RAG2$^{-/-}$x γc$^{-/-}$ mouse into RAG2$^{-/-}$ recipients treated either with the neutralizing H22 IFNγ-specific monoclonal antibody (mAb), a NK1.1 specific monoclonal antibody (PK136), or a control mAb (PIP). Tumors were harvested at day 20 and converted into cell lines, which were subsequently transplanted into naïve, syngeneic WT hosts to measure tumor free survival. We observed a statistically significant increase in the survival of WT mice transplanted with MCA-induced sarcomas that had been passaged through NK cell depleted and IFNγ-neutralized mice versus control mice (Fig. 1.6 A,B $p = 0.0042, 0.0016$), indicating that NK cells and IFNγ plays a critical role in activating the editing capacity of the innate immune system in RAG2$^{-/-}$ mice. Analysis of tumor cross sections by immunohistochemistry at day 20 showed MHC class II positive macrophages were significantly reduced with anti-IFNγ treatment (Fig. 1.6 C,D, $p = 0.0432$), even though total macrophage infiltration did not differ between hosts as determined by CD68^{+} events (Fig. 1.6 D). These results demonstrate that NK cells and IFNγ may facilitate editing by activating macrophages.

Tumor-associated macrophages (TAMs) from regressor tumors display an M1 phenotype and require NK cells and IFNγ for polarization in vivo.

Since the MHC class II^+ macrophages required IFNγ for their accumulation, we hypothesized that these macrophages were classically activated (21) M1 macrophages and next performed immunophenotyping to detect the presence of tumor associated M1 or M2 macrophages, known to have anti- or pro-tumor functions, respectively (19,20). For this purpose, we used a combination of IHC and FACS analysis combined with defining cytokine production in freshly harvested tumors. In all cases, we analyzed no fewer than three tumors across at least two experiments. We first performed IHC analysis for the M2-type macrophage marker CD206 and compared the staining pattern to that of MHC class II (known to be upregulated on M1 macrophages versus M2 macrophages) (Fig. 1.7 A). We found that regressor tumors harvested from $RAG2^{-/-}$ mice had the highest percentage of class II high events (29%) and lowest percentage of $CD206^+$ events (33%). In contrast, tumors harvested from both $RAG2^{-/-}$ mice depleted of IFNγ or $RAG2^{-/-}$x $\gamma c^{-/-}$ mice had significantly lower percentages of class II events (12% and 10%, respectively) and significantly higher percentages of $CD206^+$ events (60% and 70%, respectively) (Fig. 1.7 A). Thus, IHC analysis suggested that M1-phenotype macrophage accumulation within tumors requires both IFNγ and γc. We next used FACS analysis to gate on TAM subsets using combinations of CD11b, Ly6C, and MHC class II to differentiate between M1 and M2 macrophages (Fig. 1.7 C) as previously described (41). This gating strategy identified M1 macrophages as MHC class II^{hi}, $Ly6C^{lo}$, $CD206^{lo}$,

F4/80^{hi} cells and M2 macrophages as MHC class II^{lo}, Ly6C^{lo}, CD206^{hi}, F4/80^{hi} cells (Fig. 1.7 C, D). This analysis showed that regressor tumors contained significantly higher percentages of M1 macrophages when isolated from RAG2$^{-/-}$ mice treated with control mAb PIP (56%) compared to either RAG2$^{-/-}$ mice treated with anti-NK1.1 mAb (28%), neutralizing IFNg mAb (37%), or RAG2$^{-/-}$ x γc$^{-/-}$ (20%) mice (Fig. 1.7 B, top panel, $p < 0.0001$ for all populations). Conversely, M2 macrophage percentages were slightly increased in tumors isolated from RAG2$^{-/-}$ mice treated with anti-IFNγ (36%) and RAG2$^{-/-}$x γc$^{-/-}$ mice (37%), but not anti-NK1.1 treated mice (27%) compared to control RAG2$^{-/-}$ mice (28%) (Fig. 1.7 B, bottom panel, $p = 0.0007$, 0.002 respectively), confirming our IHC results. Tumor cell suspensions isolated from the different groups of mice did not show differences in total numbers of CD45^{+} or CD11b^{+} cells (data not shown), thus ruling out the possibility that the differences observed in TAM subsets were due to differential recruitment of immune cells in mice lacking either IFNy or γc function.

To test a functional marker of TAM polarization, we examined supernatant of matched tumor cell suspensions cultured in vitro. Cell suspensions from tumors growing in control RAG2$^{-/-}$ mice contained high levels of IL-1a and IFNγ and produced levels of IL-6 and TNF that were similar to bone marrow-derived macrophages stimulated with LPS and IFNγ, indicative of a classically activated M1 macrophage cytokine profile. In contrast, cell suspensions derived from tumors derived from anti-IFNγ-treated RAG2$^{-/-}$ mice and RAG2$^{-/-}$ x γc$^{-/-}$ mice produced significantly lower levels of each cytokine (Fig. 1.7 E, $p < 0.0001$ for all comparisons). We did not detect IL-10 or IL-4 production in any of the cultures, indicating that the M2 TAMs are not identical to alternatively activated M2 macrophages found in certain infections. No cytokine production was observed in

cultures of the tumor cell line alone (data not shown). These results demonstrates that the cytokines that were detected in the cell suspensions derived from in vivo growing tumors can be attributed to the immune subsets that infiltrate the tumor. To further characterize TAM subsets in our midel we sorted M1 and M2 macrophages from regressor tumor cell suspensions derived from RAG2-/- hosts to confirm their differentiation by qPCR. Sorted M1 TAMs contained higher transcript levels of classically activated macrophage genes TNf-a and iNOS, while containing less M2 specific genes arginase, eCAD, and GAS3 (Fig. 1.7F).

Polarization of M1 macrophages in vivo by administration of a CD40 agonist induces editing in RAG2$^{-/-}$x γc$^{-/-}$ mice.

CD40 agonist administration in vivo has been shown to have anti-tumor properties (42, 43) by activating TAMs to become tumoristatic through production of nitric oxide (NO) (44). We hypothesized that CD40 agonist treatment would activate macrophages in tumors growing in RAG2$^{-/-}$x γc$^{-/-}$ mice, thereby leading to editing of cancer cells in vivo. In order to test this, a regressor cell line was transplanted into RAG2$^{-/-}$x γc$^{-/-}$ mice receiving a single injection of either control IgG or anti-CD40 agonist monoclonal antibodies, tumor masses were harvested, and cell lines were generated and transplanted into WT mice. We found that cell lines from CD40 agonist treated RAG2$^{-/-}$x γc$^{-/-}$ mice formed tumor masses in 100% of WT recipients, whereas cell lines from isotype-treated RAG2$^{-/-}$x γc$^{-/-}$mice formed tumors in 33% of WT recipients in RAG2$^{-/-}$x γc$^{-/-}$ mice (Fig. 1.8 A, $p = 0.0009$). We then analyzed the quantity of M1 macrophages in

harvested tumor cell suspensions and found that M1 macrophage percentages were doubled in mice treated with CD40 agonist (36%) compared to control treatment (18%) (Fig. 1.8 B, upper panel, $p = 0.0003$). Correspondingly, M2 macrophages were decreased (23% vs 15%) by anti-CD40 agonist treatment (Fig. 1.8 B, lower panel, $p=0.0151$). These results suggest that TAMs can be activated in $RAG2^{-/-}x\ \gamma c^{-/-}$ mice to effectively edit tumors in vivo.

Chapter 1, in full, is an adapted version that has been submitted for publication of the material as it may appear in The Journal of Experimental Medicine, 2012, Saddawi-Konefka, Robert; Smyth Mark J.; Schreiber, Robert D.; Bui, Jack D.; The Rockefeller University Press. The disseration author was the primary co-author of this paper.

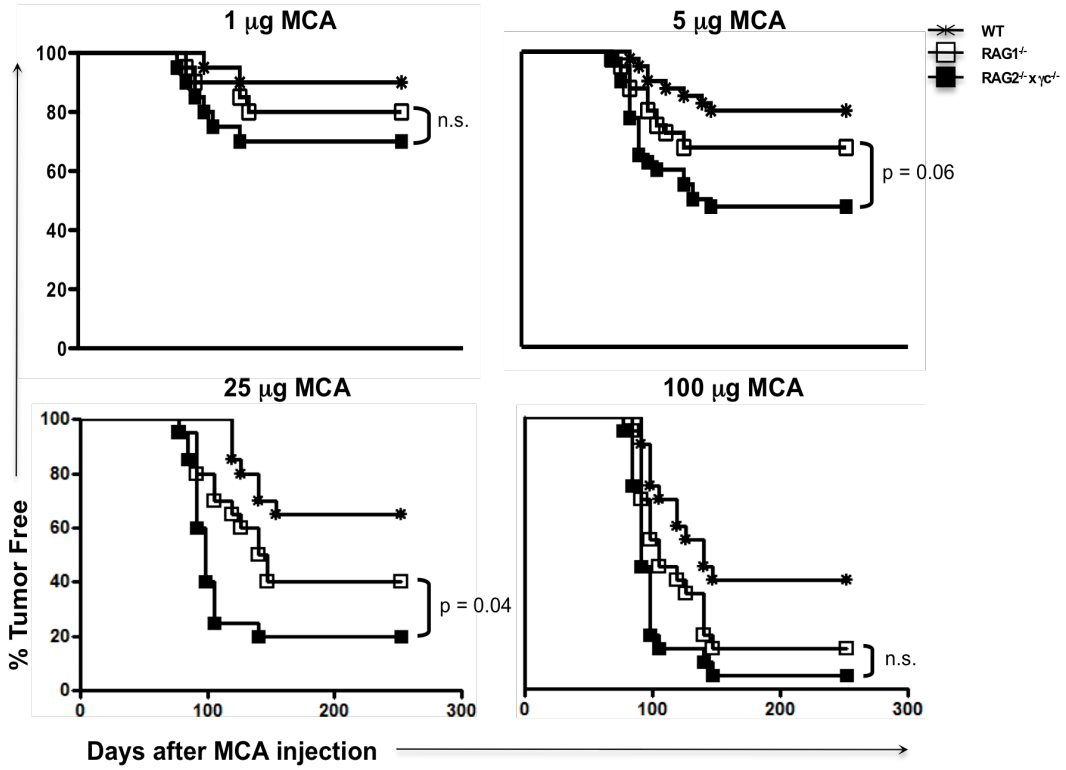

Figure 1.1 RAG2$^{-/-}$x γc$^{-/-}$ mice are more susceptible to MCA-induced sarcomas than syngeneic RAG2$^{-/-}$ and WT mice. The indicated dose of MCA was injected into the subcutaneous space of mice, and sarcoma formation was monitored over time. All cohorts consisted of 20 mice. Tumor positive mice were defined as those that harbored a progressively growing mass ≥ 25 mm^2. Similar results were found in a repeat experiment that included the 5 and 25 mg doses.

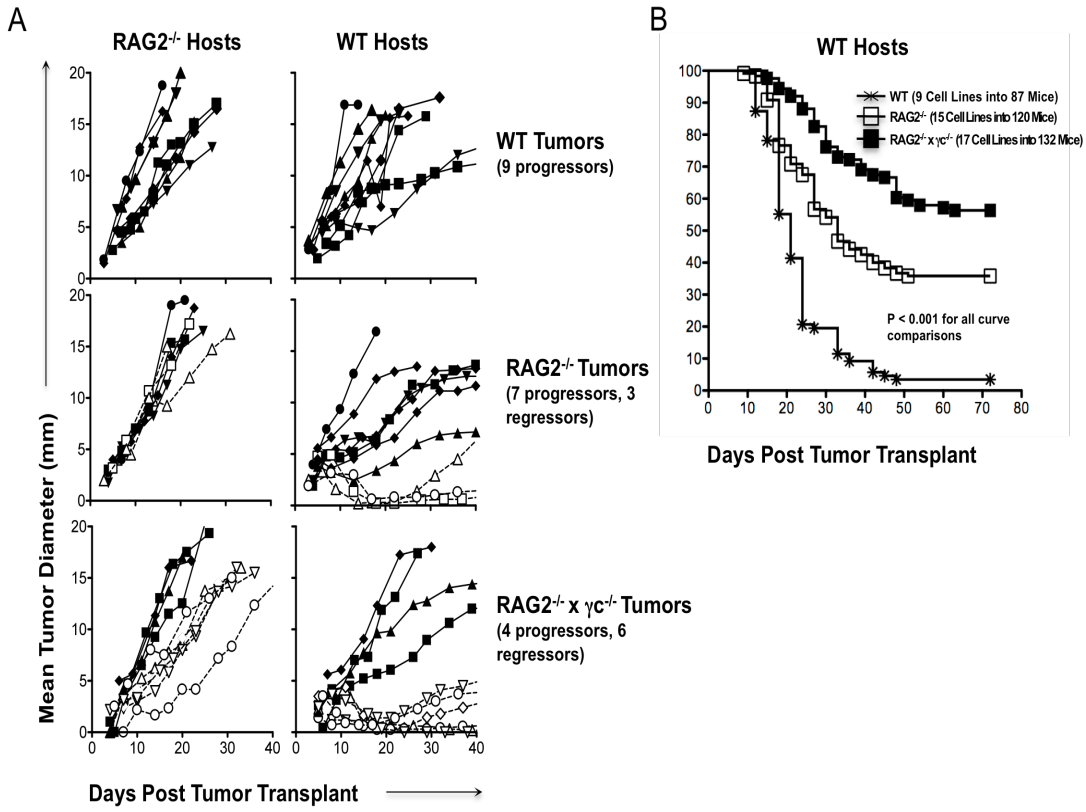

Figure 1.2 A majority of MCA-induced sarcoma cell lines derived from RAG2$^{-/-}$ x γc$^{-/-}$ mice cannot form tumors when transplanted into syngeneic WT mice. MCA-induced sarcoma cell lines were derived from tumors generated in syngeneic C57BL/6-strain WT, RAG2$^{-/-}$, and RAG2$^{-/-}$ x γc$^{-/-}$ mice. These cell lines were transplanted into syngeneic RAG2$^{-/-}$ ($n \geq 2$ for each cell line) or WT ($n \geq 5$ for each cell line) hosts, and tumor growth was measured over time. (A) The average growth for each cell line is shown (open symbols = regressor cell lines; closed symbols = progressor cell lines). (B) The percentage of WT mice that developed tumors is shown for group of cell lines. Tumor free mice were defined to have a non-enlarging mass < 9 mm in average diameter. The number of cell lines and mice are indicated in the figure.

Table 1.1 A summary of 2 independent MCA induction immunoediting experiments. A total of 71 MCA sarcoma cell lines were generated from the indicated mice and then transplanted into 474 WT, $RAG^{-/-}$, or $RAG2^{-/-}$x $gc^{-/-}$ mice, and tumor growth was monitored. Regressor frequencies from these experiments (1 & 2) are shown in Figure 1.3.

Tumor group	Growth in WT	Growth in RAG$^{-/-}$	Growth in RAG$^{-/-}$xγc$^{-/-}$
9 WT tumors into 87 WT or 22 RAG hosts (exp 1)	97% (84/87)	100% (22/22)	N.D.
15 RAG tumors into 120 WT or 7 into 15 RAG hosts (exp 1)	64% (77/120)	100% (15/15)	N.D.
17 RAGxγc tumors into 132 WT or 10 into 27 RAG hosts (exp 1)	46% (61/132)	100% (27/27)	N.D.
10 WT tumors into 35 WT or 21 RAGxγc hosts(exp 2)	100% (35/35)	N.D.	100% (21/21)
10 RAG tumors into 50 WT or 30 RAG hosts (exp 2)	60% (30/50)	100% (30/30)	N.D.
10 RAGxγc tumors into 50 WT or 30 RAGxγc hosts (exp 2)	30% (15/50)	N.D.	100% (30/30)

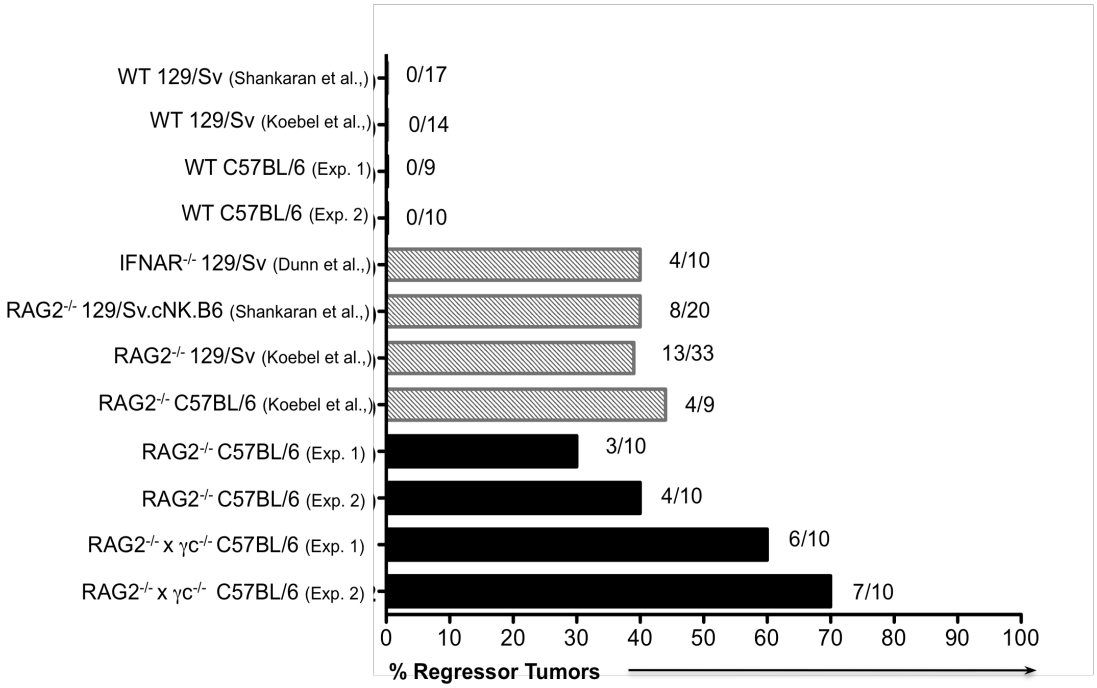

Figure 1.3 The frequency of regressor cell lines is greater from tumors generated in RAG2$^{-/-}$ x γc$^{-/-}$ mice compared to WT and other immune deficient mice. A summary of two MCA-induction experiments performed in this manuscript is plotted in the context of previous MCA-induction experiments. Previously published experiments are included for comparison purposes and are from references(Shankaran et al., 2001; Koebel et al., 2007; Dunn et al., 2005). Absolute numbers of regressors/total number of cell lines tested is shown next to the bar for each experiment.

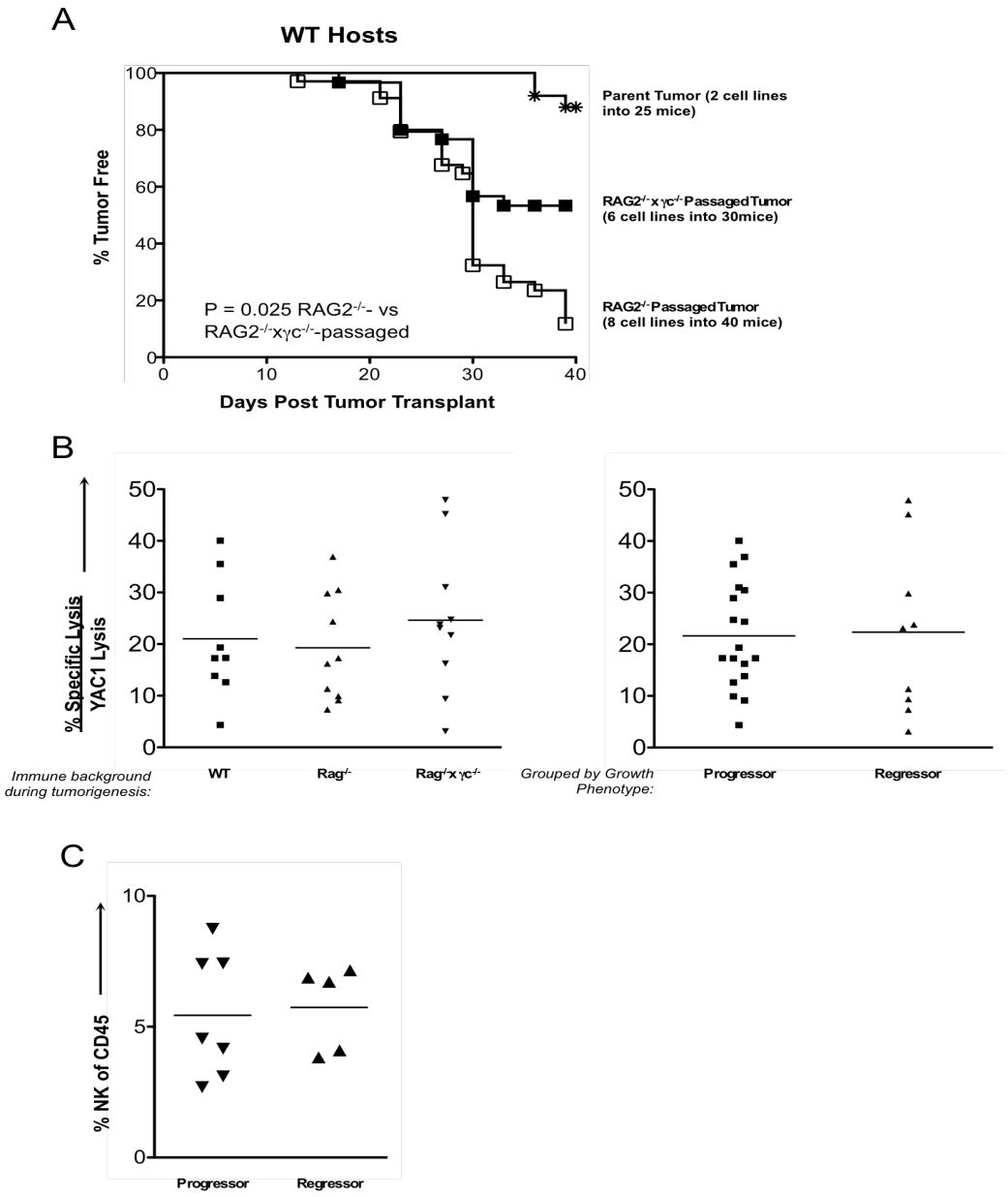

Figure 1.4 RAG2$^{-/-}$ x γc$^{-/-}$ regressors are edited when transplanted into RAG2$^{-/-}$ mice, but are not specifically recognized by NK cells. Two independent MCA-induced sarcoma cell lines generated from RAG2$^{-/-}$ x γc$^{-/-}$ mice were transplanted into syngeneic RAG2$^{-/-}$ x γc$^{-/-}$ or RAG2$^{-/-}$ mice, and tumor masses were harvested at day 25 and converted into "passaged" daughter cell lines, which were transplanted into syngeneic WT mice (number of cell lines and mice are shown in the figure), and (A) the percentage of WT mice that remained tumor free is shown for each group of cell lines. Tumor free mice were defined to have a non-enlarging mass < 9 mm in average diameter by day 40. (B) MCA sarcoma cell lines were cultured with IL-2 activated NK cells in a 5-hour chromium release cytotoxicity assay and specific lysis normalized to YAC-1 specific lysis is plotted for each cell line based on (A) immune background and phenotype. (C) Regressor and progressor cell lines were transplanted into RAG-deficient mice and analyzed for NK cells.

Figure 1.5 MHC class II macrophages preferentially infiltrate in unedited regressors. (A) Representative images of tumor sections from RAG2$^{-/-}$ or RAG2$^{-/-}$ x $\gamma c^{-/-}$ hosts stained for MHC class II. (B) Quantification of MHC class II+ events and CD68+ events in tumor sections is shown. (HPF = high power field at 200x magnification). Regressor and progressor cell lines were transplanted into RAG2-deficient mice and analyzed for (C, D, E) activated MHC class II+ macrophages. (C) Representative FACS plots of 3 regressor and 3 progressor tumors are shown. Cells were gated on a CD45^{+}PI^{-} population. (D) Percentages of activated monocyte-lineage (F4/80^{+}) cell populations are shown for regressor and progressor tumor masses. Each symbol represents a different tumor cell line transplanted into 1-3 RAG2$^{-/-}$ mice. (E) Frozen tumor cross sections of progressor and regressor tumor masses growing in RAG2$^{-/-}$ mice were stained with anti-I-A/I-E (MHC class II). Nuclei were counterstained with hematoxylin. Scale bar = 100 microns. **$p < 0.01$. Error bars are represented by $\pm$ SEM. IHC results were reproduced at least once.

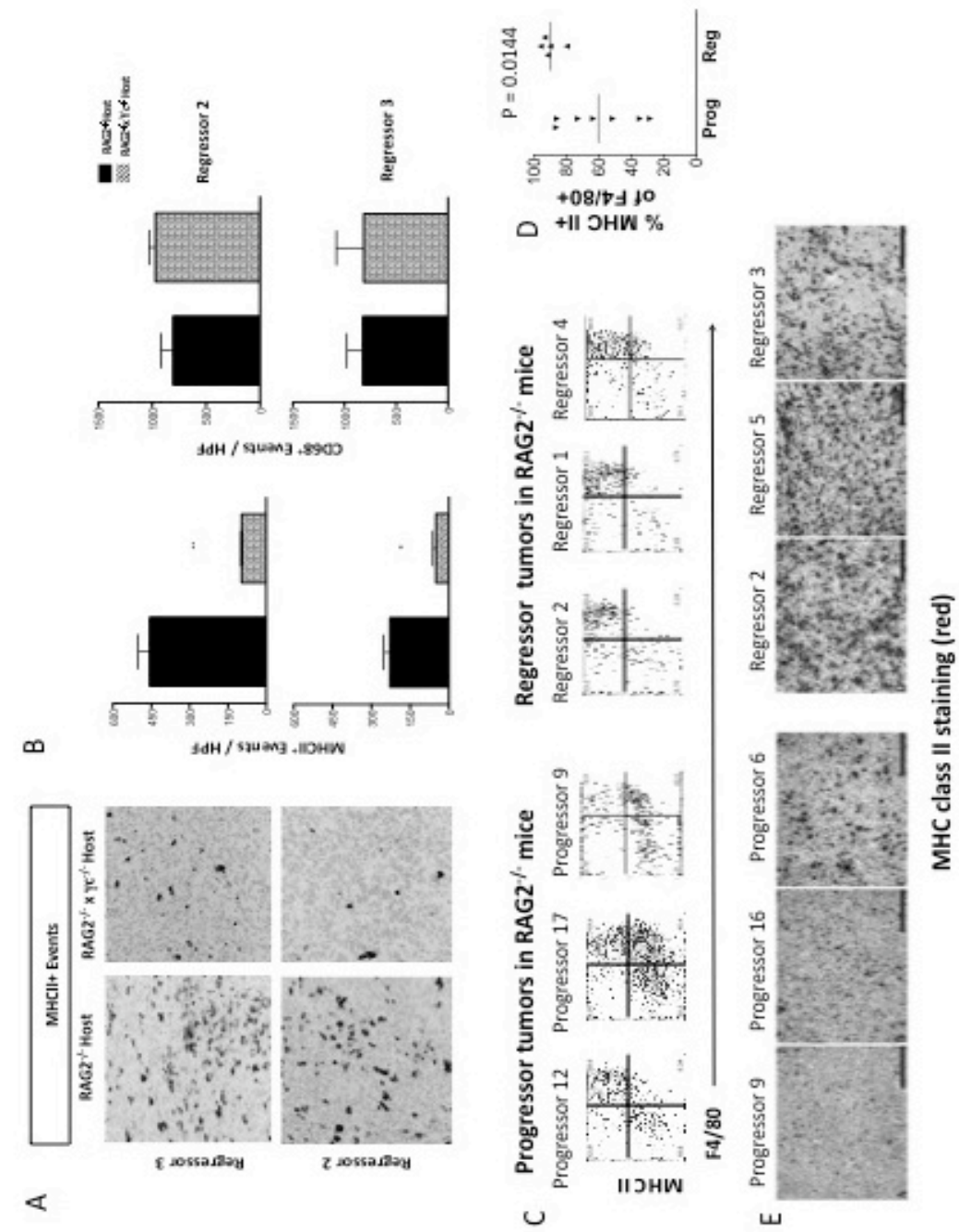
A
MHCII+ Events
RAG2-/- Host
RAG2-/- x γc-/- Host
Regressor 3
Regressor 2
B
MHCII+ Events / HPF
CD68+ Events / HPF
Regressor 2
Regressor 3
C
Progressor tumors in RAG2-/- mice
Progressor 12
Progressor 17
Progressor 9
MHC II
F4/80
Regressor tumors in RAG2-/- mice
Regressor 2
Regressor 1
Regressor 4
D
P = 0.0144
% MHC II+ of F4/80+
Prog
Reg
E
Progressor 9
Progressor 16
Progressor 6
Regressor 2
Regressor 5
Regressor 3
MHC class II staining (red)

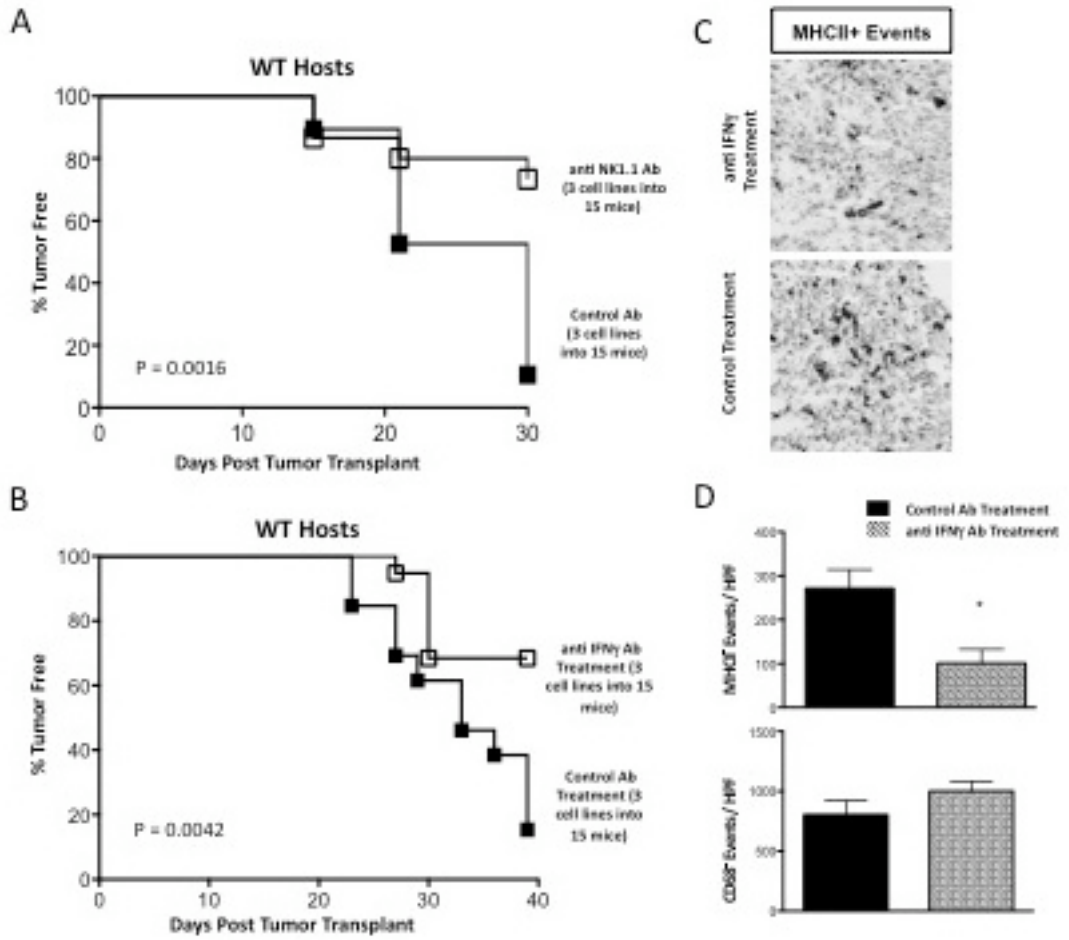

Figure 1.6 NK cells and IFN-g are necessary for innate editing of a regressor tumor and M1 macrophage accumulation. Regressor cell line 2 was transplanted into $RAG2^{-/-}$ mice treated with anti-NK1.1, IFN-g blocking antibody or control antibody, tumor growth was measured, and passaged cell lines were generated. (A,B) The passaged cell lines were then transplanted into syngeneic WT hosts (number of cell lines and mice are indicated in the figure) and tumor free survival was measured. Tumor free mice were defined to have a non-enlarging mass < 9 mm in average diameter by day 40. (C) Tumor sections from $RAG2^{-/-}$ hosts were stained for MHC class II and (D) quantitated. (HPF = high power field at 200x magnification). *$p < 0.05$. Error bars are represented by $\pm$ SEM. Results were reproduced at least once.

Figure 1.7 NK cells and IFNy are required to polarize tumor associated macrophages towards an M1-type phenotype. Regressor cell line 2 was transplanted into syngeneic $RAG2^{-/-}$ mice (injected with either isotype control, anti-NK1.1, or anti-IFNg monoclonal antibodies) or $RAG2^{-/-}$x $gc^{-/-}$ mice. Tumor masses were harvested 15 days after transplantation, disaggregated into single cell suspensions, and (A) analyzed by immunohistochemistry or (B, C) flow cytometry to measure the percentage of M1 and M2 macrophages as defined by MHC class II and CD206 expression of $CD68^{+}$ events per HPF (for IHC) or MHC class II and Ly6C expression in $CD11b^{+}$ populations (for FACS), respectively. (C, D) An example of the flow cytometry gating to quantitate M1 and M2 macrophages. M1 macrophages are 7AAD-, CD45+, Ly $6C^{lo}$, MHC class II^{hi}, F4/80+, $CD206^{lo}$ cells. M2 macrophages are 7AAD-, CD45+, $Ly6C^{lo}$, MHC $classII^{lo}$, F4/80+, $CD206^{hi}$ cells. (E) Cultured supernatant from single cell suspensions were assessed for production of the indicated cytokines after 24 hours of culture. (HPF = high power field at 200x magnification). $*p < 0.05$, $**p < 0.01$, $***p < 0.001$. Error bars are represented by $\pm$ SEM. Each symbol represents a different mouse. Results were reproduced at least once.

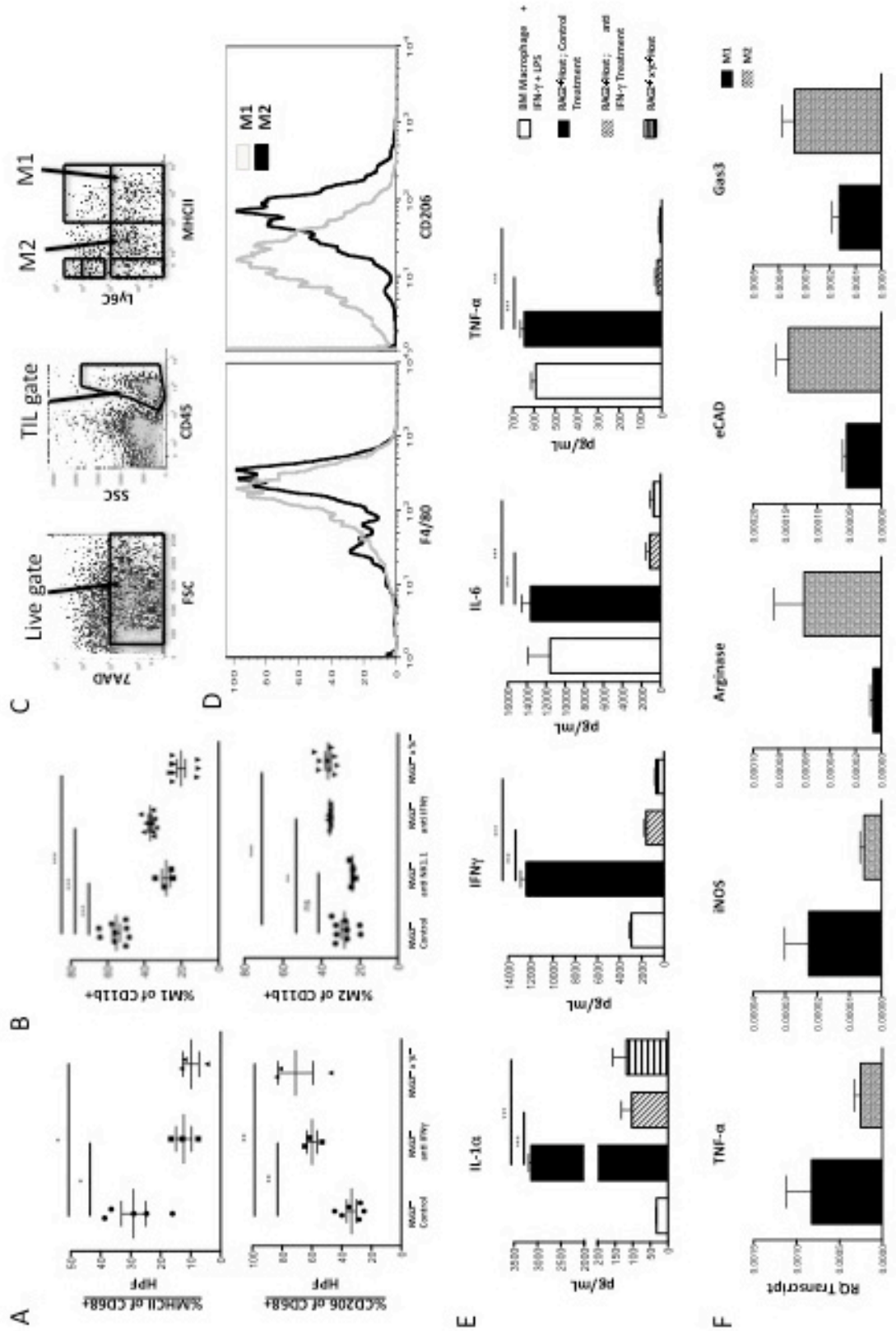
A
B
C
D
E
F
Live gate
TIL gate
M1
M2
7AAD
FSC
SSC
CD45
Ly6C
MHCII
F4/80
CD206
%MHCII of CD68+ HPF
%CD206 of CD68+ HPF
%M1 of CD11b+
%M2 of CD11b+
Wasf Control
Wasf anti NK1.1
Wasf anti IFNγ
Wasf anti IL6
Wasf -/-
IL-1α
IFNγ
IL-6
TNF-α
pg/mL
BM Macrophage + IFN-γ + LPS
Rac2-/-fos ; Control Treatment
Rac2-/-fos ; anti IFN-γ Treatment
Rac2-/-γ-/-fos
TNF-α
iNOS
Arginase
eCAD
Gas3
RQ Transcript

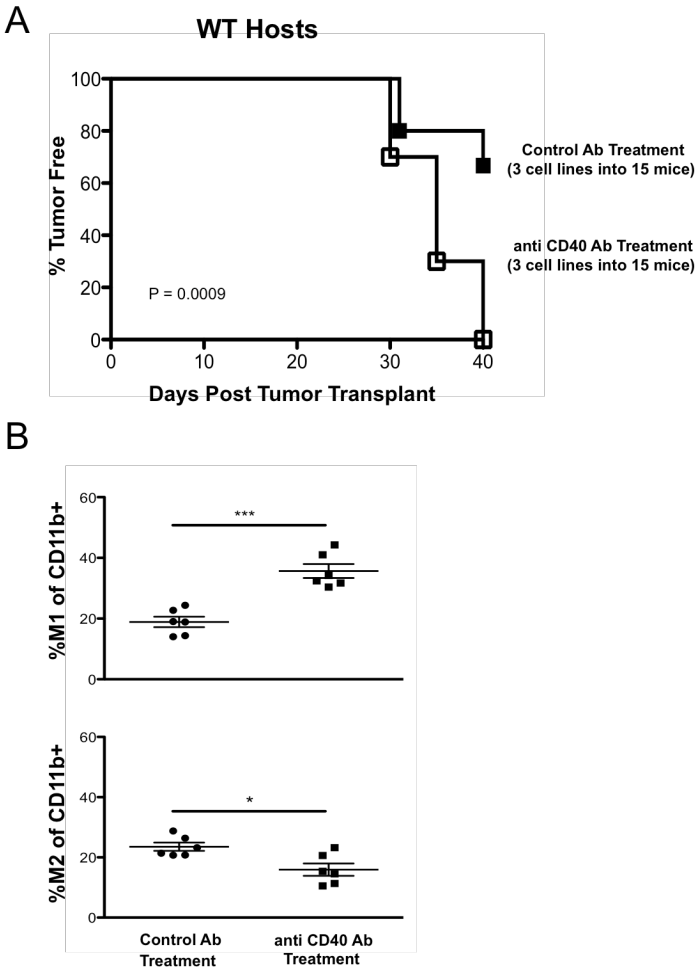

Figure 1.8 In vivo administration of CD40 agonist in RAG2$^{-/-}$x γc$^{-/-}$ mice induces effective immunoediting and intratumoral M1 macrophages. Regressor cell line 2 was transplanted into RAG2$^{-/-}$ x γc$^{-/-}$ mice receiving a single dose of either control rat IgG or anti-CD40 agonistic monoclonal antibodies on day 5. Tumor growth was measured over time. (A) Tumor masses were converted into passaged daughter cell lines which were transplanted into syngeneic WT mice and assessed for tumor formation (number of cell lines and mice are indicated in the figure). Tumor free mice were defined to have a non-enlarging mass < 9 mm in average diameter by day 40. (B) At day 15 after transplantation, tumor masses were disaggregated into single cell suspensions and the percentage of M1 (top panel) and M2 (bottom panel) macrophages were quantified in CD11b^{+} events for each condition. *p < 0.05, ***p < 0.001. Error bars are represented by ± SEM. Each symbol represents a different mouse. Results were reproduced at least once.

CHAPTER 2: CANCER IMMUNOEDITING OF THE NKG2D LIGAND H60A

Unedited tumors display a wide range of NKG2D ligand expression.

Previous carcinogenesis studies comparing primary tumor formation in WT versus NKG2D-deficient mice found no significant difference in MCA sarcoma formation (25). However, these experiments were performed using mice on a C57BL/6 background, where H60a is not expressed (32, 45). Therefore, we measured NKG2D ligand expression in MCA sarcoma cell lines generated in WT mice and mice with varying levels of immune deficiency (1, 9), all on a 129/Sv background, which display an intact H60a gene (46). Figure 2.1 shows NKG2D tetramer staining of 39 129/Sv-strain MCA sarcoma cell lines. We found that the range of NKG2D ligand expression was highest in the MCA sarcomas that developed in the most immune deficient mice ($RAG2^{-/-}$ x$STAT1^{-/-}$, denoted as RkSk, or $STAT1^{-/-}$). MCA sarcomas from $RAG2^{-/-}$ mice displayed moderate heterogeneity of NKG2D ligand expression, whereas edited MCA sarcomas that developed in immunocompetent WT mice had tightly grouped levels of NKG2D ligand expression. Although the mean level of NKG2D ligand expression was similar between the groups, using the F test to compare variances, we found that there was significant difference in the variances of NKG2D ligand expression between WT and RkSk/$STAT1^{-/-}$ groups ($p=0.0079$), WT and $RAG2^{-/-}$ groups ($p=0.043$), but not between $RAG2^{-/-}$ and RkSk/$STAT1^{-/-}$ groups ($p=0.166$). We also calculated the Levene statistic to

test the homogeneity of variances between all groups, and found significant heterogeneity in NKG2D ligand expression ($p=0.007$).

Regressor cell lines display a higher level of heterogeneous NKG2D ligand expression than matched progressor cell lines.

Previously, we found that approximately 40% of unedited MCA sarcoma cell lines tested were rejected when transplanted into syngeneic, naïve WT mice, whereas 60% grew progressively (1, 9). The regressor and progressor phenotypes of these cell lines were reproducible and were only observed in tumor cell lines derived from immunodeficient mice (either $RAG2^{-/-}$ or $IFNAR^{-/-}$). Edited tumor cell lines from WT mice all displayed progressor phenotypes. We determined whether the tumor growth phenotype was correlated with the expression of NKG2D ligands, by examining unedited MCA sarcomas from $RAG2^{-/-}$ or $IFNAR^{-/-}$ mice that had already been categorized into regressor and progressor phenotypes (1, 9). We found that the heterogeneity in NKG2D ligand levels was associated with the regressor phenotype of unedited cells (Figs. 2.2 A-B). This difference in heterogeneity was significant when the variances of the populations were compared in the group of tumors (F test, $p=0.0024$; Levene statistic $p=0.001$) from $RAG2^{-/-}$ but not $IFNAR^{-/-}$ mice.

H60a expression correlates with the heterogeneity in NKG2D tetramer staining seen in unedited tumors.

We next examined whether the heterogeneous NKG2D tetramer staining could be explained by heterogenous expression of a specific NKG2D ligand. We found that our MCA sarcoma cell lines did not express MULT1 (32), so we focused on examining the expression of H60a and RAE1 using monoclonal antibodies. We found that H60a expression was highly variable in the groups of unedited tumors (Fig. 2.3 A). This mirrored our results with NKG2D tetramer staining. Interestingly, RAE1 expression, while lower than H60a expression, also displayed heterogeneity (Fig. 2.3 B). For both H60a and RAE1, there were significant differences in variance between the RAG progressor and RkSk/STAT1$^{-/-}$ groups ($p=0.0079$ for H60a, $p=0.0014$ for RAE1) and between RAG progressor and RAG regressor groups ($p=0.0087$ for H60a, $p=0.001$ for RAE1). The Levene statistic indicated that RAE had a slightly higher level of heterogeneity than H60a ($p=0.048$ for RAE variance; $p=0.075$ for H60a variance). Although the heterogeneity in expression of H60a and RAE1 was found in similar groups of tumors, most regressor tumors expressed H60a while few expressed RAE1. Therefore, we focused on H60a.

H60a staining was bimodal in many cell lines.

In examining the expression of H60a in our cell lines, we noticed that the staining of H60a in some MCA sarcoma cell lines did not display unimodal staining, as would be expected of a homogeneous population of cells. We have chosen nine representative regressor cell lines (Fig. 2.4 A) to demonstrate that the pattern of H60a staining ranged from unimodal (d27m2, F510, h31m1), broad staining (F515, d30m4), to bimodal staining, with equal distribution (F535, d100) between the two cell populations or uneven, "shoulder"-type distribution (d38m2, d42m1), suggesting that within a cell line, there were populations of cells that expressed differing levels of H60a. RAE1 did not display this pattern of staining, even though in some regressors (d30m4, d27m2), it was highly expressed.

Cell lines with bimodal expression of H60a lose H60a expression after in vivo passage.

We were struck by the fact that bimodal H60a, but not RAE1 expression could be seen in some cell lines (F535, d100) and wondered whether H60a high cells could be edited by components of the immune system in vivo. Since d100 and F535 are both regressor cell lines that reject in WT mice, we transplanted them into immune deficient mice in order to test if partial immune function could eliminate H60a-hi cells in vivo. We transplanted d100 (derived from an $IFNAR^{-/-}$ mouse) into $RAG2^{-/-}$ mice and F535 (derived from a $RAG2^{-/-}$ mouse) into $IFNAR^{-/-}$ mice. After in vivo growth for 20-30

days, we harvested the tumor mass and generated cell lines. Figure 2.5 shows that the passaged cell lines indeed had lower expression of H60a compared to the parental cell lines. Whereas 70% of parental d100 cells had high expression of H60a (as measured by NKG2D-tet), this was significantly reduced to 35% in the passaged cell lines (Fig. 2.5 A, C, $p<0.001$). Similarly, two of the three passaged F535 cell lines completely lost the H60a-hi population of cells and became unimodally low in H60a expression, while the third passaged cell line had decreased levels of H60a-hi cells (Fig. 2.5 B, D). The loss of H60a-hi cells seen after in vivo passage was not seen in the same cell line cultured in vitro for a similar period of time (data not shown), and therefore it is unlikely due to inherent differences in proliferation or cell cycle between H60a-hi and H60a-lo cells.

The regressor tumor d100 shows delayed growth in RAG2$^{-/-}$ mice and increased NK cell infiltration.

Next, we examined the cell types that could mediate the editing process that removed H60a-hi cells. We hypothesized NK cells would infiltrate and selectively destroy H60a-hi cells. Therefore, we transplanted d100 and a control progressor cell line F244 that expresses moderate levels of H60a (data not shown) into WT and RAG2$^{-/-}$ mice. As shown previously (1, 46), d100 was rejected, but F244 grew progressively in WT mice (Fig. 2.6 A). Interestingly, in RAG2$^{-/-}$ mice, the progressor F244 developed a tumor mass greater than 5 mm (mean diameter) within 10 days of transplant (Fig. 2.6 B) while the d100 tumor remained $\leq$3 mm for more than 2 weeks after tumor transplant. This delayed growth was associated with a preponderance of infiltrating NK cells in the

tumor mass. When both tumors were harvested at the same size (roughly 13 mm), 10% of the infiltrating CD45+ cells in the regressor d100 tumor were NK cells ($DX5^{+}CD122^{+}$) compared to 3% in the progressor F244 tumor ($p<0.001$) (Fig. 2.6 C).

Passage of the d100 regressor tumor through $RAG2^{-/-}$ mice leads to reduced NK cell recognition.

Next, we examined whether the NK cell infiltration and delayed growth of d100 in $RAG2^{-/-}$ mice led to a sculpted tumor repertoire that was resistant to NK cell cytotoxicity. We performed a standard chromium release assay using IL-2 activated NK cells as effectors and the parental or $RAG2^{-/-}$-passaged cell lines as targets. As predicted, we found that the passaged cell lines were two-fold less susceptible to NK cell killing compared to the parental cell line (Fig. 2.7, $p = 0.0216$).

Passage of the d100 regressor tumor through $RAG2^{-/-}$ mice converts it into a progressor tumor through NK cell NKG2D editing of H60a-hi cells.

Having shown that NK recognition was decreased in vitro in $RAG2^{-/-}$-passaged cell lines, we next determined whether $RAG2^{-/-}$-passaging of d100 in the presence or absence of NK cells or NKG2D activity had functional consequences on tumor growth in vivo. We transplanted d100 into $RAG2^{-/-}$ mice that had received either i.p. injections of PBS, anti-ASGM1 (to deplete NK cells), or a blocking anti-NKG2D monoclonal

antibody and monitored tumor growth in vivo. Depletion of NK cells with anti-ASGM1 showed a slight increase in tumor growth in RAG2$^{-/-}$ mice compared to control PBS treatment, while there was no change in growth when NKG2D function was blocked with anti-NKG2D (Fig 2.8 A top panel). When cell lines were generated from the tumors, we found that cells passaged in the presence of functional NK cells (PBS) showed a progressive growth phenotype in WT mice, while those passaged without NKG2D function or NK cells still retained their regressor phenotype (Fig. 2.8 A bottom panel). Moreover, daughter cell lines generated in mice treated with anti-ASGM1 or anti-NKG2D still maintained ~70% H60a-hi cells (Fig. 2.8 B, $p = 0.006$, 0.03, respectively, when compared to H60a expression in cell lines passaged through mice treated with PBS), suggesting that NK cell recognition of H60a-hi cells through NKG2D leads to their elimination during RAG2$^{-/-}$-passaging.

We tested NKG2D-dependent recognition by a standard chromium release assay using IL-2 activated NK cells as effectors and the parental d100 cell line as a target incubated with IgG or anti-NKG2D antibody. Targets incubated with anti-NKG2D antibody were lysed 5 times less than control IgG, indicating that NK cell recognition through NKG2D resulted in higher killing of the d100 parental cell line (Fig. 2.9, $p = 0.0102$).

Editing of H60a by NK cells and NKG2D is required for conversion to a progressor phenotype.

It is possible that H60a serves as a surrogate marker of an editing process and is not required for tumor rejection. To test this, we restored H60a expression in RAG2$^{-/-}$-passaged d100 cell lines that were now progressor tumors by transducing with a retrovirus expressing either green fluorescent protein (GFP), or both GFP and H60a. We restored H60a expression to the level that was originally on the parent cell line (Fig. 2.10). Figure 2.8 C shows that control GFP cell lines grew progressively, while those overexpressing H60a displayed delayed growth or a rejection phenotype in vivo, confirming that the reduction of H60a by NK cells and/or NKG2D is required for the conversion of a regressor into a progressor.

Chapter 2, in full, is an adapted version of the material as it appears in The Journal of Immunology, 2011, Schreiber, Robert D.; Bui, Jack D.; The American Association of Immunologists, Inc. The dissertation author was the primary author of this paper.

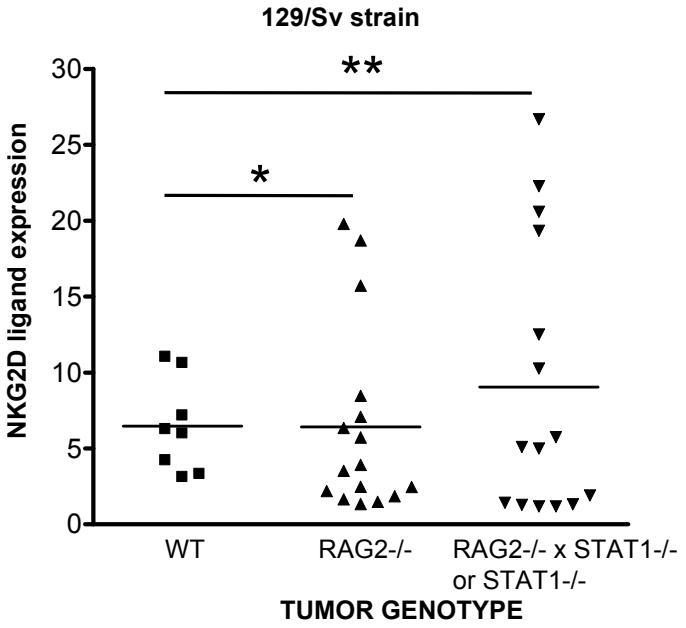

Figure 2.1 NKG2D ligand expression displays heterogeneous expression in unedited tumors. MCA sarcoma cell lines were generated in WT or immune deficient mice. Cell lines were stained with NKG2D tetramer to measure all NKG2D ligands. NKG2D ligand expression was calculated by dividing the median fluorescences of NKG2D tetramer staining and SA-PE control. Similar results were obtained when the median channel shift was calculated by subtracting the median fluorescences. Each symbol represents a different individual cell line. The F-test was used to measure significant differences in variances between groups. (* Indicates p value < 0.05, ** Indicates p value < 0.01).

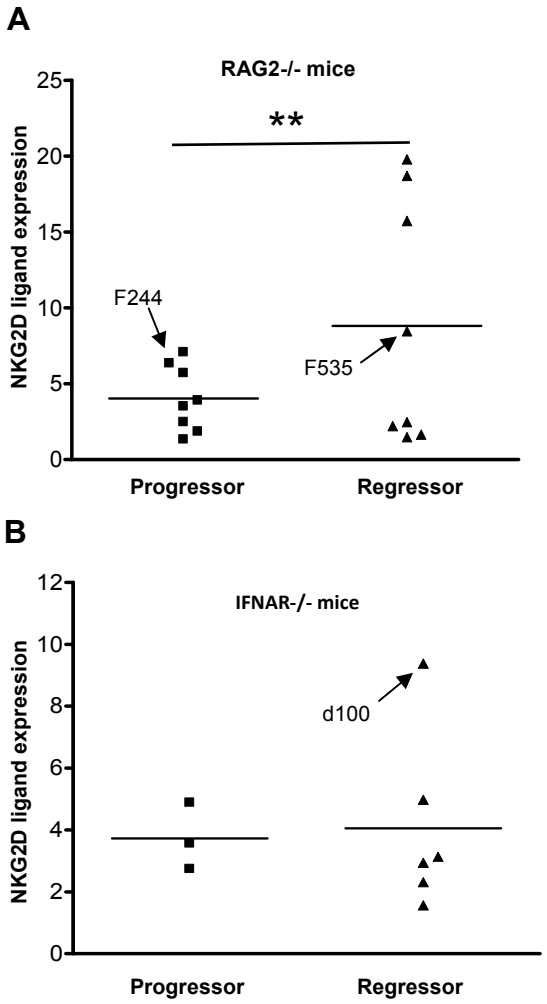

Figure 2.2 NKG2D ligand expression displays heterogeneous expression in regressor compared to progressor cell lines. MCA sarcoma cell lines derived from (A) 129/Sv RAG2-/- and (B) 129/Sv IFNAR-/- mice were categorized into progressor and regressor phenotypes, and NKG2D ligand expression was plotted similar to Figure 1. The F-test was used to measure significant differences in variances between groups. (** Indicates p value < 0.01). Several cell lines (F244, F535, d100) were chosen for later studies, and their data points are indicated in the bar graph for comparison.

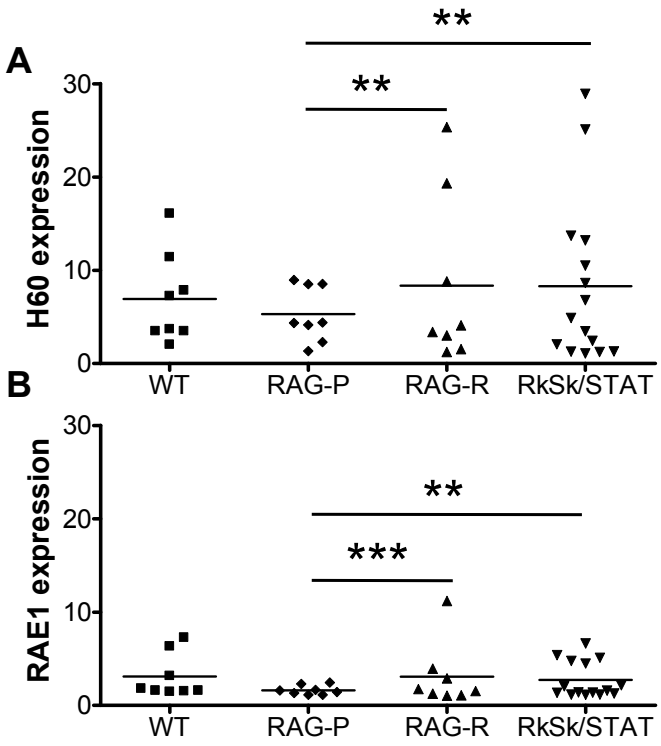

Figure 2.3 Heterogeneity in NKG2D ligand expression in 129/Sv strain tumors is seen in H60a but not RAE1 expression. H60a and RAE1 expression was determined in the indicated cell lines by flow cytometry using monoclonal antibodies. NKG2D ligand expression was calculated by dividing the median fluorescences of anti-H60a or anti-RAE-1 staining by isotype control. The F-test was used to measure significant differences in variances between groups. (** Indicates p value < 0.01, *** Indicates p value < 0.001).

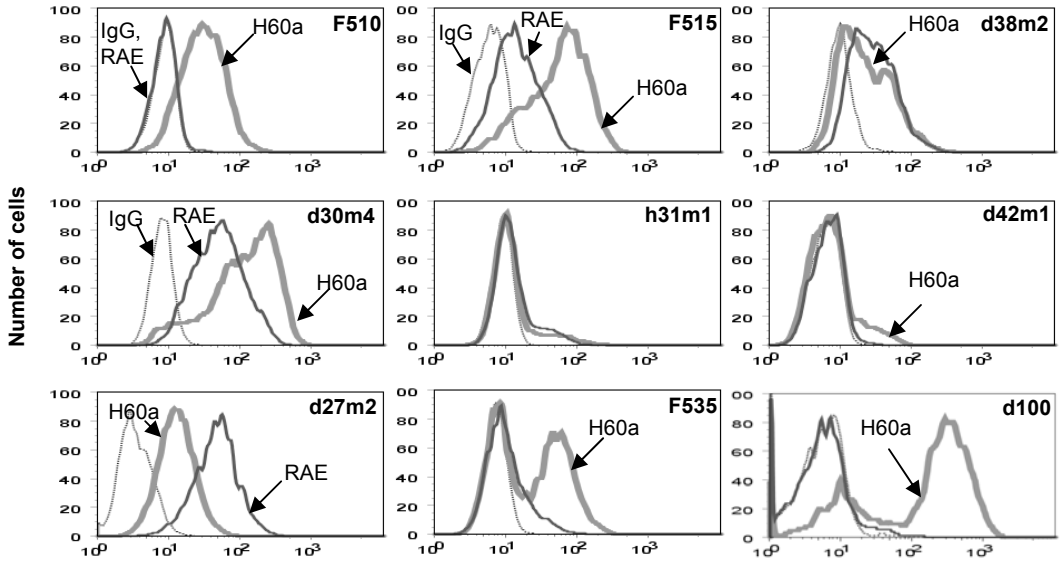

Figure 2.4 Heterogeneity in H60a expression can be seen even within a single cell line. Nine regressor cell lines were stained with control isotype (dotted line), anti-RAE (solid line), or anti-H60a (thick line).

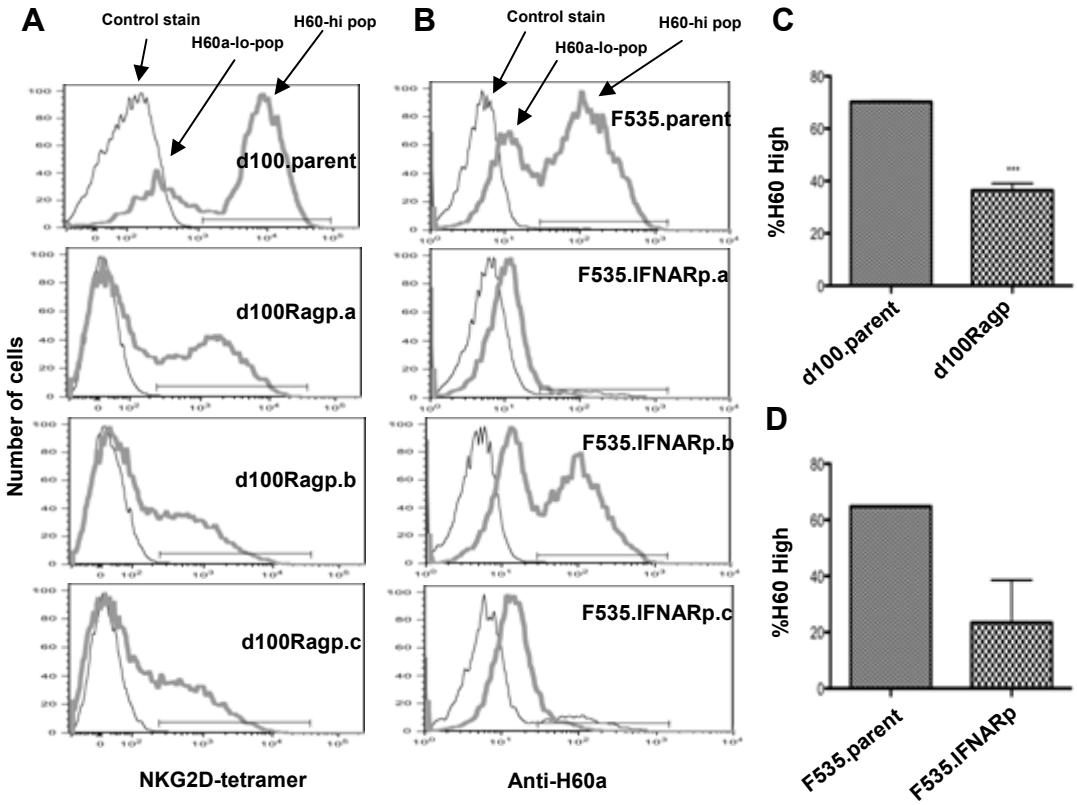

Figure 2.5 Editing of H60a-hi cells after in vivo passage. (A) The IFNAR-/--derived regressor tumor d100 was transplanted into three RAG2-/- mice, and daughter cell lines were generated, designated with the suffix "Ragp" to indicated their passage through RAG2-/- mice. Cell lines d100.Ragp.a, d100.Ragp.b, and d100.Ragp.c were obtained from three different RAG2-/- mice, and H60a expression was detected by NKG2D-tetramer. (B) The RAG2-/--derived regressor tumor f535 was transplanted into three IFNAR-/- mice, and daughter cell lines were generated, designated with the suffix IFNARp. Cell lines f535.IFNARp.a, f535.IFNARp.b, and f535.IFNARp.c were obtained from three different IFNAR-/- mice. H60a expression was detected by flow cytometry. (*** Indicates p value < 0.001).

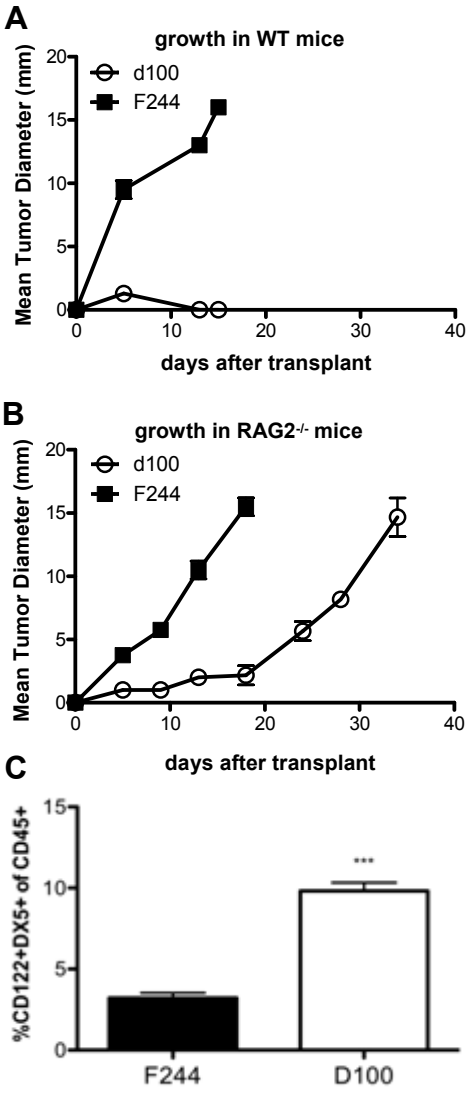

Figure 2.6 d100, a regressor tumor, shows delayed growth in RAG2-/- mice, which is associated with NK cell infiltration. The d100 and F244 cell lines were injected into (A) WT and (B) RAG2-/- mice, and tumor size was measured over time. (C) Tumor masses growing in RAG2-/- mice were harvested at day 25, disaggregated, and analyzed as a single cell suspension by FACS analysis. Infiltrating NK cells were identified as the DX5+CD122+ population from CD45+ events. Results were reproduced in an independent experiment. (*** Indicates p value < 0.001).

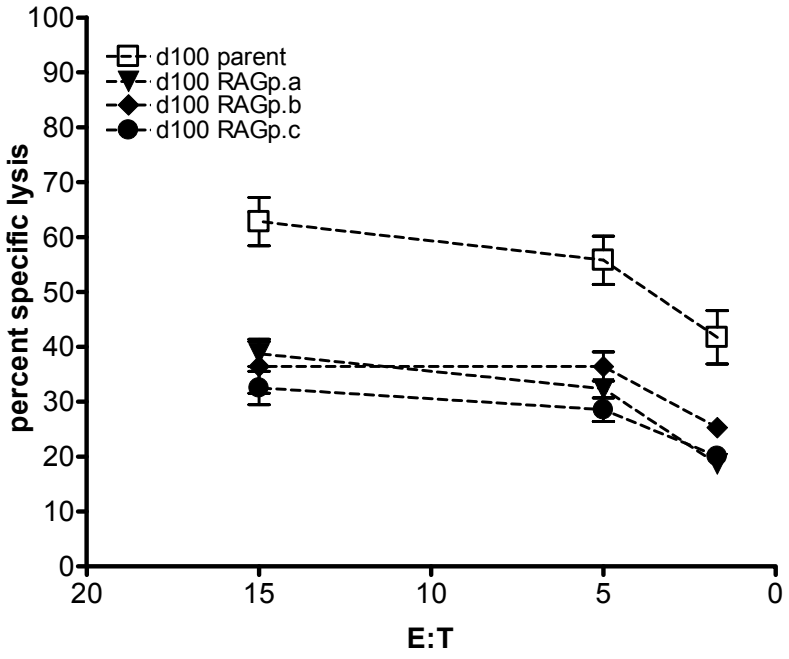

Figure 2.7 Passage of d100 in RAG2-/- mice leads to decrease in NK recognition. The parental unpassaged d100 or RAG2-/--passaged cell lines were used as targets in a conventional cytotoxicity assay using IL-2 activated NK cells as effectors. Results were reproduced in an independent experiment. (* Indicates p value < 0.05)

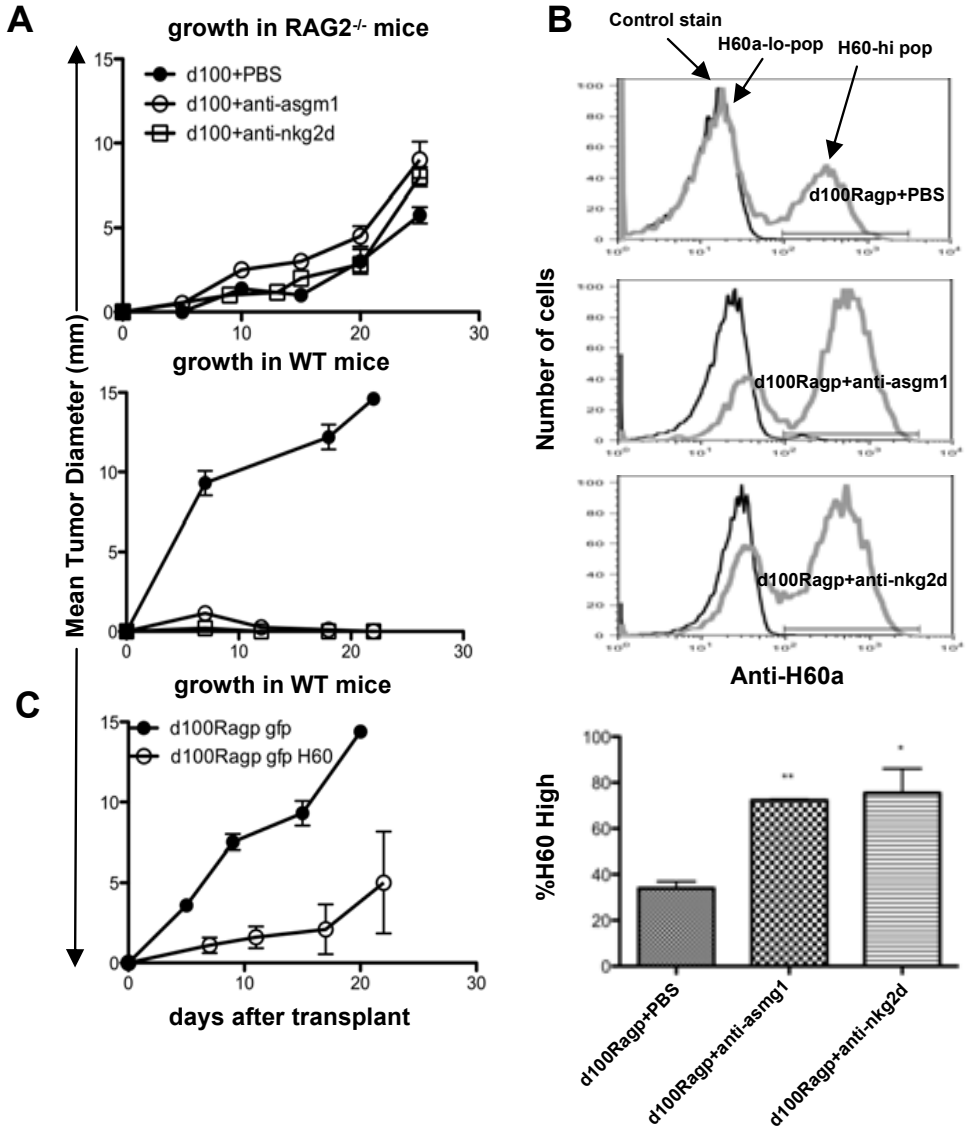

Figure 2.8 H60a is functionally edited by NK cell recognition through NKG2D. The IFNAR-/--derived regressor tumor d100 was injected into (A) Top-RAG2-/- mice that received i.p injections of either PBS, anti-ASGM1, or anti-NKG2D, and tumor size was measured over time. Bottom-Tumor masses growing in RAG2-/- mice were harvested at day 25, disaggregated, and daughter cell lines were generated and injected into WT mice. (B) H60a expression of daughter cell lines was detected by flow cytometry. (C) An edited, passaged, progressor d100 cell line was transduced either with retrovirus-expressing green fluorescent protein (GFP), or both GFP and H60a and injected into WT mice. (** Indicates p value < 0.01, * Indicates p value < 0.05).

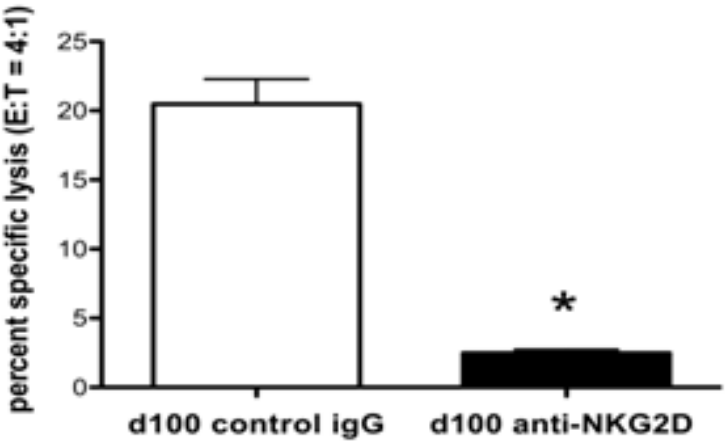

Figure 2.9 Lysis of d100 parental tumor is inhibited by blocking NKG2D in activated NK cells. Day IL-2 activated effector NK cells were used in a 4-hour chromium release assay using tumor target cell labeled with ^{51}Cr as described (20) with either control IgG or anti-NKG2D (*Indicated p value < 0.05).

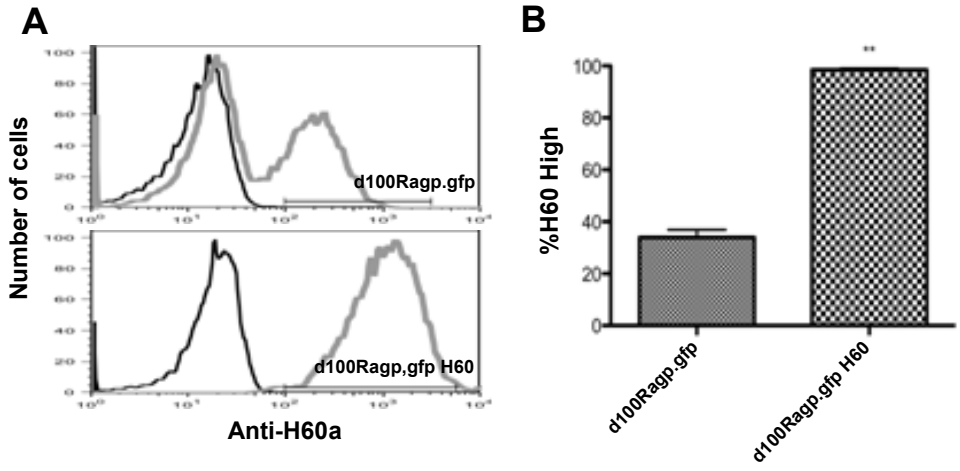

Figure 2.10 Expression of H60a. (A) Expression of H60a on the daughter cell lines generated from d100Ragp+PBS tranduced with either gfp or H60a and gfp. (B) Quantification of H60a-hi cells from daughter cell lines (** Indicates p value < 0.01).

CHAPTER 3: IL-17D MEDIATED TUMOR REJECTION

Regressor/Progressor Mixtures Reject in WT mice in a spatially dependent and antigen independent manner

To determine whether factors produced by unedited regressor cells can lead to rejection of edited progressor cells, we utilized a syngeneic panel of progressor and regressor MCA-induced sarcoma cell lines. We mixed a representative MCA-induced progressor sarcoma cell line (d30m1) with the MCA-induced regressor sarcoma cell lines d42m1 or d38m2 and transplanted the mixture into WT syngeneic mice. Interestingly, mixtures of progressor:regressor tumor cell lines were rejected when transplanted into WT mice (Fig. 1a), whereas the same quantity of progressor tumor cells grew in WT mice (Fig. 1a). This result was found with other progressor:regressor mixtures derived from regressor clones and escape variants of d42m1 (47). The rejection required that the tumors were spatially and temporally localized, since mice that had rejected d42m1 regressor tumor cell lines failed to reject subsequently transplanted d30m1 progressor tumors (Fig. 3.1 A), and placing d42m1 on the opposite flank did not lead to rejection of d30m1 (Fig. 3.2). These results suggest that immune rejection of mixed progressor:regressor tumors was not associated with common antigen expression, but rather other regressor-associated molecules.

IL-17D is highly expressed in regressor, but not progressor tumor cell lines

To identify regressor-expressed molecules that could mediate rejection of progressor:regressor mixtures, we performed microarray studies of 8 independent regressor and 16 independent progressor tumor cell lines (Fig. 3.3). We found that the novel cytokine IL-17D was highly upregulated in regressors compared to progressors as shown by microarray data (Fig. 3.1 B) and confirmed by qRT-PCR (Fig. 3.1 C, Fig. 3.4 A-C) and intracellular flow cytometry (Fig. 3.1 D). These results suggest that IL-17D was secreted in vitro at higher levels by regressor versus progressor tumor cell lines.

IL-17D is required for the rejection of regressor/progressor mixtures in WT mice

To confirm that IL-17D is required for the rejection of progressor:regressor mixtures, we silenced IL-17D in two regressor cell lines. We generated daughter cell lines transduced with scramble control (shctrl) or shRNA specific for the 3'UTR and coding regions of IL-17D (sh17D) and confirmed 90% protein knockdown (Fig. 3.5 A,B left panels). When the daughter cell lines were transplanted into WT mice, IL-17D knockdown did not alter the rejection phenotype (Fig. 3.6). Furthermore, IL-17D knockdown did not alter the in vitro and in vivo growth kinetics (in $RAG2^{-/-}$ mice) (Fig. 3.7 A,B), suggesting that IL-17D has no effect on intrinsic tumor growth and

proliferation. We did observe, however, that IL-17D was required for the rejection of progressor:regressor mixtures, as daughter sh17D tumor cell lines mixed with d30m1 progressor tumor cell lines did not reject when transplanted into WT mice (Fig. 3.1 E). These results suggest that a single gene (IL-17D) was required for the dominant rejection phenotype of progressor:regressor tumor mixtures.

Overexpression of IL-17D leads to rejection of small tumors

We then explored whether IL-17D expression in progressor tumors could mediate their rejection in WT mice in the absence of other regressor-associated molecules. Two progressor fibrosarcoma and one progressor melanoma cell line (F244, d30m1, B16 OVA) were transduced with empty vector control (ctrl) or IL-17D cDNA lentivirus (ex17D), leading to approximately five-fold overexpression of IL-17D, similar to regressor levels (Fig. 3.5 A,B,C right panels). Strikingly, the overexpression of IL-17D led to the complete rejection of both transplanted F244 and d30m1 tumors and a delay in growth of B16 OVA in WT mice (Fig. 3.1 F). This result clearly demonstrates that early expression of IL-17D can lead to tumor rejection, but does not demonstrate the efficacy of IL-17D on pre-established tumors. In order to address this, we generated a progressor tumor cell line (F244TR17D) that expresses IL-17D upon administration of doxycycline (Fig. 3.5 D). Conditional expression of IL-17D was able to induce the rejection of $25mm^2$ tumors, but not $100mm^2$ tumors (Fig. 3.1 G), indicating that early expression of IL-17D in small tumors was critical for its rejection.

IL-17D enhances NK cell recruitment to tumors, which enhance M1 macrophage polarization

To define the mechanism of IL-17D-mediated tumor rejection, we characterized the tumor infiltrating immune cells in tumors with high and low levels of IL-17D. FACS analysis of infiltrating immune subpopulations showed an approximate two-fold increase in the amount of natural killer (NK) cells at d7 and d14 in tumors overexpressing IL-17D compared to control tumors (Fig. 3.8 A,B). Moreover, when IL-17D was silenced in the d42m1 regressor, there was a decrease in NK cell infiltration compared to control tumors (Fig. 3.8 B). We also observed an approximate 1.5-fold enhancement in the accumulation of M1 macrophages in progressor tumors overexpressing IL-17D, whereas silencing of IL-17D in regressor tumors reduced M1 macrophages by approximately two-fold in both WT and $RAG2^{-/-}$, but not $RAG2^{-/-}$ x $\gamma c^{-/-}$ hosts, which are deficient in NK cells (Fig. 3.8 C). We did not observe increased NK cell lysis of progressors overexpressing IL-17D compared to controls in vitro (Fig. 3.9), suggesting NK cells are recruited rather than activated by IL-17D. Indeed, we have found a requirement for NK cells and IFNγ in the accumulation of M1 macrophages in regressor tumors during cancer immunoediting (Chapter 1), and observe a similar requirement for NK cells to polarize M1 macrophages during tumor rejection. These results suggest a model whereby IL-17D recruits NK cells to produce the cytokine IFNγ to polarize macrophages to an anti-tumor M1 phenotype.

NK cells are required for the rejection of IL-17D-overexpressing tumors, and promote adaptive immunity to establish immunologic memory.

To demonstrate the functional requirement for NK cells in IL-17D-mediated tumor rejection, we depleted NK cells from WT mice transplanted with d30m1 and F244 ex17D tumors. We found that mice treated with anti-NK1.1 but not control IgG failed to reject the IL-17D-overexpressing tumors (Fig. 3.8 D). Since it is known that NK-dependent tumor rejection can lead to priming of adaptive immune responses (34,48) we postulated that IL-17D-mediated rejection could prime anti-tumor immune responses. We challenged mice that had rejected IL-17D-overexpressing tumors with the parental tumor and found that transplanted parental progressor tumors were rejected after priming with IL-17D-overexpressing tumors (Fig. 3.8 D). These results confirm that edited tumors possessed antigens and that initiating the "correct" innate cell response through induction of IL-17D can result in productive adaptive, antigen-specific anti-tumor responses.

IL-17D recruits innate immune cells in an air pouch model of inflammation

To show directly whether IL-17D can induce the recruitment of immune cells, we used an in vivo air pouch model of inflammation in WT mice. Mice injected with sterile air pouches recruit immune cells rapidly after administration of LPS (49). Indeed, we

found that LPS, IL-17A, and IL-17D significantly recruited $CD45^+$ immune cells into air pouches compared to PBS control (Fig. 3.10 A). Whereas LPS and IL-17A recruited a larger percentage of neutrophils, IL-17D recruited a larger percentage (Fig. 3.10 B) and number (Fig. 3.10 C) of NK cells while also recruiting neutrophils and monocytes into air pouches. Although we observed recruitment of neutrophils, monocytes, and NK cells after injection of IL-17D into air pouches, we did not observe differential recruitment of either neutrophils or monocytes on d4 after F244-ex17D or ctrl tumor transplant (Fig. 3.11 A). Additionally, neutrophils were not required for IL-17D mediated rejection of d30m1 progressor tumors, as mice treated with neutrophil depleting antibodies still rejected d30m1-ex17D tumors (Fig. 3.11 B). Thus, although IL-17D can lead to the recruitment of monocytes and neutrophils in an air pouch model, IL-17D does not lead to enhanced recruitment of these cells in the context of a progressor tumor microenvironment.

IL-17D indirectly recruits NK cells through the production of MCP-1, which is required for IL-17D mediated tumor rejection.

We next examined whether IL-17D directly recruited NK cells or induced chemokines that could recruit NK cells. Using in vitro transwell assays, we found that IL-17D could not directly induce the migration of NK cells in vitro, whereas the control chemokine MCP-1 could induce robust transmigration of NK cells (Fig. 3.12 A). Furthermore, supernatant from IL-17D-expressing tumor cell lines or IL-17D-expressing

tumor cell suspensions did not differentially recruit NK cells, or contain higher levels of NK-recruiting chemokines such as MCP-1 and RANTES (Fig. 3.12 B,C), suggesting that IL-17D does not induce chemokine expression from tumor cells or infiltrating immune cells. Since IL-17A is known to induce IL-8 from endothelial cells to recruit neutrophils (50), we examined whether a similar mechanism of recruitment could be utilized by IL-17D. Indeed, we found that IL-17D induced the expression of MCP-1 in mouse air pouch lavage fluid (Fig. 3.13 A). To confirm that MCP-1 was the chemokine that mediated the IL-17D-dependent recruitment of NK cells in vivo, we repeated the air pouch experiments in the presence of blocking antibodies specific for MCP-1. We found that anti-MCP1, but not control IgG, completely inhibited IL-17D mediated recruitment of NK cells (Fig. 3.13 B) as well as neutrophils and monocytes (data not shown). Additionally, depletion of MCP-1 led to the outgrowth of F244 ex17D tumors (Fig. 3.13 C), further underscoring the importance of NK cell recruitment in anti-tumor responses in our model.

Chapter 3, in part, is an adapted version of material that is currently being prepared for submission for publication. Saddawi-Konefka, Robert; Bui, Jack D.; Mayfield, Stephen P.; Tran, Miller. The dissertation author was the primary author of this material.

Figure 3.1 IL-17D is expressed in regressor tumor cells and can mediate the rejection of progressor tumors in WT mice. (A) Tumor growth of d30m1 progressor unmixed or mixed with d42m1 or d38m2 regressors transplanted into WT mice. Tumor growth of d30m1 progressor tumors transplanted into mice immunized with d42m1 regressor tumors (B) IL-17D gene expression of 8 regressor, 8 progressor, and 8 WT progressor tumor cell lines generated from RAG2-/- and WT mice on the 129/Sv background respectively. (C) qRT-PCR analysis of mRNA from 3 independent regressor and progressor tumor cell lines (D) IL-17D intracellular protein expression of 3 regressor and 3 progressor tumor cell lines incubated with or without inhibitors of protein secretion. (E) Tumor growth of daughter (ctrl, sh17D) regressor and d30m1 progressor mixtures transplanted into WT mice. (F) Tumor growth of daughter (ctrl, ex17D) progressor tumors transplanted into WT mice. (G) Growth of conditional IL-17D expressing tumor cell line (F244TR17D) transplanted into WT mice receiving water or doxycycline continuously from d0, d5, or d12. Data are representative of two independent experiments. (*$P < 0.05$, **$P < 0.01$).

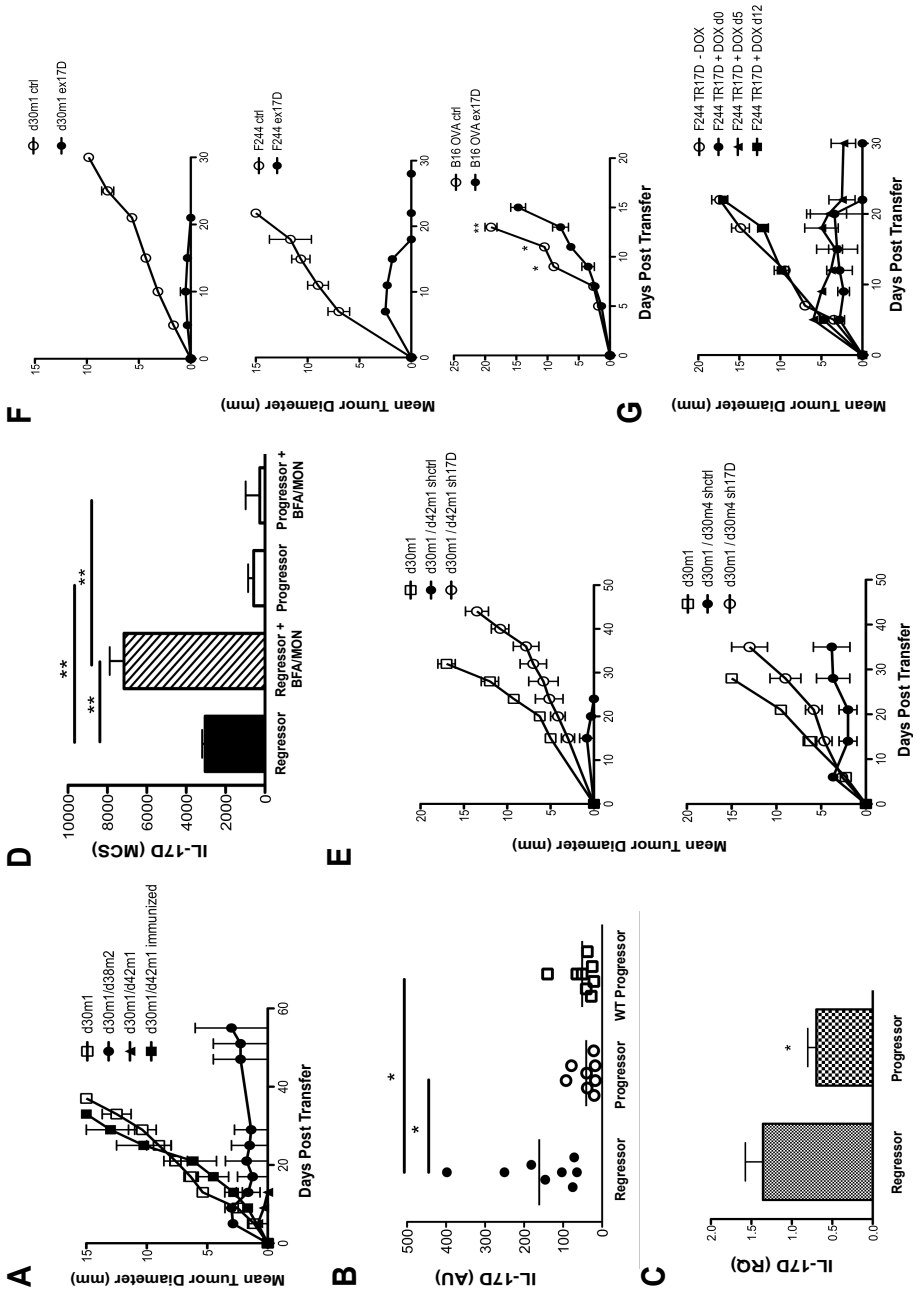
A
Mean Tumor Diameter (mm)
d30m1
d30m1/d38m2
d30m1/d42m1
d30m1/d42m1 immunized
Days Post Transfer
B
IL-17D (AU)
Regressor
Progressor
WT Progressor
C
IL-17D (RQ)
Regressor
Progressor
D
IL-17D (MCS)
Regressor
Regressor + BFA/MON
Progressor
Progressor + BFA/MON
E
Mean Tumor Diameter (mm)
d30m1
d30m1 / d42m1 shctrl
d30m1 / d42m1 sh17D
Days Post Transfer
d30m1
d30m1 / d30m4 shctrl
d30m1 / d30m4 sh17D
Days Post Transfer
F
Mean Tumor Diameter (mm)
d30m1 ctrl
d30m1 ex17D
F244 ctrl
F244 ex17D
B16 OVA ctrl
B16 OVA ex17D
Days Post Transfer
G
Mean Tumor Diameter (mm)
F244 TR17D - DOX
F244 TR17D + DOX d0
F244 TR17D + DOX d5
F244 TR17D + DOX d12
Days Post Transfer

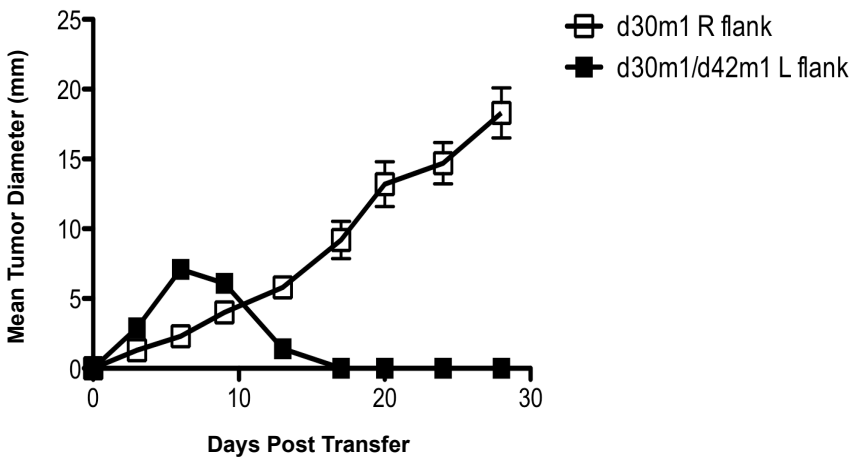

Figure 3.2 Rejection of progressor-regressor mixtures is spatially localized. Tumor growth of d30m1 progressor unmixed or mixed with d42m1 and injected into WT mice on the right and left flank respectively in the same mouse.

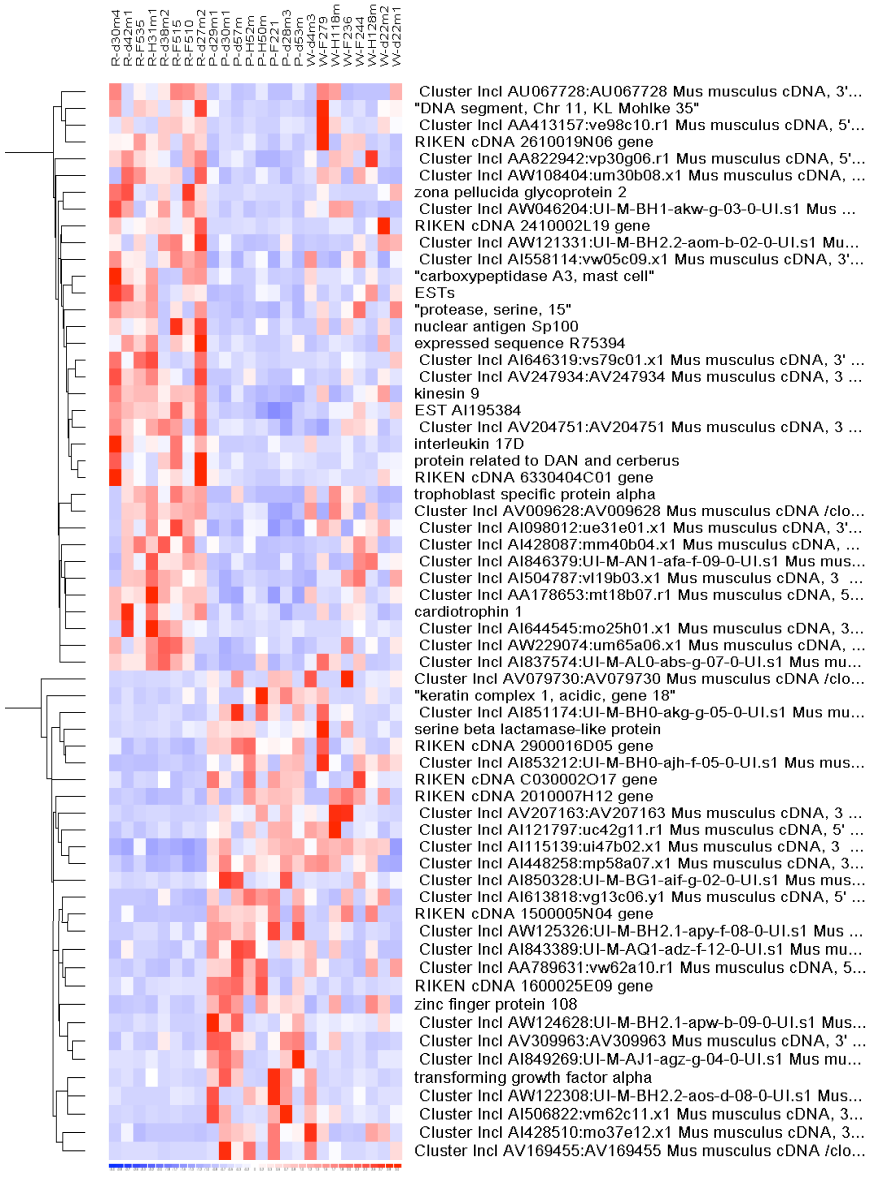

Figure 3.3 IL-17D is highly expressed in regressor tumor cell lines. Gene expression microarray clustering analysis of 8 regressor (left), 8 progressor (middle), and 8 WT progressor (right) tumor cell lines. Highly upregulated genes compared to reference are shown in dark red and highly donwregulated genes are shown in dark blue.

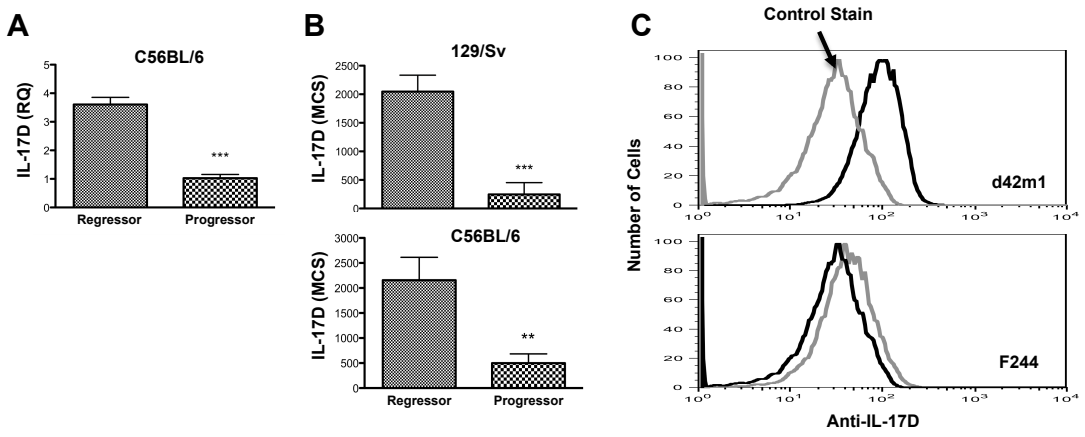

Figure 3.4 IL-17D protein is highly expressed in regressor tumor cell lines. (A) qRT-PCR analysis of mRNA from 3 independent regressor and progressor tumor cell lines generated from RAG2-/- a yc -/- mice on the C56BL/6 background. Values are normalized to GAPDH expression. (B) IL-17D protein levels measured by intracellular staining FACS anlaysis. Values are given as the mean channel shift of signal subtracted by isotype control staining as shown for a (C) representative regressor (d42m1) and progressor (F244) tumor cell lines. (**P < 0.01, ***P < 0.001).

Figure 3.5 Generation of IL-17D deficient regressor and IL-17D overexpressing progressor tumor cell lines. (A) IL-17D protein expression measured by intracellular staining FACS anlaysis of two regressor and progressor daughter tumor cell lines transduced with scramble control (shctrl) or IL-17D specific shRNA retrovirus (sh17D), and empty vector control (ctrl) or IL-17D cDNA lentivirus (ex17D) respectively. (B) Relative protein expression values for corresponding daughter cell lines normalized to percent of ctrl tranduced cell line mean channel shift**.** (C) IL-17D protein expression of F244 daughter cell lines transduced with tetR and tetO IL-17D or control tetR lentivirus after 48 hour stimulation with 100 ng/ml doxycycline. (D) IL-17D protein expression of B16 OVA daughter cell lines transduced with either empty vector control or IL-17D cDNA lentivrus.

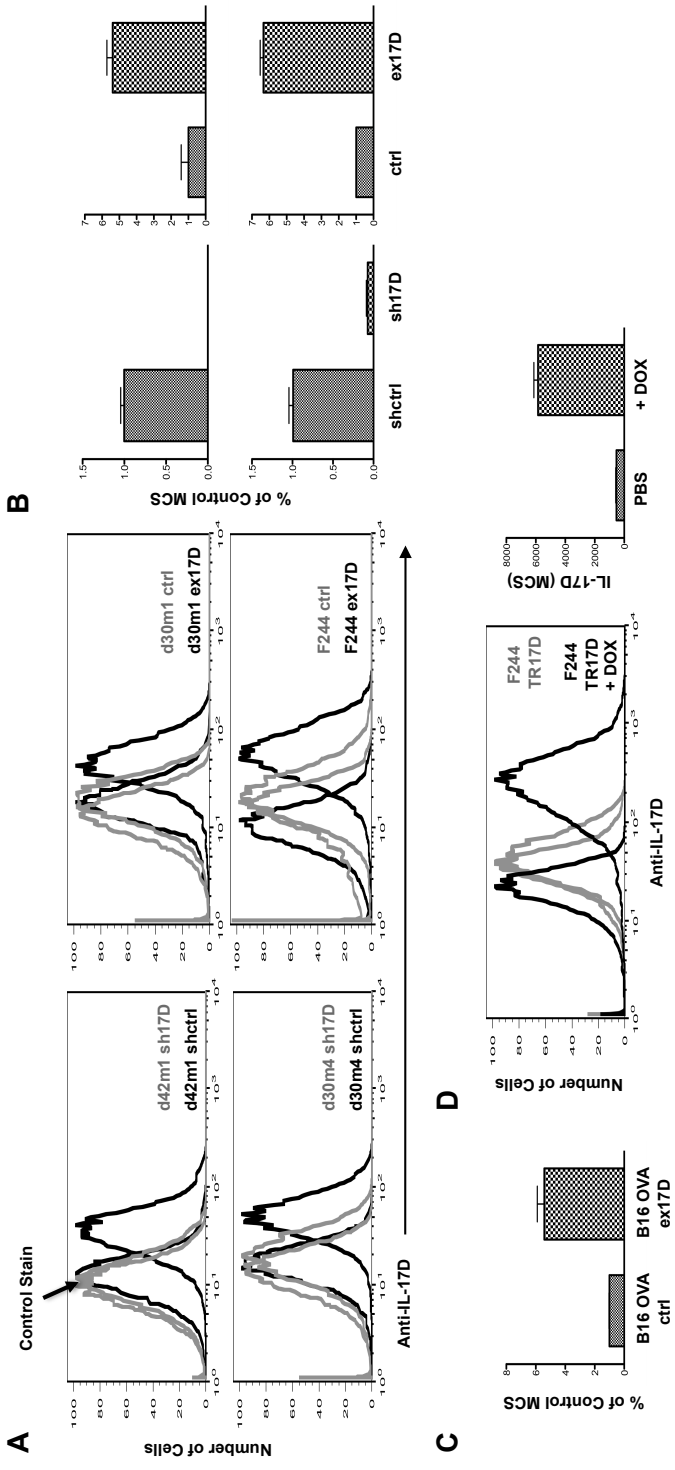
A
Control Stain
d42m1 sh17D
d42m1 shctrl
d30m1 ctrl
d30m1 ex17D
d30m4 sh17D
d30m4 shctrl
F244 ctrl
F244 ex17D
Anti-IL-17D
Number of Cells
B
% of Control MCS
shctrl
sh17D
ctrl
ex17D
C
% of Control MCS
B16 OVA ctrl
B16 OVA ex17D
D
F244 TR17D
F244 TR17D + DOX
Anti-IL-17D
Number of Cells
IL-17D (MCS)
PBS
+ DOX

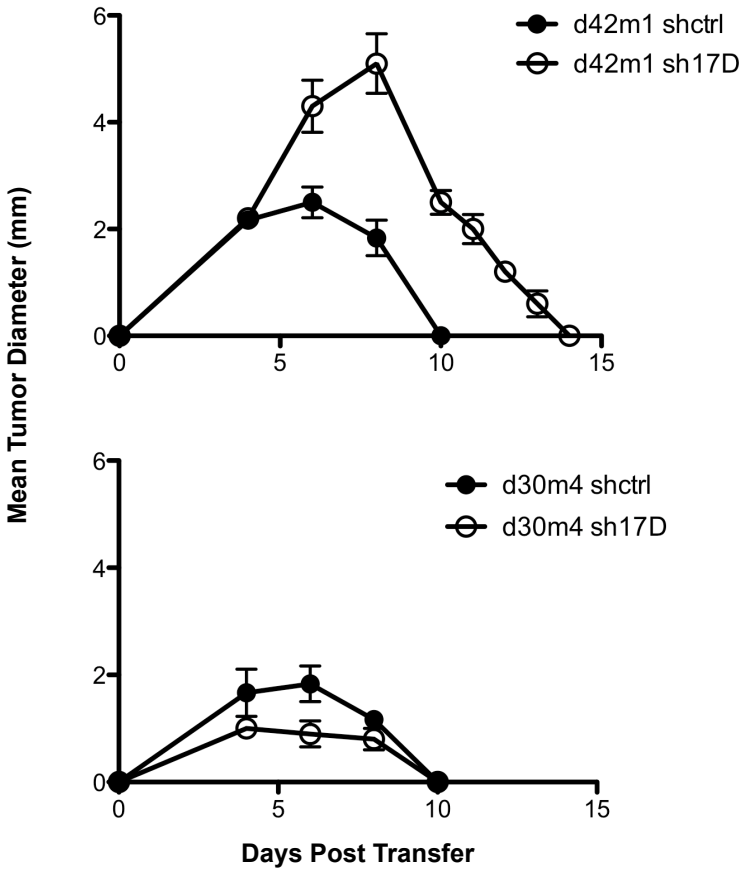

Figure 3.6 IL-17D is not required for the rejection of regressor tumors in WT mice. d42m1 and d30m4 daughter regressor tumor cell lines were injected into WT mice and growth was measured. Tumor growth was recorded as the mean of the two diameter measurements of the tumor mass.

Figure 3.7 IL-17D expression does not influence the growth rate of tumor cell in vitro or in vivo. (A) Daughter regressor and progressor tumor cell lines were plated in vitro and viable cells were counted each day using a hemocytometer. (B) Daughter regressor and progressor tumor cell lines were injected into syngeneic $RAG2^{-/-}$ mice. Tumor growth was recorded as the mean of two diameter measurements of the tumor mass.

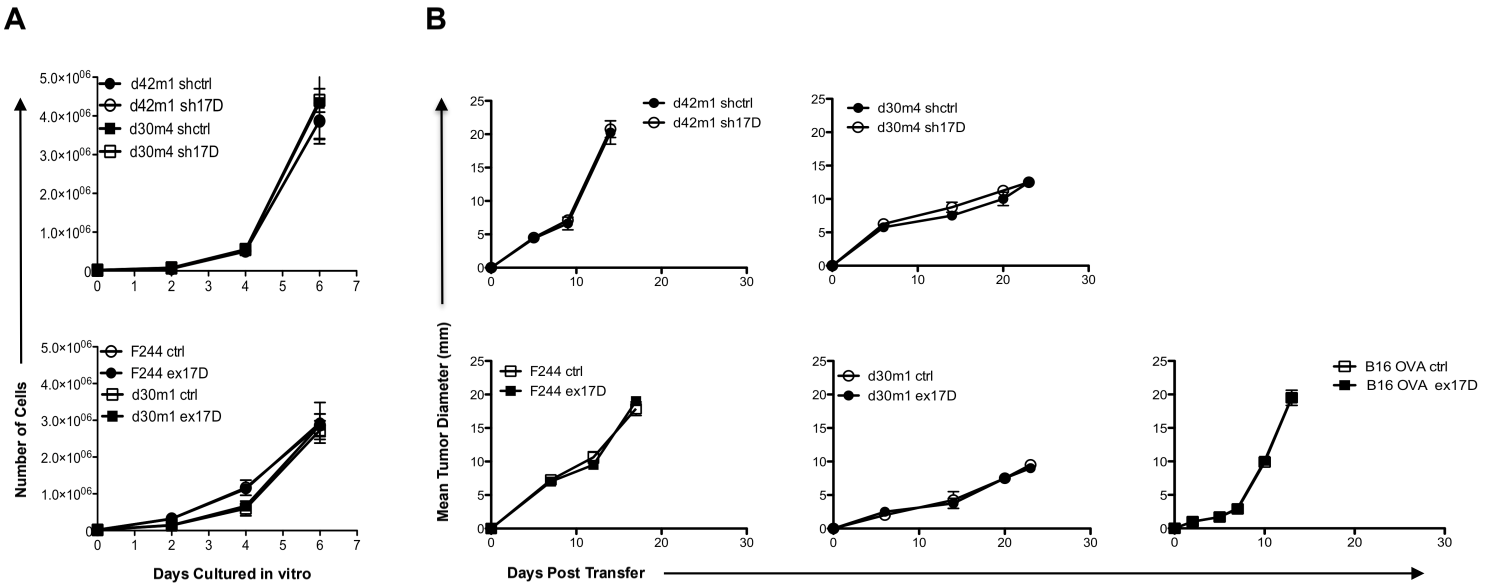
A
B
d42m1 shctrl
d42m1 sh17D
d30m4 shctrl
d30m4 sh17D
F244 ctrl
F244 ex17D
d30m1 ctrl
d30m1 ex17D
B16 OVA ctrl
B16 OVA ex17D
Number of Cells
Days Cultured in vitro
Mean Tumor Diameter (mm)
Days Post Transfer

Figure 3.8 Overexpression of IL-17D in progressor tumors recruits NK cells that are required for tumor rejection in WT mice. (A) Infiltrating immune cell FACS analysis of disaggregated tumor single cell suspensions of F244 ctrl or ex17D daughter tumor cell lines on d7 and d14 post transplantation in WT mice (B) FACS analysis of infiltrating NK cells from regressor and progressor daughter tumors on d7 post tumor transplant in WT mice . (C) FACS analysis of tumor associated M1 macrophages on d14 post tumor transplant of daughter regressor or progressor tumor cell lines into WT, $RAG2^{-/-}$, or $RAG2^{-/-}$ x $yc^{-/-}$ hosts. (D) Tumor growth of daughter (ex17D) progressor tumors transplanted into WT mice receiving either i.p. injections of anti-NK1.1/ctrl IgG, or pre-immunized with transplantation of daughter (ex17D) tumor cell lines. Data are representative of two independent experiments. (**P < 0.01, ***P < 0.001).

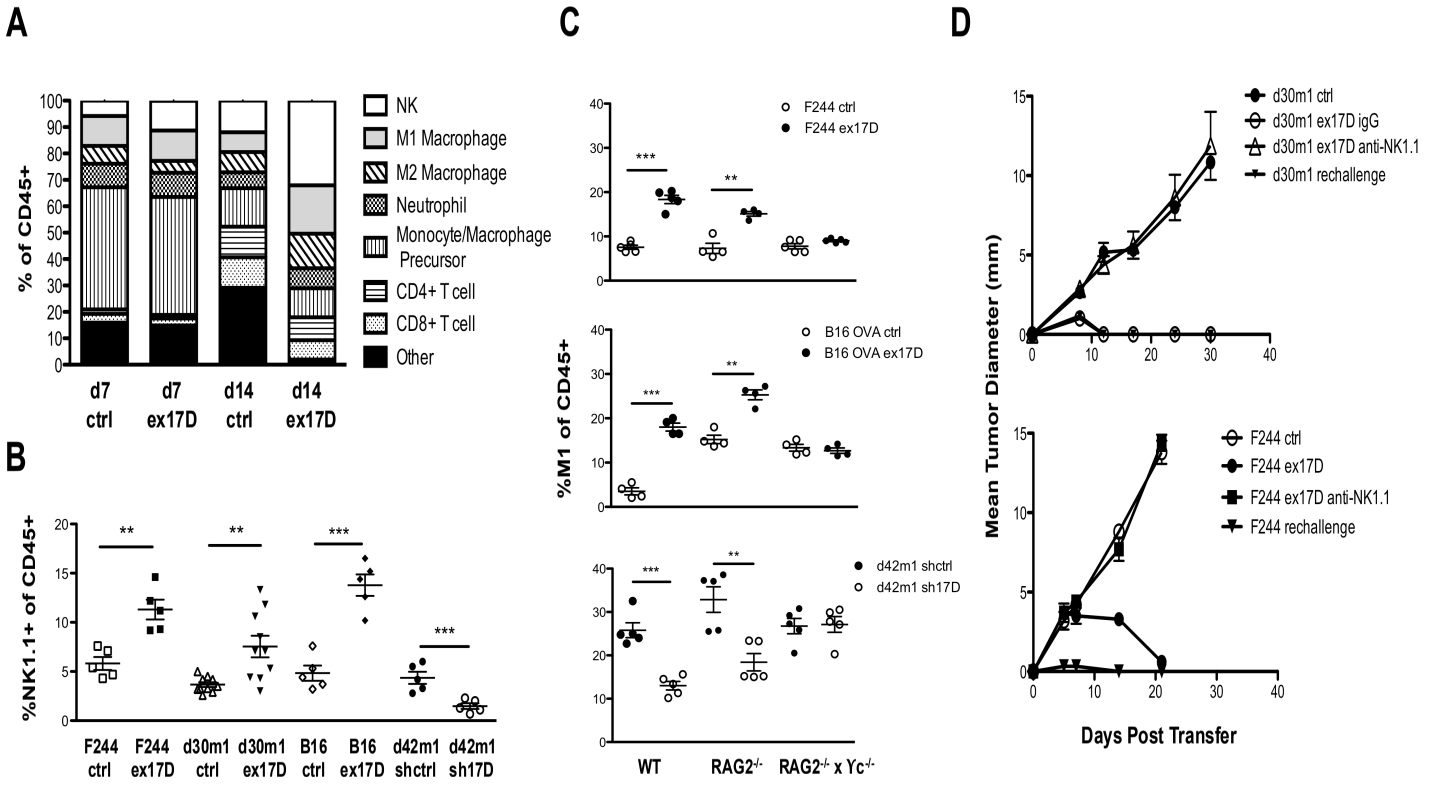
A
% of CD45+
NK
M1 Macrophage
M2 Macrophage
Neutrophil
Monocyte/Macrophage Precursor
CD4+ T cell
CD8+ T cell
Other
d7 ctrl
d7 ex17D
d14 ctrl
d14 ex17D
B
%NK1.1+ of CD45+
F244 ctrl
F244 ex17D
d30m1 ctrl
d30m1 ex17D
B16 ctrl
B16 ex17D
d42m1 shctrl
d42m1 sh17D
C
%M1 of CD45+
F244 ctrl
F244 ex17D
B16 OVA ctrl
B16 OVA ex17D
d42m1 shctrl
d42m1 sh17D
WT
RAG2-/-
RAG2-/- x Yc-/-
D
Mean Tumor Diameter (mm)
d30m1 ctrl
d30m1 ex17D igG
d30m1 ex17D anti-NK1.1
d30m1 rechallenge
F244 ctrl
F244 ex17D
F244 ex17D anti-NK1.1
F244 rechallenge
Days Post Transfer

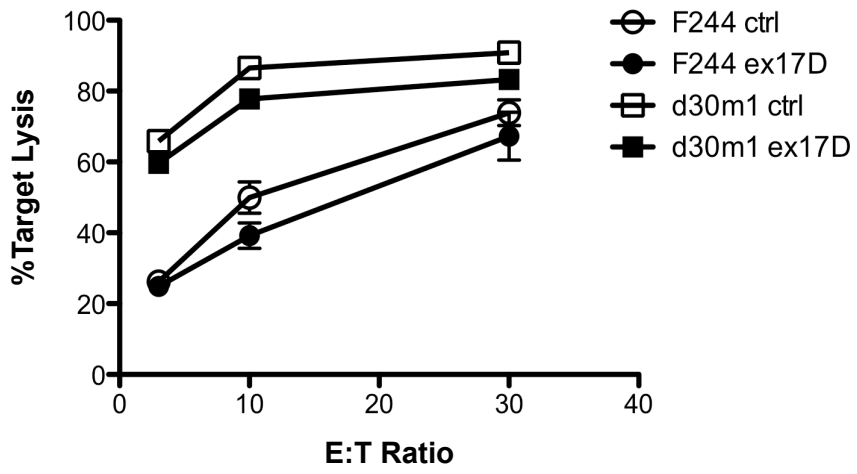

Figure 3.9 IL-17D does not increase lysis of progressor tumor cell lines in vitro. F244 and d30m1 daughter cell lines were labeled with CFSE and incubated with d7 IL-2 activated NK cells at various effector to target ratios. Specific target lysis was calculated as the percentage of 7AAD+ events from CFSE+ targets.

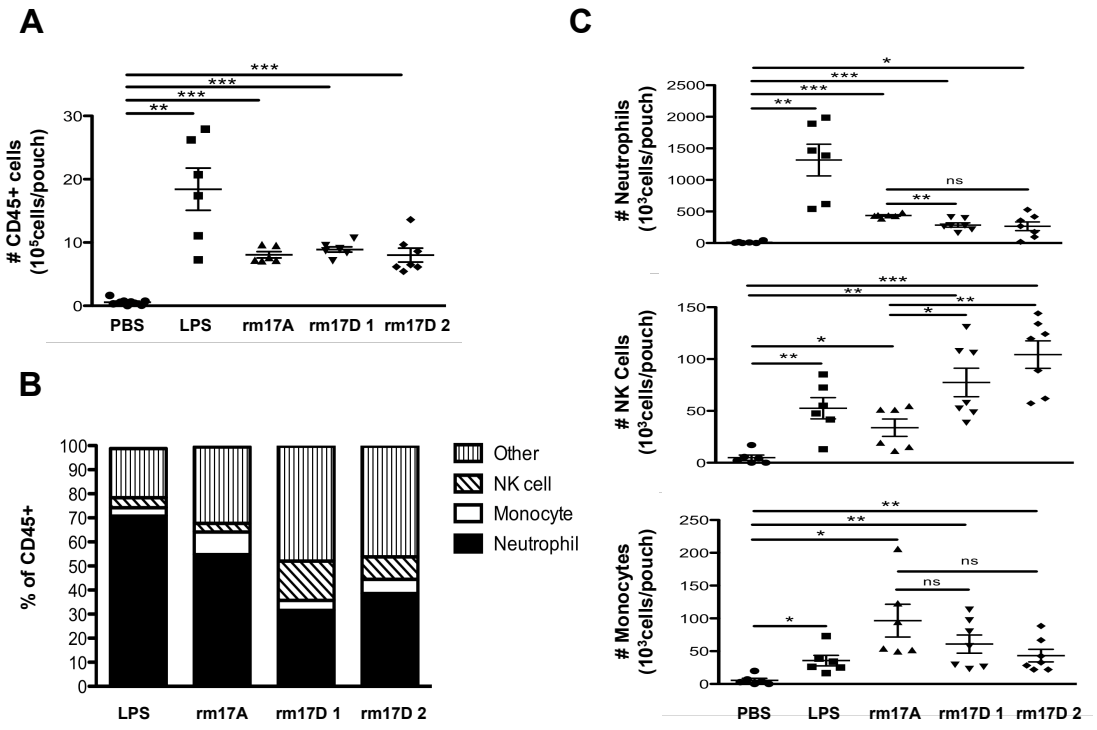

Figure 3.10 Recombinant mouse IL-17D recruits NK cells in an air pouch inflammation model. (A) Percentage of infiltrating immune cells, (B) innate cell subpopulations of total immune cells, and (C) total number of innate cell subsets per air pouch for WT mice receiving intra-pouch injections of PBS, LPS, rm-IL-17A, or rm-IL-17D . Data are representative of two independent experiments. (*P < 0.05, **P < 0.01, ***P < 0.001).

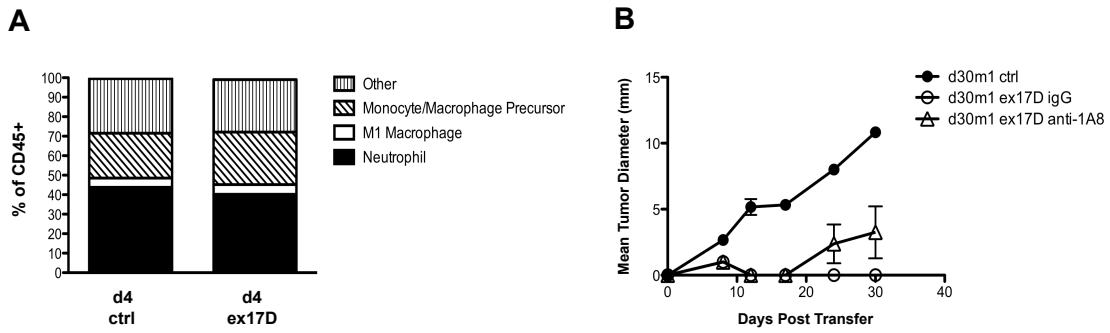

Figure 3.11 Overexprression of IL-17D does not recruit or require neutrophils during progressor tumor rejection. (A) F244 daughter ctrl or ex17D tumor cells lines were injected into mice at 10 x 10^6 cell/mouse. Tumor masses were harvested at d4, digested, and single cell suspensions were analyzed by FACS analysis. (Other indicates tissue macrophages, T cells, B cells, and eosinophils, all of which were not differentially recruited). (B) d30m1 ctrl or ex 17D daughter progressor tumor cell lines were injected into WT recipients treated with i.p. injection of ctrl IgG or anti-1A8 depleting antibodies and tumor growth was measured over time.

Figure 3.12 IL-17D does not induce chemotaxis of immune cells in vitro. Bone marrow was harvested from WT mice and 5 x 10^5 cells were plated in the top chamber of a 5 um transwell. Specific migration of innate cell populations was measured by FACS analysis as a response to various doses of (A) IL-17D and (B) tumor supernatant in the bottom chamber of the transwell. (C) F244 daughter ctrl or ex17D tumor cell lines were injected into WT or RAG2-/- x yc-/- hosts at 5 x 10^6 cells/mouse and tumor masses were harvested at d7 and d14. Tumors were disaggregated into single cell suspensions and plated at 4 x 10^4 cells/well in a 96 well plate for 24 hours. Supernatant was harvested and assayed for chemokine secretion levels compared to tumor cell line controls.

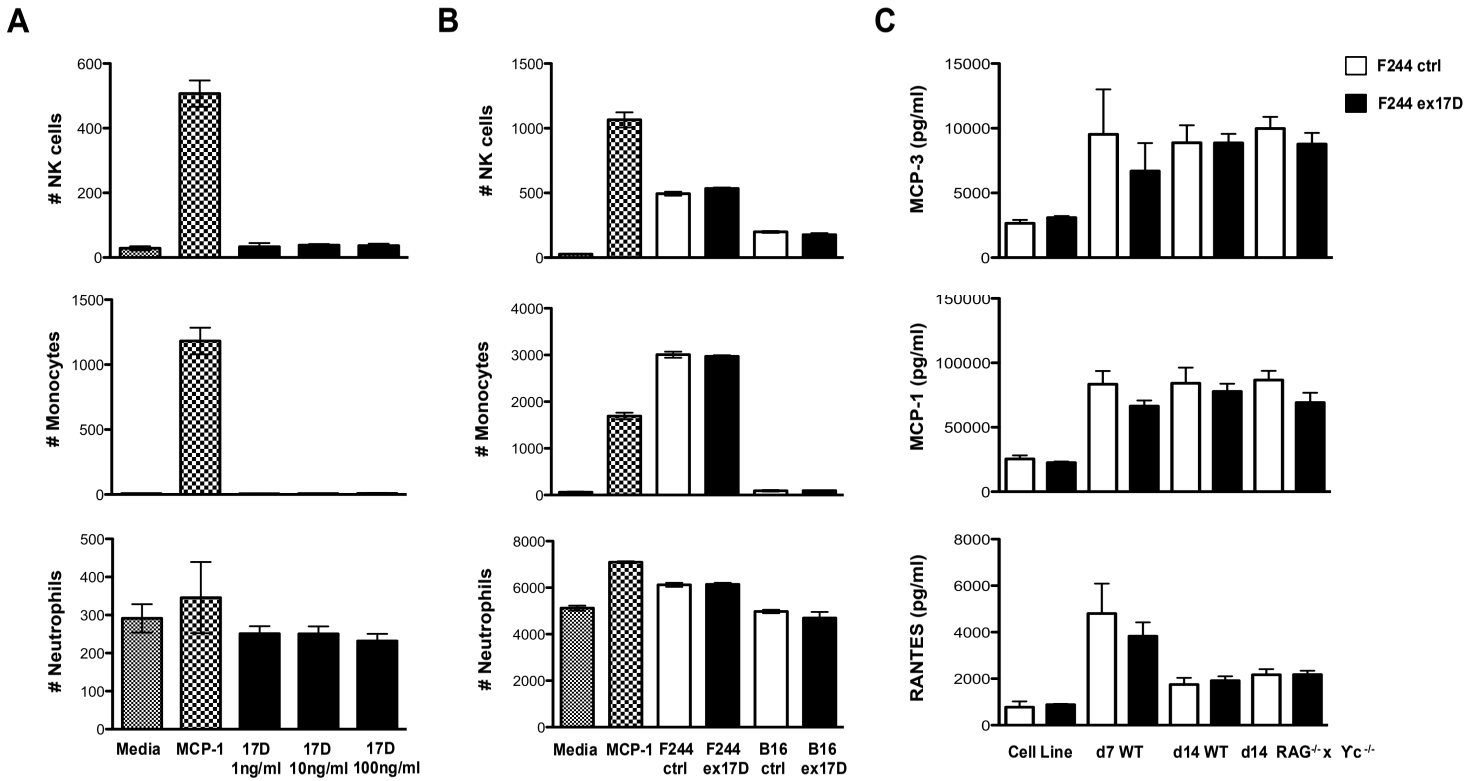
A
NK cells
600
400
200
0
Monocytes
1500
1000
500
0
Neutrophils
500
400
300
200
100
0
Media
MCP-1
17D 1ng/ml
17D 10ng/ml
17D 100ng/ml
B
NK cells
1500
1000
500
0
Monocytes
4000
3000
2000
1000
0
Neutrophils
8000
6000
4000
2000
0
Media
MCP-1
F244 ctrl
F244 ex17D
B16 ctrl
B16 ex17D
C
F244 ctrl
F244 ex17D
MCP-3 (pg/ml)
15000
10000
5000
0
MCP-1 (pg/ml)
150000
100000
50000
0
RANTES (pg/ml)
8000
6000
4000
2000
0
Cell Line
d7 WT
d14 WT
d14 RAG-/- x Yc-/-

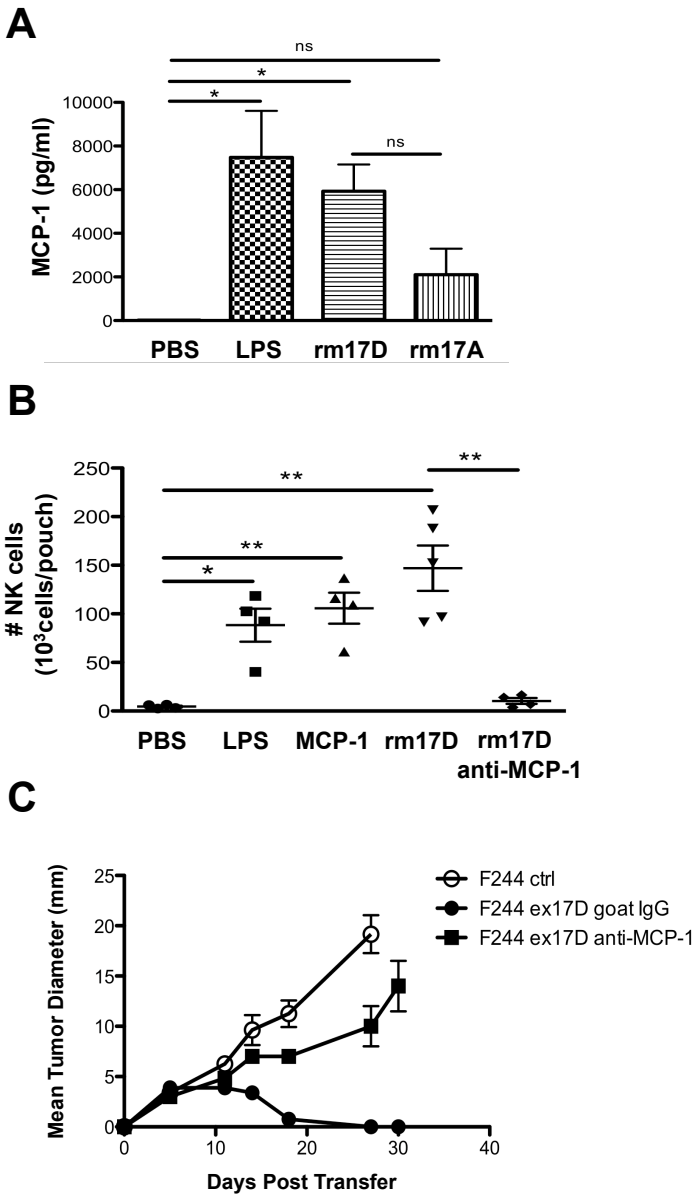

Figure 3.13 IL-17D indirectly recruits NK cells through production of MCP-1. (A) Lavage fluid chemokine levels of MCP-1 and (B) total number of innate cell subsets per air pouch for WT mice receiving intra-pouch injections of PBS, LPS, rmIL-17A, rm-IL-17D, rmMCP-1, or rm-IL-17D and anti-MCP-1 monoclonal antibodies. (C) Tumor growth of daughter F244 ex17D tumors transplanted into WT mice receiving either i.p. injections of anti-MCP-1/ctrl goat IgG. Data are representative of two independent experiments. (*P < 0.05, **P < 0.01, ***P < 0.001).

DISCUSSION

The cancer immunoediting hypothesis predicts that tumors arising in immune-deficient individuals will be more immunogenic than tumors that develop in immune-competent individuals. Although this concept is achieving wide acceptance, the relationship between the degree of host immune deficiency and the extent of cancer immunoediting have not yet been examined. We provide evidence that the extent of host immune-deficiency directly correlates with the level of cancer immunoediting. In doing so, we document that the innate immune system present in $RAG2^{-/-}$ mice can mediate to some extent the immunosurveillance and immunoediting of MCA-induced sarcomas. This editing activity is associated with M1 macrophages, IFNγ, γc, and NK cells.

Consistent with previous studies (1,3), we found that tumors arising in RAG-deficient mice are unedited and as a group, more immunogenic. Our evidence is based on studies of over 150 cell lines generated during a decade of experimentation performed in two separate sites, across two strains of mice, and using both RAG1- and RAG2-deficient models. A striking finding from our studies is that the regressor frequency of MCA-induced sarcoma cell lines derived from RAG-deficient mice reproducibly approximates 40%. Moreover, the regressor frequency of MCA-induced sarcomas generated in mice lacking RAG and yc is 60-70% in two independent experiments. These results suggest a quantitative nature to the immunoediting process, whereby a certain degree of basal immune function is associated with quantifiable levels of tumor sculpting, which can be measured by the regressor frequency. Since a majority of MCA cell lines generated from $RAG2^{-/-}$x $\gamma c^{-/-}$ mice are regressors, we speculate that the primary

tumor cell repertoire consists of mostly immunogenic tumor cells that are immunologically heterogeneous.

Tumor heterogeneity has been appreciated as an inherent characteristic of genetically unstable neoplasms (51, 52). Various studies have shown that among the cancerous cells in a tumor mass, or even within a tumor cell line, there is heterogeneity in the phenotype (53, 54), capacity to metastasize (55, 56), response to chemotherapy (57), ability to initiate new tumors (53, 56, 58), and signalling through surface receptors (54, 59). Indeed, the cancer stem cell hypothesis (53, 58) is supported by the observation that a tumor mass is heterogeneous, and therefore made of cells that have different capacities to initiate new tumors after transplantation. We have found that the expression of H60a, as a potential surrogate marker of immunogenicity, is more heterogeneous in unedited compared to edited tumor cells. This heterogeneity in H60a expression is found in groups of cell lines (unedited versus edited) and even within single unedited cell lines. These data suggest that tumor heterogeneity may be detected and eliminated by the immune system via a cancer immunoediting process, and NKG2D ligands may serve as markers for this process.

We conclude that H60a is an edited molecule, and this editing process requires NK cells and NKG2D activity. A previous study (25) using NKG2D-deficient mice found that NKG2D is not involved in the surveillance of MCA sarcomas, whereas a study from another group showed increased MCA tumor formation in mice treated with blocking antibodies to NKG2D (13). Both of these studies were performed in C57BL/6 mice, which lack H60a, and therefore do not shed light on the mechanism of H60a editing in our model system. The finding that some unedited cell lines from mice

deficient in STAT1 or γc display even higher levels of H60a points to NK cells as an effector of the editing process, since they are functionally defective in the absence of STAT1 (60) and are completely absent in mice lacking γc (39). We found increased levels of activated NK cells in the d100 regressor tumor as it is undergoing editing when transplanted into $RAG2^{-/-}$ mice compared to a progressor tumor control. In addition, daughter cell lines generated in the presence of functional NK cells showed a progressive growth phenotype in WT mice, while those generated without NKG2D function or NK cells still retained their rejection phenotype, suggesting that NK cell killing through NKG2D is required for the editing of these tumors in vivo. Overexpression of H60a into edited tumors causes their rejection in vivo, showing that H60a can be a functional marker of immunoediting for certain tumors.

We found that H60a can be expressed at higher levels in progressor than regressor tumor cell lines. These results suggest that H60a is not sufficient or necessary for tumor rejection. We envision that NKG2D ligands are only one component of the immunologic landscape of tumor cells, and tumors with very high antigenicity or innate ligands might not need NKG2D ligand expression to be rejected. On the other hand, tumor cells with moderate NKG2D ligand expression can escape immune detection if they decrease their antigenicity or increase inhibitory ligands or cytokines. In our model system using d100, the decrease in H60a expression is required for the conversion to a progressor. In contrast, although H60a is edited in F535 after passage through $IFNAR^{-/-}$ mice, the $IFNAR^{-/-}$-passaged F535 daughter cell lines remain regressors, indicating that other immune targets can be sufficient to mediate rejection. It will be interesting to examine the expression of inhibitory molecules such as CD47 (61) and B7-H1 (62) on progressors

with moderate H60a expression and innate ligands such as HMGB1 and advanced glycation end-products (63) on regressors with low levels of H60a, such as IFNAR$^{-/-}$-passaged F535 cells.

We found that some regressor cell lines displayed bimodal H60a expression. This pattern was fairly stable over time, and therefore is unlike the bimodal H60c expression that is induced via "culture shock" in primary keratinocytes (64). Nevertheless, we cannot rule out that cultured cell lines induce H60a expression via a response to the stress of in vitro growth. We consider this possibility unlikely, since others have shown previously that H60a expression on tumor cells harvested ex vivo is comparable to levels of the same tumor cell grown in vitro (33). In addition, other groups have found that primary tumor cells also express high levels of NKG2D ligands (27, 65). Regardless of whether in vitro culture induces NKG2D ligand expression, we advocate that the level of expression is an inherent characteristic of the cell line and can reflect the level of editing that the cell line has undergone in vivo.

It should be noted that regressor cell lines that are bimodal in H60a expression (d100, F535) are completely rejected in WT mice, rather than undergoing an equilibrium phase that promotes the escape of H60a-lo clones. We speculate that even though the H60a expression is bimodal, the T cell antigens may be shared among the H60a-hi and H60a-lo cell clones. Since it is known that NK cell activation and killing can lead to T cell priming (34), we envision that and adaptive immune response to H60a-lo cells is responsible for the destruction of these cells in WT mice. Future studies will address whether the H60a-hi cells can immunize against edited H60a-lo cells.

It is not known what regulatory mechanism allows for very high and very low NKG2D ligand levels in similarly treated cells. The fact that H60a expression is also heterogeneous within cell lines indicates that H60a expression could be controlled at the level of a single cell via intrinsic mechanisms. We envision that during carcinogenesis, some tumor cells suffer lesions that induce H60a expression, while others do not. These lesions could be quantitative in nature, and may loosely correlate with H60a expression.

We believe these lesions could be in the *cis* elements that regulate H60a and also throughout the genome, to be sensed by *trans* factors that regulate H60a. Although DNA damage has been shown to regulate Rae-1, Mult-1, and MICA, we have not found similar regulation of H60a (JDB, unpublished observations). We have found that the transcript levels for H60a also displayed heterogeneity and is not always correlated with H60a protein levels, implying that post-transcriptional mechanisms of H60a regulation may exist. Indeed, we and others have found that microRNAs can regulate the human NKG2D ligand MICA (66, 67) and H60a (46).

Our cell lines are not cloned, and therefore, the heterogeneous expression of H60a is likely due to multiple cell clones expressing different levels of H60a. Interestingly, when we sorted H60a-lo cells from the bimodal parental d100 cell line, these cells were unstable and gave rise to H60a-hi cells after several days of culture (data not shown). The sorted H60a-lo cells, when transplanted into WT mice as a bimodal population due to H60a instability, were still regressor cells. We could not obtain cell clones that stably expressed H60a at low levels, even after multiple limiting dilution cloning procedures. Thus, we still do not know whether the parent d100 is a mixture of cell lines or is a single "unstable" cell line that then gives rises to different daughter cells. Thus we would

predict that the d100 cell line can in fact represent a mixture of cell clones, which would be consistent with our conclusion that the substrate for editing is a mixture of various cell clones, each with differing immunogenicities. Unedited tumor would therefore be more heterogeneous and would include potential unstable cell clones.

An alternative scenario could be that H60a expression is associated with intrinsic cellular physiology, and could be related to the proliferation state of the cell, as has been shown for MICA (68). Although cell starvation is not sufficient to affect H60a levels (33), cell cycle signals could collaborate with other signals to regulate H60a. It should be noted that the Rae-1 levels in our cell lines are fairly homogeneous, i.e., displays a unimodal, narrow peak in flow cytometric analysis, and thus, the mechanisms that underlie the observed heterogeneous expression of H60a must be specific for individual NKG2D ligands.

We have provided evidence that NK cells can edit tumors and point to M1 macrophages as another participant in this process. M1 macrophages are activated classically via IFNγ and function in the removal of intracellular pathogens (21). In the context of cancer, M1 macrophages can promote tumor elimination via activation of Th1 pathways and secretion of tumoricidal levels of nitric oxide (19). In our studies, we have defined $CD45^{+}CD11b^{+}$MHC class $II^{hi}CD206^{lo}Ly6C^{lo}$ cells as M1 macrophages based not only on their phenotype but also on their classical requirement for IFNγ for their generation. Using this definition, we found a striking correlation between the presence of M1 macrophages and productive immune responses to regressor tumors. The administration of reagents that increased M1 percentages, such as CD40 agonist, enhanced editing, whereas treatments that decreased M1 percentages, such as NK cell

depletion and anti-IFNγ , blocked editing. Our findings support an anti-tumor function for macrophages that is consistent with studies performed almost forty years ago, when it was shown that activated macrophages from infected mice (69) could kill syngeneic transformed murine embryonic fibroblasts (MEFs) but not primary non-transformed MEFs (70) in vitro. This tumoricidal activity of macrophages required cell-cell contact and was induced largely by the cytokine IFNγ (71,72) in combination with additional signals such as lipopolysaccacharide (LPS) (73) or muramyl dipeptide (74). Moreover, recent studies indicate that macrophage tumoricidal activity could be enhanced in vitro and in vivo upon administration of CD40 agonistic antibodies (42,43). Although we have not shown that regressor tumor cells are killed by TAMs, we have observed that regressor tumor cells can be killed effectively by IFNγ-stimulated bone marrow macrophages *in vitro* (data not shown). Our attempts at demonstrating the tumoricidal activity of regressor-associated macrophages was limited by the poor viability of sorted TAMs. Furthermore, the contribution of regressor-associated TAMs to the editing process cannot be elucidated as clodrontate encapsulated liposomes fail to deplete TAMs in the tumor microenvironment, while achieving depletion of $CD11b^+$ macrophages in tumor bearing spleens (data not shown). Nevertheless, we favor the interpretation that M1 macrophages are the most likely editor given their abundance in the tumor, their enhanced presence in response to IFNy and NK cell activity, and their known tumoricidal activity.

We found that the accumulation of M1 macrophages in regressor tumors required IFNy and NK cells. The participation of NK cells in immunosurveillance against certain types of tumors has been clearly documented in studies showing increased tumor incidences in mice lacking NK cells or molecules associated with NK cell recognition or

effector function (12,17,18), such as NKp46 (75), NKG2D (18), DNAM-1 (76, 77), perforin (78,79), IFN-γ (78), or TRAIL (80). Therefore, we considered the possibility that there might be increased NK cell killing of MCA-induced sarcoma cells from RAG2$^{-/-}$x γc$^{-/-}$ versus RAG2$^{-/-}$ or WT mice. However, we did not find major differences in the susceptibility of unedited versus edited tumors to NK cell killing. For MCA-induced sarcomas, we advocate that the role of NK cells in eliminating and/or sculpting tumors can also be as a source of IFNγ. This is based on findings that NK cells and IFNγ is necessary for M1 macrophage polarization and subsequent editing in RAG2$^{-/-}$ mice. Although we cannot rule out the contribution of other myeloid populations to IFNγ production ex vivo, qPCR data of sorted M1 and M2 TAM's does not show any IFNγ transcript (data not shown), suggesting that NK cells are the predominant producers of IFNγ in the RAG2$^{-/-}$ host. At this time, it is unclear what stimulates NK cells to produce IFNγ in the sarcoma microenvironment, but our preliminary studies indicate that MCA-induced sarcoma cells are incapable of directly eliciting IFNγ production from NK cells in vitro. It should be noted that in RAG2$^{-/-}$x γc$^{-/-}$ mice lacking NK cells, editing could be restored with CD40 agonist treatment, suggesting that direct interaction between NK cells and tumor cells is not needed for tumor editing – as long as M1 macrophages are present.

Our model is based on the postulate that immunogenic regressors, in the presence of M1 macrophages, are converted into non-immunogenic progressors, but we have not identified the molecular basis of this phenotypic conversion. Recent studies have also found that certain tumor cells can evade macrophage killing/phagocytosis by expressing high levels of CD47 (61,81) and/or low levels of calreticulin (82). Other studies have implicated calreticulin exposure as a key initiator of innate immune responses to tumor

cells, leading to antigen presentation and productive adaptive anti-tumor responses, and the blockade of these pathways could be a mechanism of tumor escape (83). We did not find differences in the interaction between bone marrow-derived macrophages and regressor versus progressor tumor cells in vitro (TEO, RSK, JDB, unpublished observations). Furthermore, our preliminary studies indicate that CD47 and calreticulin are not different between regressor and progressor cells in vitro.

We therefore postulated that unedited tumors contained more recognition molecules or antigens than edited tumors. It has been well defined that tumors have antigens, which can lead to protective immunity from either pre-immunization with a low number of tumor cells (9) or active immunizaton with tumor-derived antigens (7,8). Antigenicity of tumors can even be traced by exome sequencing to a single neo-antigen that is sufficient to reject escape variant tumors by either re-expressing neo-antigen, or by mixing with tumors endogenously expressing neo-antigen (47). While these studies were done using clones and escape variants of the same fibrosarcoma tumor cell line, we hypothesized that mixing unedited regressor tumors with other unrelated edited tumors could in fact mediate their rejection through a dominant antigenic response. We found that regressor:progressor mixtures did in fact reject when tranplanted into WT mice, whereas unmixed progressors grew. To prove that this process was in fact due to a dominant rejection antigen, we pre-immunzied mice with regressor tumor challenge and then transplanted progressor tumors that rejected when transplanted as a mixture. To our surprise, mice were not protected against progressor challenge, and all mice tested developed progressively growing tumors. These results suggested that the edited and unedited tumors tested were in fact not antigenically related, and that other regressor-

associated molecules were responsible for the rejection of regressor:progressor mixtures in immunocompetent hosts.

Many studies have shown that tumors can inhibit immune responses through expressed factors such as TGF-b (36) and B7-H1 (37), thereby modulating growth and eventual escape. However, there have been no studies profiling endogenously expressed factors by tumors that mediate their rejection other than antigens. Using an unbiased microarray approach, we compared the gene expression profiles of regressor and progressor tumors and found that interleukin 17D (IL-17D) was expressed in higher amounts in regressor when compared to prgressor tumor cell lines. IL-17D has been implicated in inducing IL-6, IL-8, and GM-CSF expression in HUVEC cells in vitro, but does not have a known cellular receptor, endogenous cellular source, or known role during homeostasis or tumor progression. Furthermore, gene array studies in human cancer tissue samples do not show a clear pattern of expression of IL-17D compared to normal tissue (Oncomine), but qPCR validation of these studies has not been done, therefore the endogenous role of IL-17D in human cancer remains unknown. Studies in mice have shown that IL-17A can augment the progression of human tumor cell lines transplanted in nude mice by increasing neovascularization (84), while others have shown anti-tumoral properties of IL-17A using syngeniec tumors (85). We have shown that IL-17D is necessary for regressor:progressor mixtures, and can be overexpressed in progressor tumors to mediate their rejection. Furthermore, pre-immunization with IL-17D overexpressing progressors confers protection from parental progressor tumor challenge, indicting that IL-17D has potent anti-tumoral effects by establishing a rejecting microenvironment that can prime adaptive immunity.

While IL-17A and IL-17C have known roles for recruiting neutrophils in vivo (86, 87), we found that IL-17D can recruit monocytes and neutrophils similar to IL-17A, while differentially recruiting NK cells in a mouse air pouch model of inflammation. This process was dependent on the stimulation of MCP-1, which was required for NK cell recruitment to mouse air pouches and for IL-17D mediated tumor rejection. Indeed we found that IL-17D increases NK cell infiltration by two fold in progressor tumors, which are required for rejection in immunocompetent host. Others have shown similar anti-tumor properties of MCP-1 as activation of immunosenescence in liver carcinoma induced MCP-1 and facilitated the increased infiltration of NK cells (88), while suppressing metastatic potential in another model of murine colon carcinoma (89). However, increased expression of MCP-1 can increase tumor growth in various tumor mouse models (90, 91), and MCP-1 serum levels are positively correlated with advanced breast cancer stage in human patients (92). Therefore, it is important to note that while IL-17D may have implications for treatment of fibrosarcoma and melanoma, its use in breast cancer may be limited. Indeed, we have found that overexpression of IL-17D in 4T1 tumors does not alter tumor growth in WT mice (data not shown). We have shown that IL-17D can be induced to reject small, established, tumors, but cannot reject larger, or more aggressive cancers. It has been shown that Tregs have a pro-tumoral role in mouse (6, 93, 94) and human (95-97) tumors, and can suppress LPS mediated activation of the innate immune system (98). It may be possible that Tregs present in large established tumors can suppress IL-17D mediated activation of the innate immune system. Others have shown that the immunohibitory functions of Tregs can be overcome by treatment with anti-CTLA4 (99) or anti-PD-1 (100) monoclonal antibodies to decrease

various forms of cancer growth in vivo. We therefore postulate that IL-17D can be used in conjunction with anti-CTLA4 and anti-PD-1 monoclonal antibodies to prime both the innate and adaptive arms of anti-tumor immunity to increase therapeutic efficacy.

We show that NK cell IFNy mediated the polarization of M1 macrophages in the tumor microenvironment (Chapter 1), and see a similar requirement for NK cells in modulating the polarization in progressor tumors overexpressing IL-17D, as we do not see IL-17D dependent differential polarization of M1 macrophages in $RAG2^{-/-}$ x $\gamma c^{-/-}$ hosts that are deficient in NK cells. Since NK cells do not show differential lysis of progressor tumors with differential levels of IL-17D, we favor the interpretation that NK cells serve as a source of IFNγ and polarize tumoricidal M1 macrophages that can stimulate adaptive immunity to progressor tumors in immunocompetent mice. We were unable to show the requirement of M1 macrophages in IL-17D mediated rejection as clodronate encapsulated liposomes failed to deplete macrophages in the tumor, while depleting $CD11b^{+}$ macrophages from tumor bearing spleens (data not shown). Furthermore, we have not been able to show that these M1 macrophages are in fact tumoricidal in our system (discussed in Chapter 1), but have shown increased levels of iNOS mRNA of M1 polarization that suggest these macrophages kill through secretion of NO, similarly to classically activated macrophages (19).

Although we have elucidated a role for IL-17D in tumor rejection and recruitment of innate immune cell in vivo, we still do not know the cellular target or receptor of IL-17D, and still do not understand the endogenous role of IL-17D. IL-17D has been shown to stimulate cytokine production from HUVEC cells in vitro (38), but we have failed to recapitulate this result in vitro (data not shown). We hypothesize that IL-17D does indeed

act on tumor endothelial cells to stimulate the production of MCP-1 in vivo. Future studies will profile the stimulatory effect of IL-17D on chemokine secretion of sorted endothelial cells from tumors and mouse air pouches, and biotinylated IL-17D will be used with lysates from these cells to indentify the cellular receptor for IL-17D. Interestingly, the composition of immune cells recruited by IL-17D is different from IL-17A, suggesting that these two cytokines evolved to induce specific arms of the immune response, presumably to deal with specific pathogen insults. Similar to IL-17C (87), the expression of IL-17D is in non-immune tissues and may mediate local anti-viral immunity through the recruitment of NK cells. Future studies will be performed profiling the susceptibility of IL-17D KO mice to viral infections, and other pro-inflammatory diseases. IL-17D may be regulated by NRF2, as NRF2 shows a conserved binding region on the IL-17D promoter (data not shown). Additionally, preliminary data suggests that hydrogen peroxide treatment of murine embryonic fibroblasts can induce IL-17D mRNA (data not shown), suggesting that IL-17D may be induced by NRF2 in response to oxidative stress. This leads us to hypothesize that tumors can become self-destructive by responding to increased cellular proliferation and oxidative stress by inducing NRF2 and IL-17D, which subsequently mediates their rejection through recruitment of NK cells by MCP-1. Future studies will elucidate whether progressor tumors display an impaired oxidative stress response as a mechanism of escape.

In summary, we document the generation and initial characterization of a novel set of unedited MCA-induced sarcoma cell lines that may be highly stimulatory for the innate immune system. The enhanced accumulation of M1 macrophages in these highly immunogenic tumors suggests that they can serve as models to study the early events that

lead to the generation of M1 macrophages in regressing tumors. We also show that the innate immune system in $RAG^{-/-}$ mice contains sufficient cellular machinery to perform sculpting of MCA-induced sarcomas. This cellular machinery includes NK cells that can actively edit the NKG2D ligand H60a and produce IFNγ to activate macrophages to function as innate editors. IL-17D can elicit simlar innate immune activation and facilitate tumor destruction in the presence of adaptive immunity while generating long-term protective immunity of the host. Finally, we introduce a quantitative dimension to the sculpting phase of cancer immunoediting by showing that the percentage of regressor cell lines generated from MCA-induced sarcomas is reproducible and correlates with the level of immune pressure in the tumor-bearing host.

MATERIALS AND METHODS

All experiments involving mice were conducted under animal protocols approved by the Washington University Animal Studies Committee and the University of California, San Diego Institutional Animal Care and Use Committee (IACUC protocol #S06201) and were in accordance with ethical guidelines determined by the Peter Mac Animal Experimental Ethics Committee.

Mice and MCA induction.

Tumor induction by MCA was performed as previously described (1). Briefly, cohorts of C57BL/6-strain WT (Taconic Farms), $RAG2^{-/-}$, $RAG1^{-/-}$, $IFNAR^{-/-}$, $RAG2^{-/-}$ x $STAT1^{-/-}$, and $RAG2^{-/-}$x $\gamma c^{-/-}$ mice were injected with MCA dissolved in peanut oil at various doses. Experiment 1 was performed in St. Louis and used $RAG2^{-/-}$x $\gamma c^{-/-}$ mice generated by breeding IL-$2R\gamma c^{-/-}$ mice (C57/BL6 N10+1F7-strain, Jackson Laboratories, San Diego, CA) to C57BL/6 $RAG2^{-/-}$ mice (Taconic Farms, Germantown, NY). Genotyping was performed using PCR (for IL-$2R\gamma_c$, Jackson Labs protocol, http://jaxmice.jax.org/strain/003174.html) or by Southern blot for RAG2. Genomic microsatellite analysis showed that the $RAG2^{-/-}$x $\gamma c^{-/-}$ mice contained C57BL/6 markers at 97% of the loci tested (3% 129/Sv markers).

To control for inter-institutional breeding, minor strain differences, and housing variability,the $RAG2^{-/-}$ mice used in MCA experiment 1 were outcrossed from ($RAG2^{-/-}$x

$\gamma c^{-/-}$) x $RAG2^{-/-}$ breeding performed in-house. Tumors in mice were measured as described (1). In experiment 1, a dose of MCA was used such that all MCA-treated mice developed tumors. Experiment 2 was performed at the Peter Mac facility in Australia and used $RAG2^{-/-}$x $\gamma c^{-/-}$ mice provided by WEHI (Bundoora) and C57BL/6 and $RAG1^{-/-}$ mice. To rule out that $RAG2^{-/-}$x $\gamma c^{-/-}$ tumor cell lines were rejected based on minor strain differences, we also transplanted $RAG2^{-/-}$x $\gamma c^{-/-}$ regressor cell lines into F1 (C57BL/6 x 129) mice (n=30) (Taconic Farms) and obtained identical growth patterns as in C57BL/6 mice (NCI-Frederick Rockville, MD). For some tumor transplantation experiments, $RAG2^{-/-}$x $\gamma c^{-/-}$ recipient mice were purchased from Taconic Farms. No differences in tumor growth were observed in $RAG2^{-/-}$x $\gamma c^{-/-}$ recipient mice purchased from Taconic Farms or bred in-house.

We discovered in the process of routine genotyping of our mice for the current study that the $RAG2^{-/-}$ 129/Sv mice previously obtained from Taconic Farms (RAGN12 model) and used in our 2001 publication (1) contained the C57BL/6 NK-C locus. Microsatellite analysis confirmed that these mice were virtually congenic at the NK-C locus and contained approximately 22 cM of C57BL/6 sequence encompassing the following genes/markers: D6MIT261, D6MIT105, D6MIT018, D6MIT111, Nkrp1a, Nkrp1c, CD69, Nkg2d, Nkg2a, and Ly49a. These mice were therefore designated 129/SvEv.cNK-C.B6 $RAG2^{-/-}$ mice.

Since the NK-C gene locus displays allelic polymorphism and can contribute to part of the difference in NK cell activity between the C57BL/6 and 129/Sv strain,new sets of MCA-induced sarcomas were generated using $RAG2^{-/-}$ mice that had been bred by Taconic Farms to be on a pure 129/SvEv background (129S6/SvEvTac-*Rag2*^{tm1Fwa}). This

new set of MCA-induced sarcomas was published in reference 27 and further studied in Figure 3.

Cell lines and mice.

MCA-induced and passaged daughter sarcomas were isolated and passaged *in vitro* as described (1). Briefly, tumor chunks were made into single cell suspensions by mincing and collagenase treatment in HBSS (type IA 1 mg/mL, Sigma, St. Louis, MO), and multiple vials were frozen at passage 2. For transplantation and cytotoxicity assays, passage 2 cell lines were thawed, expanded, and studied at passage 4-8. Cell lines were maintained in RPMI 1640 (Cambrex, East Rutherford, NJ) supplemented with 10% FCS (Hyclone, Logan, UT) as previously described (1). The IFNAR-/- MCA sarcoma cell line d100 was passaged through RAG2-/- mice and cell lines were generated from harvested tumor masses. The passaged cell lines which were now progressors were transduced with a retrovirus expressing either green fluorescent protein (GFP), or GFP and H60a, and sorted as a >95% GFP+ population using a FACS Aria cell sorter. 129/Sv, C56BL/6 x 129/Sv F1, 129/Sv RAG2$^{-/-}$, C56BL/6 RAG2$^{-/-}$, C56BL/6 RAG2$^{-/-}$x γc$^{-/-}$ mice used were used for tumor transplantation experiments.

Tumor transplantation.

Subconfluent tumor cell lines were harvested by trypsinization, washed 3x with PBS, and injected at $1x10^6$, $5x10^6$, $10x10^6$, or $3x10^6$ regressor:$1.5x10^6$ progressor mixture subcutaneously into recipient C57BL/6, (129/Sv x C57BL/6) F1, $RAG2^{-/-}$ or $RAG2^{-/-}$ x $\gamma c^{-/-}$ strain mice as described (1). $RAG2^{-/-}$ or WT mice were injected i.p. with 200 mg of either control hamster IgG (PIP), control mouse IgG (2A3), anti-NK1.1 (PK136), anti-MCP-1, anti-ASGM1, anti-NKG2D, or anti-IFN-g (H22) on days -2 and 0 and every four days after until tumor harvest. $RAG2^{-/-}$ x $\gamma c^{-/-}$ mice were injected i.p. with 200 mg either control rat IgG or anti-CD40 agonist (FGK 45.5) on day 5. NK cell and neutrophil depletion was verified by FACS anlaysis of both spleen and tumor cell suspensions at the indicated time of harvest. For conditional expression of IL-17D in tumors in vivo, mice were administered either doxycycline (200μg/ml) (Sigma, St. Louis, MO) treated water or regular drinking water on various days post tumor transplant. Mice were monitored for tumor growth by measurement of mean tumor diameter, defined as the average of the 2 maximum dimensions of the tumor mass.

Microarray and Clustering Analysis.

Using transplantation assays, we reported that all of the tested 17 primary fibrosarcomas from wild type mice were poorly immunogenic and formed progressively growing tumors in immunocompetent naïve hosts when 1 x 10^6 cells were injected subcutaneously[1]. We designated those as WT tumors and randomly selected 8 (H128m, d4m3, F279, H118, F236, d22m1, F244, and d22m2) for microarray analysis. Sixty percent (12/20) of the $RAG2^{-/-}$ mice-derived tumors also formed progressively growing tumors in naïve host[1]. We designated those as $RAG2^{-/-}$ progressors and selected 8 (d29m1, F221, d57, d53, d30m1, d28m3, H50, and H52) randomly for analysis. In contrast, 40% (8/20) of $RAG2^{-/-}$ mice-derived tumors were significantly more immunogenic and were rejected in immunocompetent naïve mice even at high dose inoculation of tumor challenge[1]. We designated those as $RAG2^{-/-}$ regressors and 8 (d38m2, F510, F535, d42m1, F515, H31m1, d27m2, and d30m4) were used in analysis. Tumor cells were thawed and cultured for 4 or 5 days, and total RNA was extracted using Trizol reagent (Invitrogen, Carlsbad, CA) and prepared using the RNA-Bee protocol (Tel-Test, Friendswood, TX). With 20mg of total RNA, cDNA was synthesized by Super Script Choice System (Gibco BRL Life Technologies, Grand Island, NY) with T7-(dT)24 Primer (Genset Corp, San Diego, CA), and was cleaned up by Phase Lock Gels (Eppendorf-5 Prime, Inc., Boulder, CO) with Phenol/chloroform/isoamyl alcohol (Ambion, Grand Island, NY). Biotin-labeled cRNA was synthesized by BioArray HighYield RNA Transcript Labeling Kit (Enzo, Farmingdale, NY), and cleaned up by RNeasy Mini Kit (Qiagen, Valencia, CA). Murine Genome U74v2 Set GeneChip Arrays

(Affymetrix, Santa Clara, CA) were hybridized with Biotin-labeled cRNA with GeneChip Hybridization Oven 320 (Affymetrix, Santa Clara, CA), and washed and stained with GeneChip Fluidics Station 400 (Affimetrix, Santa Clara, CA). Gene signals were scanned by GeneArray Scanner (Hewlett Packard, Palo Alto, CA), and differential expression data was analyzed on Microarray Suit Software (Affymetrix, Santa Clara, CA). Data was normalized, statistically analyzed, and clustered by DecisionSite for Functional Genomics (Spotfire, Somerville, MA).

Generation of IL-17D deficient and overexpressing tumor cell lines.

Daughter ctrl and sh17D regressor tumor cell lines were generated by transducing parental regressor tumor cell lines with either a retrovirus-expressing scramble sequence (shctrl) or retroviruses expressing shRNA's specific for the 3'UTR and coding sequence of IL-17D and selected on puromyocin supplemented media for 1 week. Daughter ctrl and ex17D progressor tumor cell lines were generated by either transducing parental progressor tumor cell lines with an empty vector lentivirus (ctrl) or a lentivirus-expressing IL-17D cDNA and selected on blastocydin supplemented media for 1 week. Conditional expressing IL-17D daughter progressor tumor cell lines were generated by transducing parental F244 progrssor tumor cell line with a lentivirus-expressing the tet repressor and selected on blastocydin for 1 week. Resulting cells were then trasnduced with a lentivirus-expressing IL-17D regulated by the tet operator sequence and selected on puromyocin supplemeted media for 1 week.

Antibodies and FACS analysis.

On various days post-transplantation, tumors were excised from mice, minced, and treated with 1 mg/mL type IA collagenase (Sigma) as described (1). Cells were vigorously resuspended, washed in FACS buffer (PBS+1% FCS+0.05%NaN_3, Sigma) and filtered before staining. Antibodies to CD45, F4/80, NK1.1, CD69, CD80, CD206, Ly6C, CD11b, I-A/I-E , 1A8, and steptavidin PE were from BD PharMingen (San Diego, CA). Staining was conducted for 15-20 minutes at 4º in FACS tubes containing 1-2 million total cells, 0.5-1 ml of antibody, 1 ml of FC block (anti-CD16/32), and 100 ml of FACs buffer. 7AAD (Calbiochem) or Propidium Iodide (Sigma) was added at 1 mg/mL immediately prior to FACS analysis. M1-type and M2-type macrophages were gated as published (41). Cells were harvest with dPBS or HBSS supplemented with 2.5 mM EDTA. Trypsin was not used since it decreased NKG2D tetramer staining, presumably by cleaving the ligands. NKG2D tetramers were generated as described (20). Monoclonal antibodies to H60a, pan-RAE-1, and MULT1 were obtained from R&D (Minneapolis, MN). Secondary antibodies were obtained from Biolegend (San Diego, CA). For intracellular IL-17D staining, cells were either incubated with or without 2μM monensin (Sigma, St. Loius, MO) and 1μg/ml Brefeldin A (BD biosciences, San Jose, CA) and then harvested by trypsinization, washed once with PBS, incubated with Cytofix (BD biosciences, San Jose, CA) for 15 min at 4^o, washed twice with Perm wash (BD biosciences, San Diego) solution, and anti-IL17D (R&D Systems, Minneapolis, MN) or

rat IgG2a isotype control (eBioscience, San Diego, CA) monoclonal antibodies were added. Staining was conducted for 30 minutes at 4º in FACS tubes containing 0.5-2 million total cells, 0.5-1 ml of antibody, and 100 ml of FACs buffer (PBS+1% FCS+0.09% NaN_3, Sigma, St. Louis, MO). Cells were washed twice with Perm wash and then resuspended in FACS stain buffer. All analyses were done on live cells identified by forward and side scatter properties with a FACScanto II (BD Biosciences, San Jose, CA). IL-17D mean channel shift (MCS) is given as isotype staining subtracted from signal values. % Control mean channel shift (% of Ctrl MCS) is normalized to control sample mean channel shift values.

Generation of tumor cell line cDNA libraries and quantitative PCR.

Tumor cell lines were plated in triplicate at 6 x 10^4 cells/well in a 6 well plate and incubated for 48 hours at 37^o. Supernatant was aspirated and cells were washed twice with PBS before addition of 1ml Trizol reagent (Invitrogen, Carlsbad, CA) and RNA was prepeared using the RNA-Bee protocol (Tel-Test, Friendswood, TX). cDNA was prepared using the Applied Biosystems protocol (Branchburg, NJ). Relative qPCR was done using IL-17D specific Taqman FAM probes (Invitrogen, Carlsbad, CA) with internal GAPDH-VIC probe controls and amplified using a 7300 Real Time PCR System (Applied Biosystems, Branchburg, NJ). IL-17D transcript was quantified relative to GAPDH expression using the equation $2^{-(\Delta Ct)}$.

Immunohistochemistry.

Fresh tumor nodules were harvested, OCT-embedded, and snap frozen in cooled isopentane. Tissue blocks were cut on a cryostat into 6 μm-thick sections, mounted onto poly-L-Lysine slides, air-dried overnight, and post-fixed for 10' in acetone before staining. Purified rat anti-mouse CD16/CD32 was used as Fc block for 20' (BD Pharmingen; dilution 1:50) when appropriate. Biotin-conjugated rat anti-mouse I-A/I-E (eBioscience; dilution 1:100, 1 hr at rt) and biotin-conjugated rat anti-mouse CD206 (Biolegend; dilution 1:100, 1 hr at rt) staining was revealed using streptavidin-HRP (Vector Laboratoies; 30 minutes at rt) followed by amino-ethyl-carbazole as chromogen (BD; 10-15min at rt). Purified rat anti-mouse CD68 (Biolegend; dilution 1:100) staining was detected using a biotin-conjugated rabbit polyclonal anti-rat IgG, mouse adsorbed (Vector; dilution 1:200). Immunostained tissue sections were examined with a Leica DM 2500 or Nikon Eclipse E800 microscope; images were captured with a Leica DFC 420 or Nikon DXM 1200 digital camera, respectively. Quantitative analysis of MHC-II$^+$, CD68$^+$, CD206$^+$ cells was obtained by counting at least 10 high power fields (HPF) of tissue sections at 200x magnification.

Cytokine Secretion Assay.

On various days post-transplantation, tumors were excised from mice, minced, and treated with 1 mg/mL type IA collagenase (Sigma). Filtered tumor/immune cell suspensions were plated in triplicate wells at 40,000 cells/well in 100 mL for 24 hrs at 37^{o}C. Supernatant was analyzed for cytokines using the mouse inflammation cytometric bead array kit from BD Biosciences (San Jose, CA).

Chromium release assay.

Splenocytes from RAG2-/- mice were activated by culturing in media with 1000 U/ml human IL-2 (Chiron, Emeryville, CA). Day 7 IL-2-activated NK effector cells were used in a 4-hour 51Cr release assay using tumor target cells labeled with 51Cr as described (20) with either control IgG or anti-NKG2D. Bars depict standard error of triplicates. All experiments were done at least twice. ANOVA was used to assess statistical significance between parent and passaged cell lines.

Mouse air pouch experiments.

C56BL/6 x 129/Sv F1 mice were injected s.c with 3ml of sterilized air filtered through a 0.2μm Millipore filter (Bellerica, MA) to form air pouches on day 0 and re-

inflated again on day 3. On day 7, either 1ml of LPS (1μg/ml), 1ml of rmIL-17A (5μg/ml) (R&D Systems, Minneapolis, MN), 1ml of rmIL-17D (5μg/ml) (R&D Systems, Minneapolis, MN), 1ml rmIL-17D (5μg/ml) (Mayfield Lab), 1ml of rmMCP-1 (5μg/ml) (Peprotech, Rocky Hill, NJ), or 1ml of rmIL-17D (5μg/ml) and anti-MCP-1 polyclonal antibodies (25μg/ml) (R&D Systems, Minneapolis, MN) was injected into mouse air pouches 8h before air pouch harvest. Air pouches were lavaged with 2ml PBS and centrifuges at 1250 rpm for 5 min at room temperature. Supernatant was harvested and analyzed for chemokine protein levels using the mouse chemokine flowcytomix kit from eBioscience (San Diego, CA). Infiltrating air pouch cells were resuspended in FACS stain buffer, counted on a hemocytometer, incubated with antibodies against CD45, CD4, CD8, B220, CD11c, DX5, NK1.1, MAC1, Ly6G, and I-A/I-E for 15 min at 4^{o}, washed, and resuspended in FACS buffer containing 1ug/ml 7AAD (Sigma, St Lous, MO) to identify viable cells before analysis. Total number of infiltrating immune cell subsets were calculated from percentages obtained from FACS analysis of the total cell count for each sample.

Chemokine Secretion Assay.

On days 7 and 14 post-transplantation, tumors were excised from mice, minced, and treated with 1 mg/mL type IA collagenase (Sigma, St Louis, MO) as described[6]. Filtered tumor/immune cell suspensions were plated in triplicate wells at 40,000 cells/well in 100 mL for 24 hrs at 37^{o}C. Supernatant was analyzed for chemokines using the mouse chemokine flowcytomix kit from eBioscience (San Diego, CA).

NK cell kill assay.

Splenocytes from RAG2$^{-/-}$ mice were activated by culturing in media with 1000 U/ml human IL-2 (Chiron, Emeryville, CA). Day 7 IL-2-activated NK effector cells were centrifuged with CFSE labeled tumor cell lines at varying ratios and incubated for 6h at 37^{o}. Cells were washed and resuspended in FACS buffer containing 1ug/ml 7AAD (Sigma, St Louis, MO) to identify viable cells. % Specific target lysis is given as the percentage of CFSE+7AAD+ cells by FACS analysis.

Chemotaxis assay.

In vitro chemotaxis was performed using indicated tumor supernatant or 600μl of RPMI+ 0.5% FBS supplemented with varying doses of either rmIL-17D, or 100ng/ml MCP-1 added to 24 well plates with 5um polycarbonate membrane filter added on top. 5 x 10^5 WT bone marrow cells were added in 100μl of RPMI+0.5%FBS or complete media, added on the top of the membrane, and incubated at 37^{o} for 3h. Migrated cells were harvested by removing transwells and collecting suspended cells in the bottom well. Cells were resuspended in FACS stain buffer, incubated with antibodies against CD45, CD4, CD8, B220, CD11c, DX5, NK1.1, MAC1, Ly6G, and I-A/I-E for 15 min at 4^{o}, washed, and resuspended in FACS buffer containing 1μg/ml 7AAD (Sigma, St Louis, MO) to identify viable cells before analysis. Total viable migrating cell counts were

acquired by complete sample collection under a constant flow rate and analyzed by FACS analysis.

In vitro growth assay.

Various tumor cell lines were seeded in 96 well plates at 5 x 10^3 cells in 200µl and incubated at 37^o and expanded when necessary. At indicated time points cells were harvested by trypsinization, washed and counted using a hemocytometer.

Statistical Analysis.

Statistical significance between two groups was determined by the Welch's t-test using two-tailed analysis to obtain p-values. The Log-Rank test was used to compare the survival of mice across tumor transplantation or induction conditions. Error bars are depicted using standard error (SEM). All experiments were done at least twice.

REFERENCES

1. Shankaran, V. et al. IFNy and lymphocytes prevent primary tumor development and shape tumor immunogenicity. Nature 410, 1107–1111 (2001).

2. Dunn, G. P., Bruce, A. T., Ikeda, H., Old, L. J. & Schreiber, R. D. Cancer immunoediting: from immunosurveillance to tumor escape. Nature Immunol. 3, 991–998 (2002).

3. Koebel, C. M. et al. Adaptive immunity maintains occult cancer in an equilibrium state. Nature 450, 903–907 (2007).

4. Vesely, M. D., Kershaw, M. H., Schreiber, R. D. & Smyth, M. J. Natural innate and adaptive immunity to cancer. Annu. Rev. Immunol. 29, 235–271 (2011).

5. Schreiber, R. D., Old, L. J. & Smyth, M. J. Cancer immunoediting: integrating immunity's roles in cancer suppression and promotion. Science 331, 1565–1570 (2011).

6. Bui, J.D., Uppaluri, R., Hsieh, C.S. & Schreiber, R.D. Comparative analysis of regulatory and effector T cells in progressively growing versus rejecting tumors of similar origins. Cancer Res 66, 7301-7309 (2006).

7. Boon T. et al. Tumor Antigens Recognized by T lymphocytes. Annu. Rev. Immunol. 12, 337-365 (1994).

8. Bruggen, P. van der & Eynde, B.J. van der. T cell defined tumor antigens. Current Opinion in Immunol. 9, 684-693 (1997).

9. Dunn, G.P., A.T. Bruce, K.C.F. Sheehan, V. Shankaran, R. Uppaluri, J.D. Bui, M.S. Diamond, C.M. Koebel, C. Arthur, J.M. White, and R.D. Schreiber. A critical function for type I interferons in cancer immunoediting. Nature Immunology. 6:722–729 (2005).

10. Dunn, G., L. Old, and R. Schreiber.The immunobiology of cancer immunosurveillance and immunoediting. Immunity. 21:137–148 (2004). Smyth, M., and N. Crowe. NK cells and NKT cells collaborate in host protection from methylcholanthrene-induced fibrosarcoma. International. Immunology. 13:459-463 (2001).

11. Smyth, M.J., G.P. Dunn, and R.D. Schreiber. Cancer immunosurveillance and immunoediting: the roles of immunity in suppressing tumor development and shaping tumor immunogenicity. Advances in Immunology. 90:1–50 (2006).

12. Smyth, M.J., J. Swann, E. Cretney, N. Zerafa, W.M. Yokoyama, and Y. Hayakawa. NKG2D function protects the host from tumor initiation. The Journal of Experimental Medicine. 202:583–588 (2005).

13. Street, S.E.A., Y. Hayakawa, Y. Zhan, A.M. Lew, D. MacGregor, A.M. Jamieson, A. Diefenbach, H. Yagita, D.I. Godfrey, and M.J. Smyth. Innate immune surveillance of spontaneous B cell lymphomas by natural killer cells and gammadelta T cells. The Journal of Experimental medicine. 199:879–884 (2004).

14. Crowe, N.Y., M.J. Smyth, and D.I. Godfrey. A Critical Role for Natural Killer Cells in Immunosurveillance of Methylcholanthrene-induced Sarcomas. Journal of Experimental Medicine. 196:119-127 (2002).

15. Takeda, K., M. Smyth, and E. Cretney. Critical role for tumor necrosis factor–related apoptosis-inducing ligand in immune surveillance against tumor development. The Journal of Experimental Medicine. 195:161-169 (2002).

16. Smyth, M.J., Y. Hayakawa, K. Takeda, and H. Yagita. New aspects of natural-killer-cell surveillance and therapy of cancer. Nature Reviews Cancer. 2:850–861 (2002).

17. Raulet, D.H., and N. Guerra. Oncogenic stress sensed by the immune system: role of natural killer cell receptors. Nature Reviews Immunology. 9:568–580 (2009).

18. Sica, A., P. Larghi, A. Mancino, L. Rubino, C. Porta, M.G. Totaro, M. Rimoldi, S.K. Biswas, P. Allavena, and A. Mantovani. Macrophage polarization in tumour progression. Seminars in Cancer Biology. 18:349–355 (2008).

19. Lewis, C., and J. Pollard. Distinct role of macrophages in different tumor microenvironments. Cancer Research. 66:605-612 (2006).

20. Gordon, S. Monocyte and macrophage heterogeneity. Nature Reviews Immunology. 5:953-964 (2005).

21. Bauer, S., V. Groh, J. Wu, A. Steinle, J. H. Phillips, L. L. Lanier, and T. Spies. Activation of NK cells and T cells by NKG2D, a receptor for stress-inducible MICA. Science 285:727-729 (1999).

22. Cerwenka, A., and L. L. Lanier. Natural killer cells, viruses and cancer. Nat Rev Immunol 1:41-49 (2001).

23. Raulet, D. H. Roles of the NKG2D immunoreceptor and its ligands. Nat Rev Immunol 3:781-790 (2003).

24. Guerra, N., Y. X. Tan, N. T. Joncker, A. Choy, F. Gallardo, N. Xiong, S. Knoblaugh, D. Cado, N. R. Greenberg, and D. H. Raulet. NKG2D-deficient mice are defective in tumor surveillance in models of spontaneous malignancy. Immunity 28:571-580 (2008).

25. Smyth, M. J., J. Swann, E. Cretney, N. Zerafa, W. M. Yokoyama, and Y. Hayakawa. NKG2D function protects the host from tumor initiation. The Journal of experimental medicine 202:583-588 (2005).

26. Groh, V., J. Wu, C. Yee, and T. Spies. Tumour-derived soluble MIC ligands impair expression of NKG2D and T-cell activation. Nature 419:734-738 (2002).

27. Gasser, S., S. Orsulic, E. J. Brown, and D. H. Raulet. The DNA damage pathway regulates innate immune system ligands of the NKG2D receptor. Nature 436:1186-1190 (2005).

28. Yokoyama, W. M. Now you see it, now you don't! Nature immunology 1:95-97 (2000).

29. Cerwenka, A., A. B. Bakker, T. McClanahan, J. Wagner, J. Wu, J. H. Phillips, and L. L. Lanier. Retinoic acid early inducible genes define a ligand family for the activating NKG2D receptor in mice. Immunity 12:721-727 (2000).

30. Diefenbach, A., A. M. Jamieson, S. D. Liu, N. Shastri, and D. H. Raulet. Ligands for the murine NKG2D receptor: expression by tumor cells and activation of NK cells and macrophages. Nature immunology 1:119-126 (2000).

31. Malarkannan, S., P. P. Shih, P. A. Eden, T. Horng, A. R. Zuberi, G. Christianson, D. Roopenian, and N. Shastri. The molecular and functional characterization of a dominant minor H antigen, H60. J Immunol 161:3501-3509 (1998).

32. Carayannopoulos, L.N., O.V. Naidenko, D.H. Fremont, W.M. Yokoyama. CuttingEdge: murine UL-16-binding protein-like transcript 1: a newly described transcript encoding a high affinity ligand for murine NKG2D. J. immunol. 169: 4079-4083 (2002).

33. Diefenbach, A., E. R. Jensen, A. M. Jamieson, and D. H. Raulet. Rae1 and H60 ligands of the NKG2D receptor stimulate tumour immunity. Nature 413:165-171 (2001).

34. Girardi, M., D. E. Oppenheim, C. R. Steele, J. M. Lewis, E. Glusac, R. Filler, P. Hobby, B. Sutton, R. E. Tigelaar, and A. C. Hayday. Regulation of cutaneous malignancy by gammadelta T cells. Science 294:605-609 (2001).

35. Fridlender ZG. Et al. Polarization of tumor-associated neutrophil phenotype by TGF-beta:"N1" versus "N2" TAN. Cancer Cell 16(3), 173-174 (2009).

36. Zou W. & Chen L. Inhibitory B7-family molecules in the tumor microenvironment. Nature Reviews Immunology 8, 467-477 (2008).

37. Starnes, T., Broxmeyer, H.E., Robertson, M.J. & Hromas, R. Cutting edge: IL-17D, a novel member of the IL-17 family, stimulates cytokine production and inhibits hemopoiesis. J Immunol 169, 642-646 (2002).

38. Cao, X., E.W. Shores, J. Hu-Li, M.R. Anver, B.L. Kelsail, S.M. Russell, J. Drago, M. Noguchi, A. Grinberg, E.T. Bloom, W.E. Paul, S.I. Katz, P.E. Love, and W.J. Leonard. Defective lymphoid development in mice lacking expression of the common cytokine receptor γ chain. Immunity. 2:223–238 (1995).

39. Bui, J., L. Carayannopoulos, L. Lanier, W. Yokoyama, and R. Schreiber. IFN-dependent down-regulation of the NKG2D ligand H60 on tumors. The Journal of Immunology. 176:905 (2006).

40. Movahedi, K., D. Laoui, C. Gysemans, M. Baeten, G. Stange, J. Van Den Bossche, M. Mack, D. Pipeleers, P. In't Veld, P. De Baetselier, and J.A. Van Ginderachter. Different Tumor Microenvironments Contain Functionally Distinct Subsets of Macrophages Derived from Ly6C(high) Monocytes. Cancer Research. 70:5728–5739 (2010).

41. Rakhmilevich, A.L., I.N. Buhtoiarov, M. Malkovsky, and P.M. Sondel. CD40 ligation in vivo can induce T cell independent antitumor effects even against immunogenic tumors. Cancer Immunology, Immunotherapeutics. 57:1151–1160 (2008).

42. Buhtoiarov, I.N., H. Lum, G. Berke, D.M. Paulnock, P.M. Sondel, and A.L. Rakhmilevich. CD40 ligation activates murine macrophages via an IFN-gamma-dependent mechanism resulting in tumor cell destruction in vitro. The Journal of Immunology. 174:6013–6022 (2005).

43. Lum, H.D., I.N. Buhtoiarov, B.E. Schmidt, G. Berke, D.M. Paulnock, P.M. Sondel, and A.L. Rakhmilevich. Tumoristatic effects of anti-CD40 mAb-activated macrophages involve nitric oxide and tumour necrosis factor-alpha. Immunology. 118:261–270 (2006).

44. Samarakoon, A., H. Chu, and S. Malarkannan. 2009. Murine NKG2D ligands: "double, double toil and trouble". Molecular immunology 46:1011-1019 (2009).

45. Zhang, H., C. Hardamon, B. Sagoe, J. Ngolab, and J. D. Bui. Studies of the H60a locus in C57BL/6 and 129/Sv mouse strains identify the H60a 3'UTR as a regulator of H60a expression. Molecular immunology 48:539-545 (2010).

46. Matsushita H. et al. Cancer exome analysis reveals a T-cell-dependent mechanism of cancer immunoediting. Nature 482, 400-404 (2012).

47. Kelly, JM. et al. Induction of tumor-specific T cell memory by NK cell-mediated tumor rejection. Nat. Immunol. 3(1), 83-90 (2002).

48. Pelletier M. Bouchard A. & Girard D. In vivo and in vitro roles of IL-21 in inflammation. J Immunol 173, 7521-7530 (2004).

49. Roussel, L. et al. IL-17 Promotes p38 MAPK-Dependent Endothelial Activation Enhancing Neutrophil Recruitment to Sites of Inflammation. J Immunol. 184, 4531-4537 (2010).

50. Fidler, I. J. 1978. Tumor heterogeneity and the biology of cancer invasion and metastasis. Cancer Res 38:2651-2660 (1978).

51. Weinberg, R. A. The Biology of Cancer. Garland Science, Taylor & Francis Group, LLC, New York. (2006).

52. Reya, T., S. J. Morrison, M. F. Clarke, and I. L. Weissman. Stem cells, cancer, and cancer stem cells. Nature 414:105-111 (2001).

53. Kuwai, T., T. Nakamura, S. J. Kim, T. Sasaki, Y. Kitadai, R. R. Langley, D. Fan, S. R. Hamilton, and I. J. Fidler. Intratumoral heterogeneity for expression of tyrosine kinase growth factor receptors in human colon cancer surgical specimens and orthotopic tumors. Am J Pathol 172:358-366 (2008).

54. Yang, J., S. A. Mani, J. L. Donaher, S. Ramaswamy, R. A. Itzykson, C. Come, P. Savagner, I. Gitelman, A. Richardson, and R. A. Weinberg. Twist, a master regulator of morphogenesis, plays an essential role in tumor metastasis. Cell 117:927-939 (2004).

55. Mani, S. A., W. Guo, M. J. Liao, E. N. Eaton, A. Ayyanan, A. Y. Zhou, M. Brooks, F. Reinhard, C. C. Zhang, M. Shipitsin, L. L. Campbell, K. Polyak, C. Brisken, J. Yang, and R. A. Weinberg. The epithelial-mesenchymal transition generates cells with properties of stem cells. Cell 133:704-715 (2008).

56. Dexter, D. L., and J. T. Leith. Tumor heterogeneity and drug resistance. J Clin Oncol 4:244-257 (1986).

57. Gupta, P. B., C. L. Chaffer, and R. A. Weinberg. Cancer stem cells: mirage or reality? Nat Med 15:1010-1012 (2009).

58. Shipitsin, M., L. L. Campbell, P. Argani, S. Weremowicz, N. Bloushtain-Qimron, J. Yao, T. Nikolskaya, T. Serebryiskaya, R. Beroukhim, M. Hu, M. K. Halushka, S. Sukumar, L. M. Parker, K. S. Anderson, L. N. Harris, J. E. Garber, A. L. Richardson, S. J. Schnitt, Y. Nikolsky, R. S. Gelman, and K. Polyak. Molecular definition of breast tumor heterogeneity. Cancer Cell 11:259-273 (2007).

59. Nguyen, K. B., T. P. Salazar-Mather, M. Y. Dalod, J. B. Van Deusen, X. Q. Wei, F. Y. Liew, M. A. Caligiuri, J. E. Durbin, and C. A. Biron. Coordinated and distinct roles for IFN-alpha beta, IL-12, and IL-15 regulation of NK cell responses to viral infection. J Immunol 169:4279-4287 (2002).

60. Jaiswal, S., C. H. Jamieson, W. W. Pang, C. Y. Park, M. P. Chao, R. Majeti, D. Traver, N. van Rooijen, and I. L. Weissman. CD47 is upregulated on circulating hematopoietic stem cells and leukemia cells to avoid phagocytosis. Cell 138:271-285 (2009).

61. Dong, H., S. E. Strome, D. R. Salomao, H. Tamura, F. Hirano, D. B. Flies, P. C. Roche, J. Lu, G. Zhu, K. Tamada, V. A. Lennon, E. Celis, and L. Chen. Tumor-associated B7-H1 promotes T-cell apoptosis: a potential mechanism of immune evasion. Nat Med 8:793-800 (2002).

62. Logsdon, C. D., M. K. Fuentes, E. H. Huang, and T. Arumugam. RAGE and RAGE ligands in cancer. Curr Mol Med 7:777-789 (2007).

63. Whang, M. I., N. Guerra, and D. H. Raulet. Costimulation of dendritic epidermal gammadelta T cells by a new NKG2D ligand expressed specifically in the skin. J Immunol 182:4557-4564 (2009).

64. Groh, V., K. Smythe, Z. Dai, and T. Spies. Fas-ligand-mediated paracrine T cell regulation by the receptor NKG2D in tumor immunity. Nat Immunol 7:755-762 (2006).

65. Stern-Ginossar, N., C. Gur, M. Biton, E. Horwitz, M. Elboim, N. Stanietsky, M. Mandelboim, and O. Mandelboim. Human microRNAs regulate stress-induced immune responses mediated by the receptor NKG2D. Nat Immunol 9:1065-1073 (2008).

66. Yadav, D., J. Ngolab, R. S. Lim, S. Krishnamurthy, and J. D. Bui. Cutting edge: down-regulation of MHC class I-related chain A on tumor cells by IFN-gamma-induced microRNA. J Immunol 182:39-43 (2009).

67. Venkataraman, G. M., D. Suciu, V. Groh, J. M. Boss, and T. Spies. Promoter region architecture and transcriptional regulation of the genes for the MHC class I-related chain A and B ligands of NKG2D. J Immunol 178:961-969 (2007).

68. Hibbs, J.B., L.H. Lambert, and J.S. Remington. Resistance to murine tumors conferred by chronic infection with intracellular protozoa, Toxoplasma gondii and Besnoitia jellisoni. Journal of Infectious Disease 124:587–592 (1971).

69. Hibbs, J., and L. Lambert. Control of carcinogenesis: a possible role for the activated macrophage. Science. 177:998-1000 (1972).

70. Pace, J., S. Russell, and R. Schreiber. Macrophage activation: priming activity from a T-cell hybridoma is attributable to interferon-gamma. Proceedings of the National Academy of Sciences. 80:3782-3786 (1983).

71. Schreiber, R., J. Pace, and S. Russell. Macrophage-activating factor produced by a T cell hybridoma: physiochemical and biosynthetic resemblance to gamma-interferon. The Journal of Immunology. 131:826-832 (1983).

72. Weinberg, J.B., H.A. Chapman, and J.B. Hibbs. Characterization of the effects of endotoxin on macrophage tumor cell killing. The Journal of Immunology. 121:72–80 (1978).

73. Kleinerman, E., K. Erickson, A. Schroit, and W. Fogler. Activation of tumoricidal properties in human blood monocytes by liposomes containing lipophilic muramyl tripeptide. Cancer Research.136:2311-2317 (1983).

74. Gazit, R., R. Gruda, M. Elboim, T.I. Arnon, G. Katz, H. Achdout, J. Hanna, U. Qimron, G. Landau, E. Greenbaum, Z. Zakay-Rones, A. Porgador, and O. Mandelboim. Lethal influenza infection in the absence of the natural killer cell receptor gene Ncr1. Nature Immunology. 7:517–523 (2006).

75. Gilfillan, S., C.J. Chan, M. Cella, N.M. Haynes, A.S. Rapaport, K.S. Boles, D.M. Andrews, M.J. Smyth, and M. Colonna. DNAM-1 promotes activation of cytotoxic lymphocytes by nonprofessional antigen-presenting cells and tumors. Journal of Experimental Medicine. 205:2965–2973 (2008).

76. Iguchi-Manaka, A., H. Kai, Y. Yamashita, K. Shibata, S. Tahara-Hanaoka, S.I. Honda, T. Yasui, H. Kikutani, K. Shibuya, and A. Shibuya. Accelerated tumor growth in mice deficient in DNAM-1 receptor. Journal of Experimental Medicine. 205:2959–2964 (2008).

77. Street, S.E.A. Perforin and interferon-gamma activities independently control tumor initiation, growth, and metastasis. Blood. 97:192–197 (2001).

78. van den Broek, M.E., D. Kägi, F. Ossendorp, R. Toes, S. Vamvakas, W.K. Lutz, C.J. Melief, R.M. Zinkernagel, and H. Hengartner. Decreased tumor surveillance in perforin-deficient mice. The Journal of Experimental Medicine. 184:1781–1790 (1996).

79. Cretney, E., K. Takeda, H. Yagita, M. Glaccum, J.J. Peschon, and M.J. Smyth. Increased susceptibility to tumor initiation and metastasis in TNF-related apoptosis-inducing ligand-deficient mice. The Journal of Immunology. 168:1356–1361 (2002).

80. Majeti, R., M.P. Chao, A.A. Alizadeh, W.W. Pang, S. Jaiswal, K.D. Gibbs Jr, N. van Rooijen, and I.L. Weissman. CD47 Is an Adverse Prognostic Factor and Therapeutic Antibody Target on Human Acute Myeloid Leukemia Stem Cells. Cell. 138:286–299 (2009).

81. Chao, M.P., S. Jaiswal, R. Weissman-Tsukamoto, A.A. Alizadeh, A.J. Gentles, J. Volkmer, K. Weiskopf, S.B. Willingham, T. Raveh, C.Y. Park, R. Majeti, and I.L. Weissman. Calreticulin Is the Dominant Pro-Phagocytic Signal on Multiple Human Cancers and Is Counterbalanced by CD47. Science Translational Medicine. 2:63ra94–63ra94 (2010).

82. Zitvogel, L., O. Kepp, L. Senovilla, L. Menger, N. Chaput, and G. Kroemer. Immunogenic tumor cell death for optimal anticancer therapy: the calreticulin exposure pathway. Clinical Cancer Research. 16:3100 (2010).

83. Numasaki M, Fukushi J, Ono M, et al. Interleukin-17 promotes angiogenesis and tumor growth. Blood. 101(7): 2620-2627 (2003).

84. Benchetrit F, Ciree A, Vives V, et al. Interleukin-17 inhibits tumor cell growth by means of a T-cell-dependent mechanism. Blood. 99:2114-2121 (2002).

85. Miyamoto M, Prause O, Sjostrand M, et al. Endogenous IL-17 as a mediator of neutrophil recruitment caused by endotoxin exposure in mouse airways. J Immunol. 170:4665-4672 (2003).

86. Ramirez-Carozzi V. et al. IL-17C regulates the innate immune function of epithelial cells in an autocrine manner. Nat. Immunol. 12, 1159-1166 (2011).

87. Xue, W. et al. Senescence and tumour clearance is triggered by p53 restoration in murine liver carcinomas. Nature. 445:656–660 (2007).

88. Huang S, Singh RK, Xie K, Gutman M et al. Expression of the JE/MCP-1 gene suppresses metastatic potential in murine colon carcinoma cells. Cancer Immunol. Immunother. 39: 231–8 (1994).

89. Nakashima E, Mukaida N, Kubota Y, Kuno K, et al. Human MCAF gene transfer enhances the metastatic capacity of a mouse cachectic adenocarcinoma cell line in vivo. Pharm Res 12:1598–604 (1995).

90. Stathopouloulos G, Psallidas A, Moustaki A, Moschos C, et al. A central role for tumor-derived monocyte chemoattractant proetin-1 in malignant pleural effusion. J. Natl. Cancer Inst. 100:1464-1476 (2008).

91. Lebrecht A, Grimm C, Lantzsch T, Ludwig E, et al. Monocyte chemoattractant protein-1 serum levels in patients with breast cancer. Tumour Biol 25:14–7 (2004).

92. Onizuka S, Tawara I, Shimizu J, Sakaguchi S, Fujita T, & Nakayama E. Tumor rejection by in vivo administration of anti-CD25 (interleukin-2 receptor α) monoclonal antibody. Cancer Res. 59: 3128–33 (1999).

93. Shimizu J, Yamazaki S, Sakaguchi S. Induction of tumor immunity by removing $CD25^{+}CD4^{+}$ T cells: a common basis between tumor immunity and autoimmunity. J Immunol 163: 5211–8 (1999).

94. Attia P, Maker AV, Haworth LR, Rogers-Freezer L, & Rosenberg SA. Inability of a fusion protein of IL-2 and diphtheria toxin (Denileukin Diftitox, DAB389IL-2, ONTAK) to eliminate regulatory T lymphocytes in patients with melanoma. J Immunother. 28: 582–92 (2005).

95. Dannull J, Su Z, Rizzieri D, Yang BK, et al. Enhancement of vaccine-mediated antitumor immunity in cancer patients after depletion of regulatory T cells. J Clin Invest. 115: 3623–33 (2005).

97. Litzinger MT, Fernando R, Curiel TJ, Grosenbach DW, et al. IL-2 immunotoxin denileukin diftitox reduces regulatory T cells and enhances vaccine-mediated T-cell immunity. Blood. 110: 3192–201 (2007).

98. Tiemessen M, Jagger A, Evans H, van Herwijnen JC, et al. CD4+CD25+Foxp3+ regulatory T cells inducealternate activation of human monocytes/macrophages. PNAS. 109:19446-19451 (2007).

99. van Elsas, A. et al. Elucidating the autoimmune and antitumor effector mechanisms of a treatment based on cytotoxic T lymphocyte antigen-4 blockade in combination with a B16 melanoma vaccine: comparison of prophylaxis and therapy. J. Exp. Med. 194, 481–489 (2001).

100. Hirano F, Kaneko K, Tamura H, Dong H, Wang S, et al. Blockade of B7-H1 and PD-1 by monoclonal antibodies potentiates cancer therapeutic immunity. Cancer Res. 65, 1089–96 (2005).